Winter 1-1-2020

Life Cycle And Morphological Characterization of Colpodella Sp. (atcc 50594) In Hay Medium

Troy A. Getty
Cleveland State University

LIFE CYCLE AND MORPHOLOGICAL CHARACTERIZATION OF *COLPODELLA* SP. (ATCC 50594) IN HAY MEDIUM

TROY A. GETTY

Bachelor of Science in Biology

Shippensburg University of Pennsylvania

May 2018

submitted in partial fulfillment of requirements for the degree

MASTER OF SCIENCE IN BIOLOGY

at the

CLEVELAND STATE UNIVERSITY

December 2020

We hereby approve this thesis for

TROY A. GETTY

Candidate for the Master of Science in Biology degree

for the Department of Biological, Geological and Environmental Sciences

and the CLEVELAND STATE UNIVERSITY'S

College of Graduate Studies by

Thesis Chairperson, Tobili Y. Sam-Yellowe, Ph.D.

Department & Date

Thesis Committee Member, Girish C. Shukla, Ph.D.

Department & Date

Thesis Committee Member, B. Michael Walton, Ph.D.

Department & Date

Date of Defense: 12/11/20

ACKNOWLEDGEMENTS

I would like to say thank you to Dr. Tobili Sam-Yellowe for her guidance and wisdom throughout the project. I also want to thank Dr. John W. Peterson for letting us come in Saturday mornings and capture IFA images at the Cleveland Clinic Learner Research Institute Imaging Core. I want to thank Dr. Hisashi Fujioka for processing and imaging samples for TEM. I would like to thank Dr. Brian Grimberg for providing the AMA1 antibody. Dr. Marc-Jan Gubbels provided us with the anti-IMC3, anti-IMC3 FLR and anti-IMC7 antibodies, and I would like to thank him for his contribution. I would like to thank Dr. Girish Shukla and Dr. B. Michael Walton for serving on my thesis committee and helping me. I would also like to thank Kush Addepalli for setting up the staining protocols. Aidan Walsh provided professional life cycle models so I would like to thank her. I would like to thank Lauren Dulik and Darshita Siddhpura who were summer research assistants for the Undergraduate Research Awards (2017 and 2019). Lastly, I would like to give a thank you to MR4-BEI Resources for providing us with anti-*Plasmodium falciparum* antibodies; anti-EBA175, anti-plasmepsin 2, and anti-Py235.

LIFE CYCLE AND MORPHOLOGICAL CHARACTERIZATION OF *COLPODELLA* SP. (ATCC 50594) IN HAY MEDIUM

TROY A. GETTY

ABSTRACT

Colpodella species are free living biflagellated protists that prey on algae and bodonids in a process known as myzocytosis. *Colpodella* are phylogenetically closely related to Apicomplexa. Cyst and trophozoite stages have been identified in *Colpodella* species, however the mechanisms of encystation and excystation are unknown. The timing and transition of the life cycle stages are unknown. In the present study I investigated the life cycle of Colpodella sp. (ATCC 50594). *Colpodella* sp. were grown in diprotist cultures in tissue culture flasks containing Hay medium bacterized with *Enterobacter aerogenes* and containing *Bodo caudatus* as prey. I wanted to know the timing and duration of the life cycle and the transition stages of *Colpodella* sp. Time course experiments were performed to determine the duration of the life cycle stages, to investigate the transition of stages within the life cycle, and to identify the predominant cyst stage in resting cultures. The first four time courses were performed to identify the active stage of the life cycle. In all time course experiments cells were fixed and stained with Sam-Yellowe's trichrome for visualization by light microscopy. Confocal and differential interference contrast (DIC) microscopy was performed to determine cross reactivity of Plasmodium specific antibodies against *Colpodella* species proteins. Transmission electron microscopy was performed to visualize the ultrastructure of *Colpodella* sp. The data shows that the duration of *Colpodella* species life cycle is thirty-six hours. *Colpodella* sp. were most active between 20-28 hours as *Colpodella* sp. were

observed actively swimming, feeding, forming transient cysts, and excysting. *Bodo caudatus* was observed to excyst and encyst earlier in the culture. Previously undocumented stages were identified in the *Colpodella* species life cycle. Precyst stages, multinucleate cysts, egress of trophozoites with incomplete cytokinesis, and single nuclei mature cysts were identified. Multinucleate cysts of Colpodella species are reminiscent of Apicomplexa schizonts. Immunofluorescence confirmed there was reactivity between antiserum 686 and *Colpodella* sp. proteins. Differential interference contrast and transmission electron microscopy identified asynchronous and asymmetric mitosis in *Colpodella* cysts. Knowledge of the life cycle and stages of *Colpodella* sp. will allow investigators to perform studies in cell biology and biochemistry of *Colpodella* species.

TABLE OF CONTENTS

LIST OF TABLES

LIST OF FIGURES

LIST OF ABBREVIATIONS

AMA-1	Apical Membrane Antigen
ATCC	American Type Culture Collection
BSA	Bovine serum albumin
clpC	ATP-dependent protease
DAPI	4′,6-diamidino-2-phenylindole
DNA	Deoxyribonucleic Acid
DIC	Differential interference contrast
dPBS	Dulbecco's phosphate buffered saline
EBA-175	Erythrocyte Binding Antigen 175
GAP45	Glideosome-associated protein 45
IFA	Immunofluorescent assay
IMC3	Inner membrane complex protein 3
IMC7	Inner membrane complex protein 7
MIC2	Microneme protein MIC2
mL	Milliliter
MyoA	Myosin A
NMS	Normal mouse serum
NRS	Normal rabbit serum
PAGE	Polyacrylamide gel electrophoresis
PBS	Phosphate-buffered saline
PCR	Polymerase Chain Reaction
PKG	cGMP-dependent protein kinase

PLP1	Sporozoite microneme protein
PL2	Plasmepsin II Antigen
RhopH-3 / Rhop-3	High molecular weight complex rhoptry protein 3
RNA	Ribonucleic Acid
RON 2	Rhoptry neck protein 2
RON 4	Rhoptry neck protein 4
RON 5	Rhoptry neck protein 5
SDS	Sodium Dodecyl Sulfate
SSUrRNA	Small subunit ribosomal ribonucleic acid
sufB	FeS cluster assembly protein
TEM	Transmission electron microscopy
TRAP	Thrombospondin-related anonymous protein
TREP	Transmembrane protein
µl	Microliter

CHAPTER I

INTRODUCTION

1.1 Outline of Chapter I

Colpodellids are a group of free-living alveolate protists that are predators. They prey on other protists and algae in a process known as myzocytosis (Cavalier-Smith and Chao 2004; Simpson and Patterson 1996; Schnepf and Deichgraber 1984). There are two known life cycle stages associated with this group which are a cyst and trophozoite. *Colpodella gonderi* and *C. tetrahymenae* are two species which are considered ectoparasites that attach to the outside of a prey protist and aspirate cytoplasmic contents (Olmo et al. 2011; Cavalier-Smith and Chao 2004). Multiple species of *Colpodella* have been identified and studied to understand their phylogenetic relationship to the parasitic apicomplexans. *Colpodella* species have been isolated from different environments; including soil, freshwater, and marine environments (Simpson and Patterson 1996; Kuvardina et al. 2002, Leander et al. 2003). *Colpodella* species have been reported to be an opportunistic pathogen in two case studies that were published in China. One woman presented symptoms similar to malaria. A polymerase chain reaction (PCR) test was used to amplify the *Colpodella* DNA from the patient (Yuan et al. 2012). A second woman presented with neurological symptoms as a result of a tick bite. *Colpodella* DNA was

also amplified by PCR (Jiang et al. 2018). The life cycle stages causing infection in both cases were not identified. The literature reviewed in the introduction discusses the classification of the alveolates, relationship of the apicomplexans to other alveolates, investigations of the life cycle in photosynthetic alveolates like *Chromera velia* and *Viterella brassicaformis* and their relationship to the colpodellids. The literature review also discusses the dinoflagellates like *Perkinsus marinus* that share an apical complex with the apicomplexans, colpodellids and chromerids. Phylogenetic studies and transcriptome analysis are also discussed and the importance of the plastid in apicomplexans is also discussed.

The objective of this project is to understand the timing of each life cycle stage, find cross reactivity with apicomplexan specific antibodies, and identify morphology of *Colpodella* sp. using electron microscopy. In this study, *Colpodella* sp. (ATCC 50594) was cultured in Hay medium with the prey *Bodo caudatus* and staining techniques for light microscopy were used to identify the life cycle stages (Sam-Yellowe et al. 2019). Confocal, differential interference contrast (DIC) and transmission electron microscopy (TEM) were used identify life cycle stages of *Colpodella* sp.

1.2 Protozoan Infrakingdom Alveolata & Phylogeny

Within the domain of Eukarya there is a large infrakingdom of protists called the Alveolates (Cavalier-Smith and Chao, 2004). There are several structural characteristics that are common in each organism that define this group. The first and most significant structure is the alveoli which are membrane sacs that line the outer layer of the cell which come together and form the pellicle (Goodenough et al. 2018). Other important characteristics of note in these types of protists are mitochondria with tubular cristae and

a form of locomotion using either cilia or flagella. There are nine different classification groups that make up the Alveolata kingdom: Ciliates, Acavomonidia, Colponemidia, Dinoflagellates, Perkinsozoa, Chromerida, Voromonadida, Apicomplexa, and Colpodellida (Cavalier-Smith and Chao 2004). Each of these subgroups has diverged through the process of evolution and possess specific characteristics that are not shared among other alveolates. The specific characteristics differentiate these protists into different species. The apicomplexa are parasitic alveolates which contain a structure known as an apical complex which is highly conserved. Within the phylum there are three subgroups: Coccidians, Gregarines, and Haemosporidians (Roberts et al. 2013). Gregarines are apicomplexa that infect arthropods and mollusks. An example of this would be *Monocystis lumbrici.* Coccidians are closely related to gregarines but a difference is that they parasitize epithelial cells of vertebrates. The genus *Toxoplasma* and *Sarcocystis* contain important human parasites. Haemosporidia is the final subgroup of apicomplexa and are parasites of erythrocytes. They have an arthropod and vertebrate host (Roberts et al. 2013). Haemosporidia is the most well-known group as it contains *Plasmodium* and *Babesia* species which cause important human infections (Roberts et al. 2013).

1.3 Dinozoa & Ciliates

Ciliates are in a large group called Ciliophora that diverged very early in the history of Alveolates and are defined by their cilia, which are small hair like structures used for movement (Cavalier-Smith and Chao, 2004). An example in this group would be *Colpoda steinii* which is found in soil. *Colpodella gonderi* is an ectoparasite of *C. steinii.* (Olmo et al. 2011). Dinozoa is a larger classification that contains two important sister

groups of dinoflagellates which include perkinsids which diverged from a common ancestor. Phylogenetic analysis using actin and rRNA genes showed that *Perkinsus* was genetically different enough from apicomplexa and related to dinoflagellates (Kuvardina et al. 2002). Perkinsids are flagellates that are parasites of oysters and other bivalves of economic importance. An example species of *Perkinsus* is *P. marinus* which parasitizes oysters in the ocean. Dinoflagellates can be plankton that are found in mostly marine environments, or sometimes in freshwater. Dinoflagellates with active plastids perform photosynthesis to obtain food and energy for cell growth (Kuvardina et al. 2002). *Pfiesteria piscicida* is a very significant species of dinoflagellate that is responsible for killing thousands of fish in the ocean and detrimental to the seafood industry (Cavalier-Smith and Chao 2004*). Pfiesteria piscicida* kills marine life by conglomerating into large groups and releasing toxins in the waves (Cavalier-Smith and Chao, 2004*).*

1.4 Plastids

Apicomplexans evolved from free living ancestors (Templeton and Dain 2015; Gubbels and Duraisingh 2012). The events that led to the development of intracellular parasitism are not well known. Most apicomplexans contain a plastid. The plastid is not photosynthetic but remains essential for cell survival. There is a dependency on the nonphotosynthetic organelle as it provides different pathways for enzyme and isoprenoid biosynthesis (Janouskovec et al. 2015). Overtime apicomplexans lost the photosynthetic function of the plastid as they relied on their host to obtain nutrients. There are two very close free-living relatives to the apicomplexans which are the Chromerids and Colpodellids. Chromerids are free living unicellular marine organisms and have a functioning plastid that is used for photosynthesis (Janouskovec et al. 2015). *Colpodella*

species are free-living predators that are a sister group to apicomplexa and share many of the same cellular structures as their parasitic counterparts. Janouskovec et al. (2015) link the plastid genome loss in apicomplexans to two genes which are sufB and clpC. The evolution of parasitism is not due to acquiring new structures, but from loss or modification of organelles that were already present in the cell (Janouskovec et al. 2015).

Apicomplexans such as *Plasmodium* species are known to have a plastid that is non-photosynthetic, but still functions for producing necessary metabolites. There is much confusion and debate about the evolutionary origin of this structure in some parasites. Scientists are unsure if the photosynthetic plastid originated in red or green algae. Using *C. velia* and algae CCMP3155, Janouskovec et al. (2015) were able to isolate the plastid genomes. The *C. velia* plastid genome exists as a linear molecule. The *C. velia* plastid genome is larger than that of CCMP3155 (121.2 kb vs. 85.5 kb), with a lower gene density and stronger strand polarity. Eighteen genes found in the alveolate gene set are never found in green algal or plant plastids, but all are present in plastids of heterokonts, hacrobians, and red algae, consistent with the red algal origin of all alveolate plastids. Another characteristic uniting red algal plastids and their descendants is the ribosomal superoperon, which originated by the fusion of the str and S10+spc+alpha operon clusters. It is important to note that chromerids have a working photosynthetic plastid while *Colpodella* species and *Voromonas pontica* do not have a plastid. Although possessing a plastid, *C. velia* is thought to have an endosymbiotic relationship with coral because that is where they have been isolated from.

1.5 Apicomplexans

Apicomplexan taxonomy is split into the subgroups of gregarines, coccodia, and haemosporidia. Gregarines contain the order Eugregarinorida which has two suborders Aseptatorina and Septatorina and their life cycles include stages such as gametocytes and oocysts which transmit infection (Roberts et al. 2013). A similar organism to gregarines is *Cryptosporidium* species which includes the human parasite *C. parvum*. The distinguishing feature of the phyla is the apical complex which consists of unique structures and organelles that allow the apicomplexans to invade host cells. The specific structures include the conoid that are made of microtubules that give structural support to the cell and polar rings around the neck of the cell. Apicomplexans have rhoptries and micronemes to allow the parasite to secrete proteins and enter the host cell followed by formation of a parasitophorous vacuole in most species. Other structures found in this group are typical of an Alveolate such as a pellicle, mitochondria, Golgi apparatus, and nucleus.

Cavalier-Smith and Chao (2004) argued that the phylum Apicomplexa should never have been used and the Sporozoa name should have been retained. The Colpodellida have now been grouped in the subphylum Apicomplexa within the phylum of Myozoa. Cavalier-Smith and Chao (2004) used *Colpodella tetrahymenae* and *Voromonas ponitca* as model organisms to study their ultrastructure and phylogeny with 18S rDNA. In their phylogenetic tree analysis, they proposed that *V. pontica* is closely related to sporozoa rather than *Perkinsus*. There was also strong indication that *Perkinsus* species were closer phylogenetically with dinoflagellates than sporozoa. The reasons for including *Colpodella* in sporozoa is because they have very similar ultrastructure and

having two different groups for them would be considered over-splitting. Both groups of organisms use gliding motility and contain the same apical complex organelles such as polar ring, micronemes, and rhoptries.

Janouskovec et al. (2015) sequenced 18S rRNA of five species, two chromerids and three colpodellids to perform phylogenetic analysis and to identify genes shared among colpodellids, chromerids and apicomplexans. They found that *Chromera* and *Colpodella* form a sister monophyletic group and are therefore referred to as chrompodellids. Surprisingly, they found that *Colpodella* are more closely related to *Viterella brassicaformis*, a chromerid while *Vormonas pontica* is closer to the chromerid, *Chromera velia*. Photosynthesis was lost in apicomplexans, *Alphamonas*, and *Colpodella* at different individual time points. The loss of plastids is thought to be due to low level requirements needed for biosynthesis pathways if each species can acquire the necessary substances from their environments. In apicomplexans plastid genome loss is due to two genes, sufB and clpC, which are relocated to the nucleus. It was observed that apicomplexans share genes for cell division and oocyst wall formation with their relatives, but none of the genes are linked to the origin of parasitism. Investigators conclude that free-living organisms did not gain novel structures that allowed them to parasitize the host, but that already existing structures were lost or modified (Janouskovec et al. 2015).

Figure 1 shows the close phylogenetic relationship of *Colpodella* sp. with apicomplexan parasites. Kurvadina et al. (2002) utilized the transcriptome of *Colpodella* sp. to perform a phylogenetic analysis of nuclear-encoded genes. The results show that *Colpodella* species are in close relation with parasites such as *Plasmodium* species and

with chromerids. The use of small subunit RNA for phylogenetic analysis also supports the findings of the close relationship between chromerids and parasitic apicomplexans (Kurvadina et al. 2002; Leander et al. 2003). Chromerid and apicomplexans transcriptomes were analyzed to complete the relationships found in Figure 2. This lab also wanted look at the four pathways of metabolism that were found in the apicoplast of apicomplexans such as *Plasmodium* and the genes/ proteins that make them function. *Colpodella* did not retain any plastid genes but there is evidence that *Colpodella* contain nuclear encoded genes for apicoplast pathways.

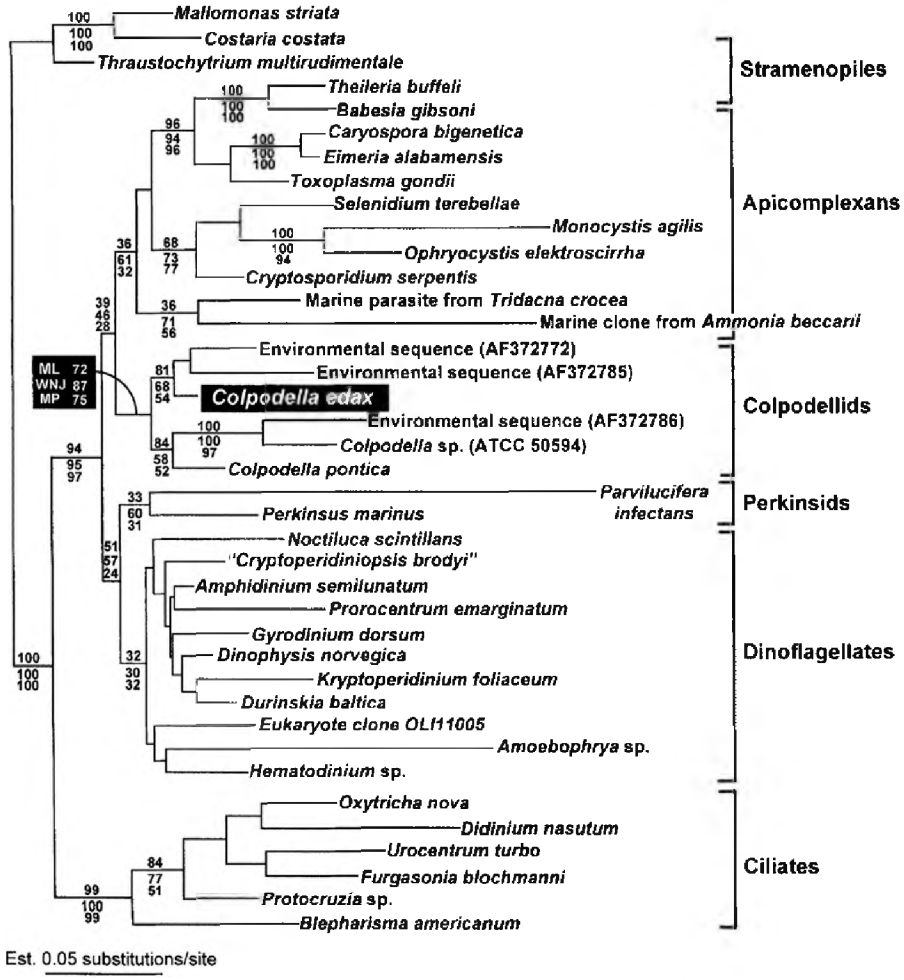

Figure 1. Phylogenetic tree showing the close relationship of *Colpodella* sp. with parasitic apicomplexans. This figure was taken from *The phylogeny of Colpodellids (Alveolata) using small subunit rRNA gene sequences suggests they are the free-living sister group to apicomplexans* (Kuvardina et al. 2002).

Apicomplexans invade a host cell by forming a tight junction between the invasive stage and the host cell membrane. Apical membrane antigen-1 (AMA-1), a microneme protein and RON proteins which are rhoptry neck proteins are crucial for this invasion event to occur (Bargieri et al. 2014) (Figure 2). Several microneme and rhoptry proteins involved in host cell invasion have been identified among parasitic apicomplexans (Table 1). Although chromerids and colpodellids possess apical complex organelles, proteins involved in the process of predation known as myzocytosis similar to the host cell invasion process, have not been identified.

When an apicomplexan such as *Plasmodium falciparum* infects a human host, the infective stage is called a sporozoite that is injected into the circulatory system by a female *Anopheles* mosquito vector. The sporozoites are then carried to the liver where they invade hepatocytes. A few rounds of asexual reproduction called schizogony occur and the cells eventually release merozoites into the blood stream. Merozoites invade erythrocytes and form a trophozoite which matures into a multinucleate schizont. The schizonts will undergo numerous rounds of asexual division and bud merozoites from the mature schizonts. The erythrocyte will then burst to release up to 32 merozoites that will infect new red blood cells to form schizonts or male and female gametocytes. If the gametocyte-infected red blood cells are aspirated by the vector, then the parasite will undergo sexual reproduction. Microgametes will form by exflagellation to fertilize macrogametes and create zygotes. The zygote matures to become an ookinete and then transforms to an oocyst. The oocyst has multiple rounds of asexual division until it releases many sporozoites which migrate to the salivary glands of the vector. Other forms of apicomplexan asexual reproduction include endodyogeny and endopolygeny which

occurs in *Toxoplasma gondii*. Endodyogeny involves two daughter cells being formed inside a single mother cell, while endopolygeny is internal budding forming two or more daughter cells (Gubbels et al. 2020). In order to understand the origins of parasitism from the free-living colpodellid and chromerid relatives, it is important to identify the type of cell division that occurs in the life cycle and to determine if similar asexual stages occur in their life cycles. These stages have not been identified and the details of the life cycles of chromerids and colpodellids are unknown. Closed mitosis seems to be the prevalent form of division among apicomplexans, where the nucleus remains intact. Closed mitosis is considered the more ancient form of cell division, while open mitosis is more recent in evolution. Open mitosis occurs when the nuclear envelope breaks down before the chromosomes separate, this usually happens in mammals (Gubbels et al. 2020).

Table 1. List of Apicomplexan proteins and kinases that function in host cell invasion and egress of parasites from host cells following schizogony. This figure was taken and modified from *Host cell invasion by apicomplexan parasites: The junction conundrum* (Bargieri et al. 2014).

Proteins	Function	Species	Reference
RON2	Receptor for AMA-1	*Toxoplasma gondii*	Murata el al. (2012)
RON4	Associates with the parasitophorous vacuolar membrane	*T. gondii*	Giovannini et al. (2011)
RON5	Organizes RON complex to form tight junction	*T. gondii*	Beck et al. (2014)
AMA1	Forms junction with RON2 for invasion	*Plasmodium falciparum*	Mital et al. (2005)
MIC2	Used in host cell invasion	*T. gondii*	Bossier et al. (2005)
TRAP	Host cell recognition and invasion, motility	*P. falciparum*	Sultan et al. (1997)
TREP	Used in gliding motility	*P. falciparum*	Combe et al. (2009)
Aldolase	Enzyme in the glycolytic cycle	*P. falciparum*	Shen et al. (2014)
Actin	Involved in motility cytoskeleton, and transport of molecules	*T. gondii*	Egarter et al. (2014)
IMC	Gives structure to cell and helps in cytokinesis	*P. falciparum*	Kono et al. (2016)
MyoA	Used in actin-myosin motor complex in cell invasion	*P. falciparum*	Meissner et al. (2002)
GAP45	Membrane anchored protein that helps invade cells	*P. falciparum*	Frenal et al. (2010)
PLP1	Disrupts host cell membrane	*P. falciparum*	Hale et al. (2017)
PKG	A protein kinase that triggers egression	*P. falciparum*	Hale et al. (2017)

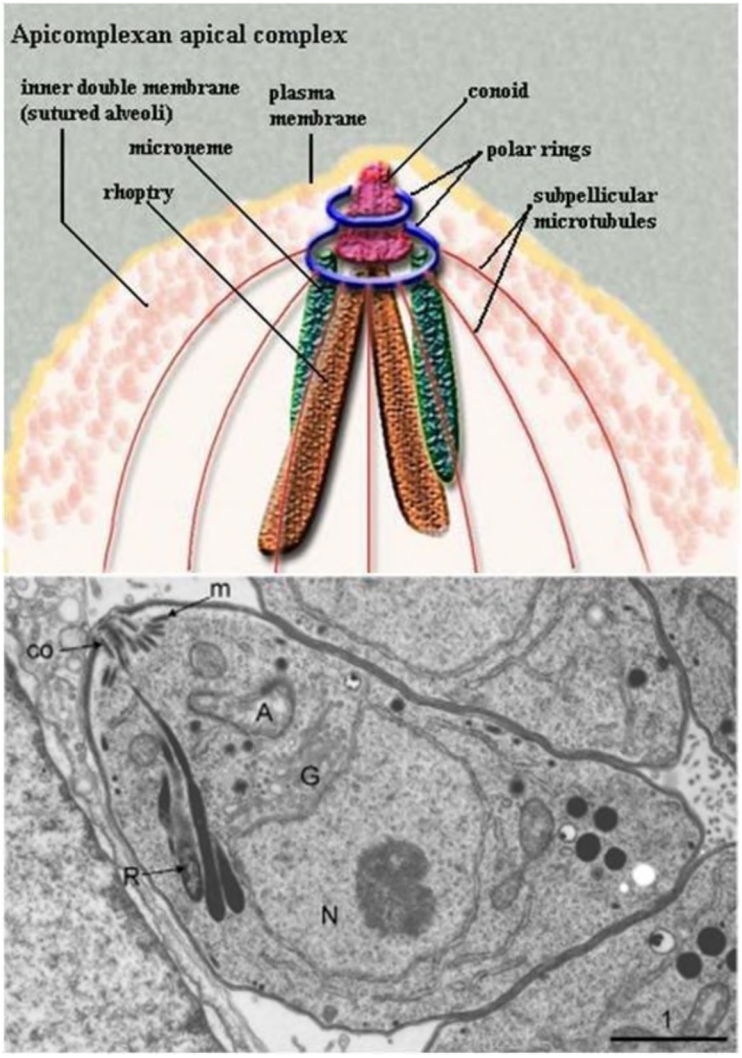

Figure 2. Apical complex found in apicomplexans that is used for host cell invasion. The electron micrograph below shows an image of the apical complex in a *T. gondii* tachyzoite (Peixoto 2009).

1.6 *Colpodella* Species

Colpodella species are unicellular alveolate flagellates that are considered predators with a few labeled as ectoparasites. Light and transmission electron microscopy has been used to investigate the morphology of *Colpodella* species to identify structural components that may or may not be unique to this group such as flagella development and the entirety of the apical complex. There are several species of *Colpodella* that have

been identified from the environment and cultured in laboratories (Simpson and Patterson 1996). They include: *Colpodella pugnax, Colpodella perforans, Colpodella gonderi, Colpodella edax, Colpodella vorax, Colpodella angusta, Colpodella turpis*, *Colpodella pseudoedax, Colpodella unguis, Colpodella tetrahymenae, and Colpodella pontica* (which is now *Voromonas pontica)* (Brugerolle 2002; Mylnikov 2009; Mylinkov and Mylnikova 2008; Cavalier-Smith and Chao 2004; Simpson and Patterson 1996). *Colpodella* species can be found in soil, fresh water, and marine environments.

1.6.1 *Colpodella pugnax*

Colpodella pugnax has a trophozoite stage which has concave ventral sides and is around 7-15 micrometers long. The rostrum in the front of the cell is curved and takes up approximately 40% of the body length, each cell also two flagella longer than the body which point to the rear and anterior. Trophozoites swim in a spiral pattern on a longitudinal axis. The ultrastructure shows a nucleus that contains a nucleolus with anterior mitochondria that are vesicular. The cell has two membranes with microtubules as structural support and the surface contains micropores. The rostrum contains an apical complex which houses the conoid, rhoptries, and polar rings (Simpson and Patterson 1996).

1.6.2 *Colpodella turpis*

Colpodella turpis is a lesser studied species and is about 14-22 micrometers long with a large rostrum that is hooked ventrally. The flagella are longer or equal to the body length and when the cysts divide, they can produce either two or four daughter cells (Simpson and Patterson 1996).

1.6.3 *Colpodella pseudoedax*

Colpodella pseudoedax reproduces by longitudinal fission into two daughter cells and has a pseudoconoid in the rostrum that is surrounded by vesicles which are right beside the 1.5 micrometer long rhoptries. A pellicle of 30nm with 3 membranes surrounds the cell supported by microtubules with micropores on the surface. Flagellar kinetosomes are situated at right angles where the flagella start from and are located next to the central microtubules. Oval mitochondria, vesicular cristae, and a dark matrix are present as well. Trichocysts which are extrusive organelles, line the pellicle from the inside of the cell while a Golgi apparatus and vacuole are found in the posterior of the cell (Mylnikov 2009).

1.6.4 *Colpodella unguis*

Colpodella unguis has a plasmalemma and expanded alveoli, as well as two heterodynamic flagella located perpendicular to one another. The cell has a longitudinal groove that is supported by two microtubular bands and trichocysts. The largest difference between *C. unguis* and C. *pseudoedax* is the way of reproduction as *C. unguis* uses fission inside the cysts instead of longitudinal fission (Mylnikov 2009).

1.6.5 *Voromonas pontica*

Voromonas pontica has no alveoli near or in the pseudoconoid and has three or four bands of microtubules passing through it. This is a marine species that is isolated from oceans and had its genus name changed from *Colpodella* to *Voromonas* (Cavalier-Smith and Chao 2004). *Voromonas pontica* has trichocysts which is similar to dinoflagellates. *Voromonas pontica* does not have a rostrum that houses the pseudoconoid and microtubules.

1.6.6 *Colpodella edax*

Similar to *V. pontica* and *C. angusta*, *Colpodella edax* has most of the same features except that the pseudoconoid lies close to the kinetosome of the front flagella then bends into an arc. This does not create a cone shape and the pseudoconoid is not locked unlike the Perkinsids (Mylinkov and Mylnikova 2008).

1.6.7 *Colpodella vorax*

Colpodella vorax looks like a rain drop about 12 micrometers long and 5 micrometers wide with the flagella extending from the base of the rostrum. They have no ventral gutter unlike *C. edax* and *C. angusta*. The rhoptries are bulbous shaped and have a globular head with microfibrils. A small posterior root and oblique root are attached to the posterior flagella which is unique. Pellicular microtubules come into close contact with the endoplasmic reticulum and the Golgi body is located next to the nucleus (Brugerolle 2002).

1.6.8 *Colpodella angusta*

Colpodella angusta consists of a pellicle with an outer plasmalemma and flattened vesicles that are absent near the pseudoconoid. Rhoptries lie in the pseudoconoid cavity forming pear shapes pointing anteriorly and micronemes are located in the conoid and posterior of the cell (Mylinkov and Mylnikova 2008).

1.6.9 *Colpodella tetrahymenae*

Colpodella tetrahymenae is an ectoparasite that closely resembles *Colpodella gonderi* in its ultrastructure. This species has a cytoplasm that is packed with a large number of ribosomes and contained by an inner membrane complex inside the membrane with some microtubules (Cavalier-Smith and Chao 2004). The rostrum appears long and

attached to one side of its prey which is the ciliate *Tetrahymena species.* The mitochondrial reticulum has ampulliform cristae (Cavalier-Smith and Chao 2004). Cavalier-Smith and Chao (2004) used electron microscopy to examine the ultrastructure of *C. tetrahymenae* and *V. pontica. Colpodella tetrahymenae* is known to feed on the ciliate *Tetrahymena* and lacks a covering on the plasma membrane. The apical end has a pseudoconoid which houses the rostrum for myzocytosis. It contains a posterior food vacuole that expands as the cell aspirates contents from the prey until it is ready to encyst. *Colpodella tetrahymenae* forms four trophozoites inside a single cyst. In a similar sister group, *Chromera velia* has been described to usually divide into four coccoid cells, but more than four has been observed.

1.6.10 *Colpodella gonderi*

Colpodella gonderi is an ectoparasite that has two flagella of even size and ranges from 10-12 micrometers long (Olmo et al. 2011). The cytoplasm contains granules as well as a large inclusion toward the posterior of the cell. The nucleus was located in the center and no vacuoles were found when observing this species. *C. gonderi* is a predator of the scuticociliate *Pseudocohnilembus pusillus* and many species of ciliates (Olmo et al. 2011).

1.6.11 *Colpodella sp* (ATCC 50594)

The *Colpodella* species maintained by the American type culture collection is the model *Colpodella sp.* used by investigators to study the phylogeny of *Colpodella* species and to investigate the origins of parasitism among the apicomplexa. Using organisms closely related to apicomplexans Janouskovec et al. (2015) wanted to examine the origins of parasitism by observing cell characteristics and genes that are conserved. They also

wanted to understand any factors mediating plastid dependency in apicomplexans as they do not function for photosynthesis. Five organisms were collected for phylogenetic analysis which included two photosynthetic chromerids and three predatory colpodellids: *C. velia and V. brassicaformis,* and *Colpodella, Alphamonas, and Voromonas*, respectively. They obtained sequences for each alveolate and used apicomplexan specific primers targeting 18S rRNA in polymerase chain reaction (PCR) to create phylogenetic lineages. Phylogenetic trees constructed showed that chromerids and colpodellids branch off together and are basal to apicomplexans. The transcriptomes of all five organisms were sequenced and eighty-five transcripts were examined from previously tested eukaryotic wide phylogenies to infer phylogenetic groups. They found that chromerids and colpodellids form a single monophyletic group (Janouskovec et al. 2015). The genes clpC and suf B, thought to be important for retention of the plastid was found in apicomplexans. The genes help retain the plastid for biosynthetic pathways crucial for survival of the apicomlexans. Orthologs of suf B and clpC genes were observed in all five chrompodellids. Some molecules shared between chrompodellids and Apicomplexa consist of apical complex genes such as microneme and rhoptry genes. Other genes examined include genes that were acquired from bacteria. These were not specific to apicomplexans and have also been found in their relatives. Specific genes such as IspH (isoprenoid), FECH (tetrapyrrole), FabG (fatty acid synthesis), GlnA (glutamine metabolism), YgFa (folate metabolism), and nucleotide conversion (PNP, PUS, and DUT) are shared between these two groups. Ribonucleotide reductase and PREX (specific DNA polymerase) only thought to be found in apicomplexans were also found in chromopodellids. Proteins only specific to apicomplexa include rhoptry, microneme,

and dense body proteins. Chrompodellids and apicomplexans share oocyst wall proteins, flatten alveoli, PKSI, FASI, GAPMS, closed conoids, inner membrane complex, rhoptry neck proteins (RON1, RON6, RON 10), PRP2, Myosin proteins, and GAP45.

Sidall et al. (2001) used the ATCC obtained species in phylogenetic studies also showed using SSU rDNA sequences that *Colpodella* sp. is a close ancestor of parasitic Apicomplexa and also a sister clade. Some of the close relatives of *Colpodella* sp. identified in their analysis include *Tridacna crocea, Ophryocystis elehiroscirrha, Monocystis agllis,* and *Toxoplasma gondii.* Previous studies in our lab investigated methods for culturing *Colpodella* sp. and identified Hay medium as suitable for maintaining diprotist cultures containing *Colpodella* sp. and its prey *Bodo caudatus* (Yadavalli and Sam-Yellowe 2017; Sam-Yellowe and Yadavalli 2018). Colpodellids and chromerids identified from different environmental sources have been maintained in short term culture using different types of culture media (Table 2), for use in ultrastructural and phylogenetic studies. Antibodies against *Plasmodium* rhoptry protein RhopH3 was also used to identify apical complex proteins cross reacting with the *Plasmodium* antibodies. RhopH3 cross reactivity was identified in *Colpodella* sp. in immunofluorescence assays (IFA) and confocal microscopy studies and exon 7 of the RhopH3 gene was amplified from *Colpodella* sp. DNA sequence analysis demonstrated conservation of the Rhop3 gene in *Colpodella* sp. (Sam-Yellowe et al. 2019). In order to visualize and differentiate life cycle stages of *Colpodella* sp. and *B. caudatus*, Sam-Yellowe's Trichrome stain was developed to aid differentiation. Cyst and trophozoite stages were identified using this method. The trichrome staining protocol was used in the current investigation to identify life cycle stages in the process of constructing the life cycle of *Colpodella* sp. and to aid

interpretation of the ultrastructure of *Colpodella* sp. by transmission electron microscopy (TEM). In order to use the *Colpodella* sp. for cell biology studies, we need to understand the timing of life cycle stage transformations and to accurately identify the stages present in the life cycle of *Colpodella* sp.

Table 2a. Table showing *Colpodella* species and their characterizations

Species	Method of Obtaining	Prey/Food	Medium of Growth	Fixation/Suspension/ DNA Extraction	Observation Method
[a] *Colpodella pseudoedax* & [b] *Colpodella unguis*	Institute of Biology of Inland Waters, Russian Academy of Science	Bacteriotrophic flagellates *Spumella* sp. *Procryptobia sorokini*	Pratt medium and Schmalz-Pratt medium	Centrifuged and fixed in mixture of 2% OsO4 and 0.6% Glutaraldehyde On Schmalz-Pratt media for 15-30min at 1C. A series of dehydrations occur in alcohols and anhydrous acetone, then placed in Araldite and Epons resins	First used BIOLAM-I microscope with phase contrast device KF-5 in passing light and water immersion. Second, used transmission electron microscope on thin sections
[c] *Colpodella gonderi*	Upland grassland site at Sourhope research station of Macaulay Land Use Research Institute, land was mid-altitude and temperate, shallow brown soil with poor minerals, pH at 4.5-4.8 taken at a depth of 5 cm, transported in 4C dark boxes to lab	*Colpoda steinii, Grossglockneria acuta, Psuedoplatyophyra nana*	Soil spread evenly in 15cm Petri dishes at room temp for 6 days, soil then passed through 3.35 sieve and homogenized, 5g air dried soil and 15 ml rainwater mixed into petri dish and incubated at 15C for 4 days	50 microliters of runoff put in Sedgewick-Rafter counting chamber and observed, ciliates identified by silver impregnation techniques (pyridinated silver carbonate methods)	Sedgewick-Rafter counting chamber, electron microscopy
[d] *Colpodella vorax*	Pond water that had dead leaves and grass	*Bodo caudatus, Spumella* sp. *Synura petersenii, Chilomonas paramaecium, Euglena gracilis, Colpoda cucullus*	Multiplied in pond water, Petri dish	Predator phase collected with pipette using a stereomicroscope, cells centrifuged and fixed by 1 vol of 1% glutaraldehyde in 0.1 M cacodylate buffer pH 7 and 1 vol of 1% osmium tetroxide for 1 hour, wash in distilled water cells are pre-embedded in 1% agar contrasted "en bloc" by saturated uranyl acetate in 50% ethanol then dehydrated in alcohol series, final embedding in Epon 812 resin	Using small chambers with ring of Vaseline on slide covered by slip C. vorax and a prey are photographed for hours/days with phase contrast microscopy, sections from Reichert Ultracut S microtome contrasted by lead citrate for 15 min and coated with carbon for EM

Table 2b. Table showing *Colpodella* species and their characterizations

Species	Method of Obtaining	Prey/Food	Medium of Growth	Fixation/Suspension/ DNA Extraction	Observation Method
[e] *Voromonas pontica*	1)Isolated from coastal waters of Black Sea near Yalta, Institute of Biology of Inland Waters, Russian Academy of Science	*Escherichia coli, Bodo sorokini*	Schmaltz-Pratt medium (1L H2O, 28.15g NaCl,0.67g KCl, 5.51g MgCl26H2O, 6.92g MgSO47H2O, 1.45g CaCl2H2O, 0.1g KNO3, 0.01g K2HPO43H2O), 20-22% salinity	DNA extracted from pellets using hexadecyltri-methylammonium bromide	small subunit rRNA purified amplified with primers and PCR and seen on agrose gel, products isolated with ultraclean purification kit and inserted in 1) pGEM-T vector and 2) pCR 2.1 vector, each was sequenced with ABI big dye reaction mix using primers
[f] *Colpodella pugnax*	Artificial hypersaline (26% NaCl) lagoon at Whyalla, South Australia	*Dunaliella viridis*	28C, lighting conditions varied	Centrifuged and fixed for 30 mins in solution of 5% glutaraldehyde and 1% osmium tetroxide in a buffer of 18% NaCl, 110 HEPES, and 20 mM EDTA. Then wash in half strength buffer embedded in 2% agar and stained with saturated uranyl acetate in 50% ethanol for 2 hours, after blocks are dehydrated through ethanol series then embedded in Araldite resin	Light microscopy, Photomicrography, serial sections cut and collected on pioloform-coated slot grids and coated with carbon then stained with lead citrate for EM
[g] *Colpodella angusta*	Unknown	*Procryptobia soronki, Spumella sp., Parabodo caudatus*	Unknown	Centrifugation and total RNA was reversed transcribed using SMARTer Pico PCR cDNA kit, DNA extraction kit, Phylogenetic research, GenBank	PCR, phylogenetic trees

Species	Method of Obtaining	Prey/Food	Medium of Growth	Fixation/Suspension/ DNA Extraction	Observation Method
[h] *Chromera velia*	First isolated from stony coral *Pleslastrea versipora* in Australia, this was obtained from Boothbay Harbor, ME from the culture collection of marine phytoplankton	*Procryptobia soronki, Spumella sp., Parabodo caudatus*	Cultivated in f/2 medium in sea water with a 12-hour light and dark cycle at 26 degrees with a 3.15 Watt intensity light	Cells could be fixed with glutaraldehyde and then pelleted and post fixed with OsO4 and dehydrated in acetone. Pellets were frozen using a high-pressure freezer and frozen substitution with liquid nitrogen. The temperature was slowly raised over a period of time and the cells were washed with acetone and resin. They were occasionally microwaved to allow the resin to polymerize. Sections were cut and stained with uranyl acetate and lead citrate and then carbon coated for TEM.	Light microscopy, electron microscopy, transmission electron microscopy, to look at morphology and ultrastructure.
[I] *Vitrella brassicaformis*	Isolated from One Tree Island, the Great Barrier Reef from a stony coral *Leptastrea purpurea*	*Procryptobia soronki, Spumella sp., Parabodo caudatus*	f/2 medium in saltwater at 22 degrees	Centrifuged for pellets and mixed with lysis buffer, RNA extracted using RNA kit	Scanning electron microscopy, Light microscopy, transmission electron microscopy
[j] *Colpodella sp.* (ATCC 50594)	American Type Culture collection (Manassas, VA)	*Bodo caudatus, Klebsiella pneumoniae*	ATCC culture medium 802 (Sonneborn's Paramecium), Hay medium	rRNA extraction for phylogenetic tree relationship, DNA extracted for sequencing and PCR, cells pelleted and fixed for staining	Transmission electron microscopy, light microscopy, confocal light microscopy
[k] *Colpodella tetrahymenae*	Rainforest soil from La Selva, Costa Rica	*Tetrahymena pyriformis*	Soil with natural mix of bacteria	DNA isolation and amplification, Phylogenetic analysis	Scanning electron microscopy, Light microscopy, transmission electron microscopy

Table 2c. Table showing *Colpodella* species and their characterizations

[a]. *Colpodella pseudoedax*, Mylnikov 2009. [b]. *Colpodella unguis*, Simpson and Patterson 1996. [c]. *Colpodella gonderi*, Olmo et al. 2011. [d]. *Colpodella vorax*, Brugerolle et al. 2002. [e]. *Voromonas pontica*, Cavalier-Smith and Chao 2004. [f]. *Colpodella pugnax*, Simpson and Patterson 1996. [g]. *Colpodella angusta*, Janouškovec et al. 2015. [h]. *Chromera velia*, Obornik et al. 2011. [i]. *Viterlla brassicaformis*, Obornik et al. 2012. [j]. *Colpodella* sp. (ATCC 50594), Sam-Yellow et al. 2019. [k]. *Colpodella tetrahymenae*, Janouškovec et al. 2015.

1.7 Morphology and Life Cycle of *Colpodella Species*

Each of the species of *Colpodella* described may differ slightly in some features, but for the most part all of them have the same basic ultrastructure. *Colpodella* trophozoites have a cone shaped microtubular structure at the neck which forms the pseudoconoid, which is contained in the rostrum that is used for feeding. *Colpodella* species contain a pellicle and apical complex just like pathogenic apicomplexans that includes rhoptries, polar rings, micronemes, and microtubules which serve to penetrate the host cell. There is a presence of heterodynamic flagella that are situated in the flagellar kinetosomes and transversal plates that produce locomotion that allow the cell to move around and catch its prey (Mylnikov and Mylnikova 2008). Universally, alveolates have a nucleus and nucleolus that lie in the center of the cell and oval mitochondria that have tubular and vesicular cristae. Some alveolates have unique structures called trichocysts which are organelles that push against the pellicle from inside the cell and are long fibrous shafts that are ejected in response to stimuli (Brugerolle 2002). *Colpodella* species have a Golgi apparatus as well as a food vacuole located at the posterior. The food vacuole is originally shrunken, but as the trophozoite feeds the vacuole becomes very large taking up most of the cell body. In the first stage of the life cycle, immature trophozoites emerge from the cyst and move with their two flagella in a rapid oscillatory motion usually in a helical path in search of prey (Brugerolle 2002). The prey of *Colpodella* species is usually either a species of ciliate or bodonid. Feeding is initiated when the predator attaches onto the prey organism using its rostrum where the apical complex is located. A tubular bridge forms between the predator and prey which is used to aspirate the cytoplasm of the prey. This way of feeding is known as myzocytosis

(Brugerolle 2002). Multiple predators can attach to a single prey either at the posterior or sides, and it is thought the rhoptries secrete proteins that help the predators feed. The species *C. gonderi* and *C. tetrahymenae* remain attached to their prey for long periods of time and are described as ectoparasites. Once the *Colpodella* species feed and have a large food vacuole they encyst and divide into two then four cells, that eventually excyst to release trophozoites so the cycle may continue. Two types of cysts are found in *Colpodella* species. The first is a temporary cyst and the second is a resting cyst. However, the duration of the life cycle and mechanisms of encystation and excystation are unknown.

1.8 *Colpodella sp.* as Opportunistic Parasites

There are two reported cases of illness believed to be caused by *Colpodella* species in humans (Jiang et al. 2018; Yuan et al. 2012). Both cases reported involved women in their late fifties from China. In the first case, a 57-year-old woman with natural killer cell deficiency had an erythrocyte parasite that caused symptoms such as fevers and persistent cough. Blood samples used for PCR and sequencing found that amplified DNA did not match any of the known apicomplexan parasites in the database. A search in Genbank found a close match of the DNA to *Colpodella tetrahymena.* Drugs known to be effective for *Plasmodium* and *Babesia* were effective against the *Colpodella* infection, resulting in resolution of symptoms and decreased parasitemia (Yuan et al. 2012). The second case involved a tick bite and transmission of *Colpodella* sp. as a vector borne infection. The second case was a 55-year-old woman that presented with neurological symptoms. A search for ticks in the woods around the woman's house led to the

identification of *Ixodes persulcatus* which tested positive for *Colpodella* sp. (Jiang et al. 2018).

1.9 Life Cycle and Morphology of *Chromera Velia.*

There are studies about the ultrastructure and life cycle of *C. velia* which share some similarities and differences with *Colpodella* sp. *Chromera velia* are important research models because they contain an active plastid and are the closest photosynthetic relative of apicomplexan parasites. This species was isolated from a stony coral found in Australia; the procedures used to obtain this organism coincides with that of intracellular endosymbionts of corals such as dinoflagellates. Through phylogenetic analysis of nuclear and plastid genes investigators determined the close relationship between this species and apicomplexans (Obornik et al. 2011). The life cycle of *C. velia* was investigated using light microscopy of cells grown in simple cultivation medium. A 12-hour light and dark cycle with optimal light intensity at 26 °C supported the growth of the cells well. Three stages were discovered in the life cycle of *C. velia:* coccoid, cysts and flagellates. The prevalence of each of these life cycle stages depended upon the culture conditions. The oval coccoid stage was the most abundant in every culture condition. Obornik et al. (2011) found that these cells undergo binary fission. After binary fission, another round of division can lead to a cyst or flagellate stage. The transformation from coccoid stage to motile stage was found to take a few minutes and was in response to light stimulus (Obornik et al. 2011). The flagellate stage possesses heterodynamic flagella, never exceed more than 1% of all the cells in the culture and most of the flagellate cells were seen between day 7 and day 11 in the culture. After a few hours the motile cells usually transform back into coccoid cells. Investigators speculate that that *C.*

velia evolved to possess the flagellate stages to help them avoid intense light or to find nutrients. Obornik et al. (2011) performed scanning electron microscopy (SEM) to understand the structure of *C. velia* cysts in the life cycle. They observed that within the cyst wall there were 4 coccoid cells and in between the cells was space filled by sporulation residuum. This study also revealed that both flagella come out of the interior portion of the cell (Obornik et al. 2011). This is similar to *Colpodella* species as both organisms have two heterodynamic flagella and each cyst contains four cells which excyst.

Transmission electron microscopy was performed with high pressure freezing and freeze substitution because the cell walls were resistant to normal fixatives. Granules reminiscent of apicomplexans and a large plastid were observed. In the stationary cultures, the cytoplasm of the coccoid cells had many granules and inclusions, and in the active cultures, the coccoid cells had very few granules. Another feature of *C. velia* is that they have a plasmalemma and alveoli like apicomplexans. Other structures that are present which are identical to apicomplexans include subpellicular microtubules and a pseudoconoid which is found in *Colpodella* species. In sections of the pseudoconoid they could see electron dense structures that were similar to micronemes or rhoptries of apicomplexa. A unique structure identified is called the chromerosome which resembles a giant extrusome or trichocysts identified in some *Colpodella* species and in dinoflagellates. Overall, *C. velia* contains a mixture of structures described in apicomplexans, *Colpodella* and dinoflagellates. The placement of microtubules is related to that of the dinoflagellate *Perkinsus* because there is a gap between each microtubule. The pseudoconoid is synthesized during the transformation of the coccoid stage into the

flagellate stage. Additionally, lamellar connectors between basal bodies of both flagella were identified but were less significant than those in *Colpodella* species. *Chromera velia* is not supported by a paraflagellar rod and actually ejects the flagella from its cytoplasm as described for *Plasmodium* species. Both *Colpodella* species and *C. velia* have similar life cycle stages in that there is a resting cyst stage and an active trophozoite stage. In their motile stages, they are able to hunt for microscopic prey such as algae and bodonids for *Colpodella* species and bacteria for *C. velia*. Both organisms live in some of the same environments such as marine water. Both life cycles show a response to stimulus as the coccoid cells of *C. velia* become motile in response to light while *Colpodella* cysts excyst when they are freshly cultivated. One major difference is that there are three stages in *C. velia* which include the coccoid stage that is not seen in *Colpodella* and mature cysts have not been recorded in *C. velia* (Obornik et al. 2011).

Intraflagellar transport is the movement of building blocks used to create flagella. The components are shipped from the cytoplasm to where they are needed in flagella by specific proteins. In apicomplexans flagella are restricted to male gametes in sexual reproduction and some species have even lost the ability to synthesize them. *Plasmodium* species use a process called exflagellation where the flagella are built completely in the cytoplasm and then expelled outside the cell membrane upon completion. Several studies have investigated the synthesis and of flagella proteins and development of flagella among the alveolates closely related to the apicomplexan in order to understand the evolution of the flagella apparatus from the free-living relatives to the parasitic apicomplexans. *Chromera velia* was investigated to determine if the flagella is expelled from within or built externally to the cell membrane. The life cycle of *C. velia* has cysts

which can release immobile coccoid cells or motile flagellates. The motile stages are biflagellate and have two heterodynamic flagella. Investigators propose that *C. velia* assembles axonemes and completes the process of building flagella in their cytoplasm similar to *Plasmodium* (Okamoto and Keeling 2014; Portman et al. 2014). Using live imaging, time lapse and TEM to capture *C. velia* in culture led to the identification of two types of cysts in the life cycle of *C. velia.* The cysts were designated as types 2 and type 4. Type 2 indicates that two daughter cells excyst and type 4 indicates four daughter trophozoites excyst. The cysts can further be divided into types 2C and 2F, type 4C and 4F. The C signifies that coccoid cells are excysting, while F means the biflagellated motile stage is eggresing. Type 4C is the predominant stage in cultures and type 4 only makes up 1% of the total culture. There were a few cysts that were seen that contained more than 4 cells within which shows they undergo multiple rounds of mitosis (Portman et al. 2014). Results showed that flagella synthesis occurs through the process of cell division and not by transformation of the cell. Using electron microscopy, they could also see the pseudoconoid in the flagellate forms.

1.10 Life Cycle and Morphology of *Vitrella Brassicaformis*

A second chromerid with close relationship to apicomplexans and *C. velia*, with links to dinoflagellates is *Vitrella brassicaformis*. This chromerid can be differentiated from C. velia through differences in morphology, life cycle and plastid genome (Obornik et al. 2012). Investigators were able to show a relationship between apicomplexa and *V. brassicaformis* through molecular phylogeny, structure of the plastid, and other ultrastructural characteristics. This new chromerid contains alveoli, a micropore, and a pseudoconoid. Morphologically the flagellates of *V. brassicaformis* are similar to

Colpodella because of the pseudoconoid. The difference between *C. velia and V. brassicaformis* is that *C. velia* has a linear genome that lacks inverted repeats of rRNA. *V. brassicaformis* has a conserved circular plastid genome with a high GC content. It also uses the canonical code for all tryptophans in the plastid encoded genes like the Apicomplexa. Under light microscopy, non-motile coccoid cells with storage granules were identified. The cyst stage possesses a thick wall, and depending on the development of the cells, there could be formation of two different types of structures known as sporangia. The first type is a mature green autosporangia that can produce non-motile autospores. A second type of sporangia that can be produced are motile flagellate zoospores which have no pigmentation. The zoospores are very tiny and are bi-flagellated. The zoospores develop more quickly than the autospores and both contain circular operculum in their walls. Scanning electron microscopy was used to show that there are several layers in the cell wall which varied in thickness and are independent of each other. Transmission electron microscopy showed that autosporangia contained autospores that were filled with granules and a thylakoid containing plastid. The zoospores were shown to have two heterodynamic flagella and subpellicular microtubules. *Colpodella* are similar to this species of chromerids as they both have cyst stages and flagellate stages in their life cycles. Some structural characteristics they share include alveoli, subpellicular microtubules, and two flagella. The research is uncertain as to why there are two stages of the life cycle for *V. brassicaformis* and what induces the motile stage. It is unknown if the new species has a pseudoconoid or not like *C. velia. Vitrella brassicaformis* was isolated from an Australian stony coral at One Tree Island, Great Barrier Reef (Orbornik et al. 2012).

1.11 *Perkinsus Marinus*

Perkinsus marinus is an intracellular parasite that infects oysters of the *Crassostrea* genus causing their tissues to degrade. This is a major problem as it affects the seafood industry. It belongs to the Alveolata group and is a protozoan. The life cycle of this pathogen consists of a motile zoospore and a non-motile trophozoite which is ingested during filter feeding (Joseph et al. 2010). Leibowitz et al. (2017) studied the proteome of *P. marinus* in vitro. Heat shock proteins were discovered which give the protist an advantage in surviving different water temperatures. Proteases such as serine protease and iron-containing superoxide dismutase play a role in causing damage to the cells of the oyster. *P. marinus* has an apical complex with rhoptries like that of apicomplexan parasites that they use to secrete ROP proteins and other virulent products like serine-threonine kinases and protein phosphatases. An interesting fact is that three different retroviruses genomes have been found in the parasite, but it has only been speculated that these are for survival or pathogenicity (Leibowitz et al. 2017). Even though *Perkinsus marinus* invades a host's hepatocytes and erythrocytes similar to apicomplexans, Janouškovec et al. (2015) demonstrated through phylogenetic analysis that this species is much more closely related to dinoflagellates. It is important to note that this alveolate does not have a plastid like other dinoflagellates.

1.12 Objectives

The overall goal of my research is to characterize the life cycle of *Colpedella* species (ATCC 50594) in Hay medium. Morphological changes in trophozoite and cyst stages were investigated. The life cycle of *Colpodella* species (ATCC 50594) has not been investigated. Phylogenetic analysis of the Colpodellids shows that they are the

closest sister lineage to the Apicomplexa. *Colpodella* species vary in the morphological stages identified. Some species are ectoparasites on ciliates such as *C. gonderi* and *C. tetrahymenae.* Some species divide by longitudinal fission and some species do not encyst during the lifecycle. In order to understand how intracellular parasitism developed among the apicomplexans, the life cycle stages involved in myzocytosis, encystation and excystation in *Colpodella* species (ATCC 50594) need to be investigated. These types of studies have not been performed with *Colpodella* sp. ATCC 50594. The ATCC maintained *Colpodella* species is used as a model organism for phylogenetic and electron microscopic studies. The life cycle for many of the *Colpodella* species remains unclear and incomplete. The life cycle of the *Colpodella* sp. (ATCC 50594) has not been studied. Recent studies from our lab demonstrated that *Colpodella* sp. can be successfully cultured in Hay medium, with its prey, *Bodo caudatus* in a diprotist culture. In addition, new trichrome staining protocols developed in our lab facilitated differentiation of cyst stages from predator and prey. The culture conditions and staining techniques were used to grow cells and characterize the life cycle. The *Colpodella* species for the ATCC maintained culture is unknown. My hypothesis is that the ATCC maintained *Colpodella* sp. has life cycle stages representative of the known cyst forming *Colpodella* species.

The following objectives guided the proposed research:

Objective 1

The life cycle of *Colpodella* species (ATCC 50594) in a diprotist culture was investigated using light and confocal microscopy.

a. Time course experiments were performed to identify morphological stages present in culture during the life cycle.

b. Developmental stages were identified using light and confocal microcopy.

Objective 2

a. Transmission electron microscopy was performed to investigate the ultrastructure of *Colpodella* sp.

CHAPTER II

MATERIALS AND METHODS

2.1 Culturing

Colpodella species (ATCC 50594) were maintained in Hay medium as a diprotist culture. Hay medium was bacterized with *Enterobacter aerogenes* in tissue culture flasks as described (Sam-Yellowe and Yadavalli 2017). *Bodo caudatus* in the diprotist culture serves as prey for *Colpodella* species (ATCC 50594). Cultures were examined using an inverted microscope to observe different stages of trophozoites and cysts as described (Yadavalli and Sam-Yellowe 2017).

2.2 Fixation of Cells

Colpodella species in diprotist cultures were fixed using 5% formalin as described (Sam-Yellowe et al. 2019). Briefly, a viable diprotist culture was mixed with equal volume of 10% formalin directly in the culture flask and incubated for ten minutes at room temperature (Sam-Yellowe and Yadavalli 2018). The fixed cells were scraped gently with a cell scraper and the cells were transferred to a 50 mL centrifuge tube for centrifugation as described previously (Sam-Yellowe and Yadavalli 2018). Following centrifugation, the supernatant was discarded, and the pellets were resuspended in 1X dPBS and centrifuged. The dPBS supernatant was discarded, and the pellets were

resuspended in 100µl of PBS. Ten µl of cells was placed on glass slides to prepare smears. The slides were left to air dry at room temperature and then used for staining and immunofluorescent assays.

2.3 Staining

For light microscopy, formalin fixed cells were stained with Giemsa, Kinyoun's Carbol Fuchsin, and Sam-Yellowe's trichrome stains (Sam-Yellowe et al. 2019). Giemsa staining differentiates trophozoites of *Colpodella* species and *Bodo caudatus*. Sam-Yellowe's trichrome stains (Table 3) identify and differentiate *Colpodella* species and *B. caudatus* cysts and trophozoites (Sam-Yellowe et al. 2019). Staining was performed as described (Sam-Yellowe et al. 2019).

Table 3. Sam-Yellowe's Trichrome series for *Colpodella* sp. and *B. caudatus* cyst and trophozoite identification. This table was taken from *New trichrome stains identify cysts of Colpodella sp. (Apicomplexa) and Bodo caudatus* (Sam-Yellowe et al. 2019).

	Name	Staining Dyes and Incubation Conditions				
		1% Brilliant Green	1% Neutral Red	0.3% Methylene Blue	Safranin	Crystal Violet
Sam-Yellowe's Trichrome A	MBBGNRΔ	5 minutes	1 minute	1 minute	--	--
Sam-Yellowe's Trichrome B	MBBGNR#	2 minutes	3 minutes	30 seconds	--	--
Sam-Yellowe's Trichrome C	MBBGS	5 minutes	--	1 minute	1 minute	--
Sam-Yellowe's Trichrome D	CVBGNR	2 minutes	1 minute	--	--	30 seconds
Sam-Yellowe's Trichrome E	CVBGS	2 minutes	--	--	1 minute	30 seconds
Sam-Yellowe's Trichrome F	MBNRBG	2 minutes	3 minutes	30 seconds	--	--
***Abbreviations: BG→Brilliant Green, MB→Methylene Blue, NR→Neutral Red, S→Saffranin, CV→Crystal Violet**						

2.4 ImmunoFluorescence

Immunofluorescence (IFA) was performed on the diprotist culture fixed using 5% formalin. Formalin-fixed cells were permeabilized with 0.1% Triton X-100 then blocked with 3% BSA. After blocking, incubation occurred for 1h at room temperature (RT) with primary antibodies that bind to the antigen in a humid chamber. This incubation was followed by three washes with 1x dPBS and then the smears were incubated with species specific secondary antibody conjugated to an Alexa fluorophore, for 1h at RT in a humid chamber. Following three washes in 1x dPBS and one wash in distilled water, smears were mounted with fluoroshield containing DAPI (4', 6-diamidino-2-phenylindole) (Abcam) or Fluoromount-G (Southern Biotech, Birmingham, AL, USA). Some of the Alexa fluorophores used include Alexa 488 and Alexa 647. Antibodies specific to apical complex proteins were used to identify *Colpodella* sp. proteins as described (Sam-Yellowe et al. 2019). IFA slides from time course five were examined with normal rabbit serum (NRS) at 1:100 and 1:500 dilutions and normal mouse serum (NMS) at 1:100 dilution as negative controls. Antiserum 686 (Yang et al. 1996) was also used on these slides in the same dilutions. Other antibodies observed include: Anti-Py235 (Holder and Freeman 1981), Anti-plasmepsin II (Bonniec et al. 1999), EBA175 (Sim et al. 1990), AMA1 (Crewther et al. 1990), IMC3, IMC 3 FLR, and IMC7 (Goodenough et al. 2018; Anderson-White et al. 2007; Dubey et al. 2017). IFA slides were examined by confocal microscopy at the imaging core (Learner Research Institute, Cleveland Clinic, Cleveland, OH).

2.5 Time Course *of Colpodella Sp.* Development in Culture

In order to identify life cycle stages of Colpodella species in Hay medium culture, a time course analysis of *Colpodella* sp. development was performed (Table 3) with cells cultured in slide culture chambers and tissue culture flasks (Figure 3). Subculture of resting cyst stages of *Colpodella* sp. *and B. caudatus* was performed. The initial subculture of cells were collected at T=0 and then cells were collected every four hours for 36 hours (T= 1, T=2, T=3, T=4, T=5, T=6, T=7, T=8, and T=9). Encysted cultures were then collected 5 and 7 days after encystation to identify the morphology of the resting cyst stages. Time course five was performed to observe culture flasks when cells are most active in a forty-hour life cycle. Cells were collected for fixation every four hours up until twenty-two hours. At twenty-two hours cells were collected every hour until hour thirty. Then cells were collected for staining every two hours until forty hours. A final time course six was performed in culture flasks where cells were collected every twenty-four hours for eight days. The purpose of this experiment was to demonstrate the predominant cyst stage of *Colpodella* sp. in resting cultures. Day five and seven slides were observed for counting one hundred cysts on each slide to get a percentage of each *Colpodella* life cycle stage found in resting cultures. Cells collected at each time point were formalin-fixed for staining with Sam-Yellowe's trichrome staining and for IFA.

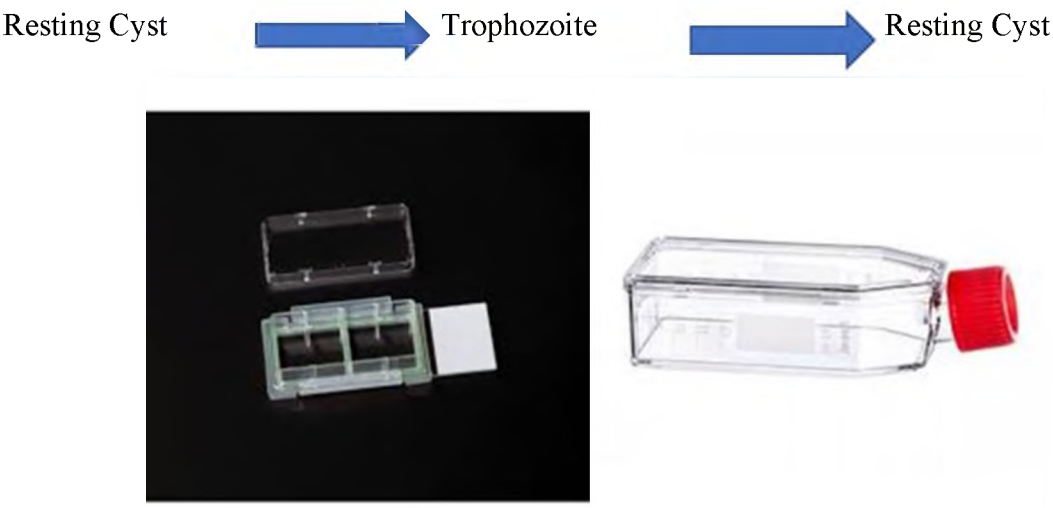

Figure 3. Images of slide culture chamber and culture flask which the time courses were performed from.

2.6 Electron Microscopy

An aliquot of *Colpodella* sp. in culture medium was added to an equal volume of 8 % paraformaldehyde in 0.1 M cacodylate buffer and spun down for 10 min at 3500 rpm. The cell pellet was fixed with 2.5 % glutarladehyde, 2 % paraformaldehyde in 0.1 M cacodylate buffer. The fixation continued in the same fixative solution for a total of 2 hours at room temperature. The pellets were thoroughly rinsed in 0.1 M cacodylate buffer, and then postfixed for 2 hours in an unbuffered 1:1 mixture of 2% osmium tetroxide and 3% potassium ferrocyanide. After rinsing with distilled water, the specimens were soaked overnight in an acidified solution of 0.25% uranyl acetate. After another rinse in distilled water, they were dehydrated in ascending concentrations of ethanol, passed through propylene oxide, and embedded in a EMbed 812 embedding media (Electron Microscopy Sciences, PA). Thin sections (70nm) were cut on a RMC MT6000-XL ultramicrotome. These were mounted on T-300 mesh nickel grids (Electron Microscopy Sciences, PA) and then sequentially stained with acidified methanolic uranyl

acetate and stable lead staining solution. These were coated on a Denton DV-401 carbon coater (Denton Vacuum LLC, NJ), and observed in a FEI Tecnai Spirit (T12) transmission electron microscope with a Gatan US4000 4kx4k CCD.

CHAPTER III

RESULTS

3.1 General Staining

Three staining protocols were used to stain formalin-fixed cells of *Colpodella* sp. Giemsa, Kinyoun's Carbol Fuchsin, and Sam-Yellowe's trichrome stains. Sam-Yellowe's trichrome stain was used to visualize different stages of the *Colpodella* sp. life cycle. Two major life cycle stages occur in *Colpodella*, which are cysts and trophozoites. The trophozoites have two heterodynamic flagella and the cysts are non-motile. In their motile stage *Colpodella* sp. form an attachment to their prey *Bodo caudatus* in the process of myzocytosis, shown in the Giemsa-stained image in Figure 4 and with Kinyoun's stain in Figure 5. During myzocytosis the predator aspirates the cytoplasmic contents out of its prey and into their food vacuole. There can be two or more predators attached to a single prey (Figure 5). *Colpodella* sp. cysts can be differentiated from cysts of the prey using Sam-Yellowe's trichrome stain. Early *Colpodella* sp. cysts have a demilune appearance that looks like a half-moon when using the Sam-Yellowe's trichrome stain (Figure 6 and 7). Mature *Colpodella* sp. cysts stain a red-blue color and can have asymmetric or symmetric number of juvenile trophozoites (Figure 6, arrow, and Figure 8) while *B. caudatus* cysts are pink. Figure 9 shows a predator and pair in myzocytosis with the prey

almost completely aspirated. Trophozoites that have egressed from cysts and showing incomplete cytokinesis are shown in panels A-C of Figure 10. Following myzocytosis, the food vacuole formed in *Colpodella* sp. becomes the cyst. Figure 11 shows the precyst stage with the enlarged food vacuole and disintegrating anterior end of the trophozoite. Multiple prey can attach to one prey at time for feeding in the process of myzocytosis. In the image show, as many as six predators can be seen attached to one prey (Figure 12, panels A and B).

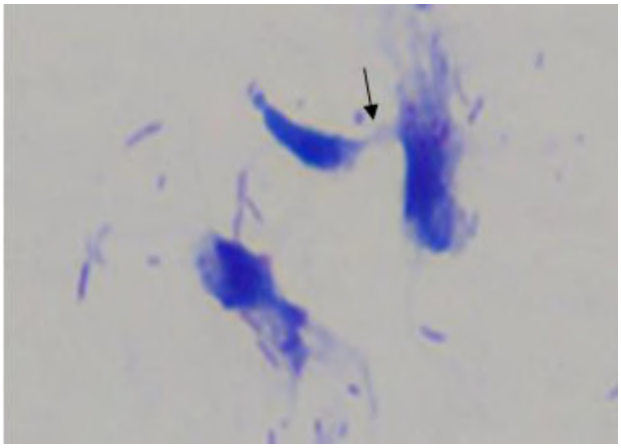

Figure 4. Giemsa stain image of myzocytosis (arrow) between a *B. caudatus* and *Colpodella* sp. trophozoite.

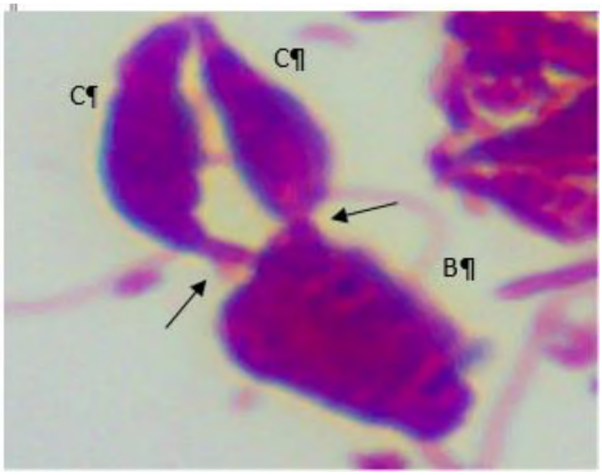

Figure 5. Kinyoun's Carbol Fuchsin stain of multiple *Colpodella* sp. tethered onto one *Bodo caudatus* trophozoite (arrows). The flagella of the trophozoites can be visualized.

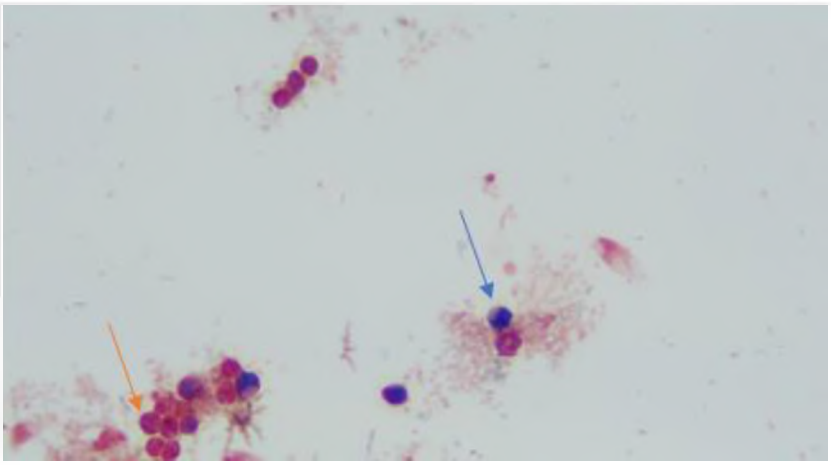

Figure 6. Sam-Yellowe's trichrome differentiating the *Colpodella* sp. (blue arrow) and *Bodo caudatus* cysts (orange arrow). The *Colpodella* sp. cysts appear purple and can have a demilune or multiple nuclei depending on maturity. *Bodo caudatus* cysts are pink.

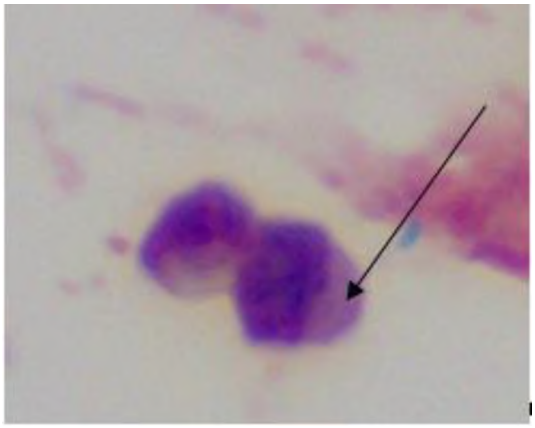

Figure 7. A *Colpodella* sp. early cyst stained with Sam-Yellowe's trichrome showing the characteristic demilune pattern with the cysts partially stained blue and white (arrow).

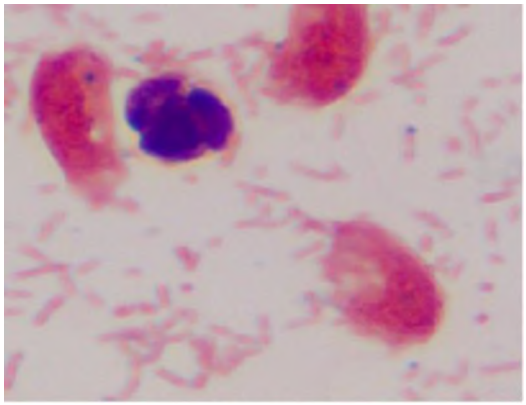

Figure 8. Mature *Colpodella* sp. three nuclei surrounded by three *B. caudatus* trophozoites using Sam-Yellowe's trichrome.

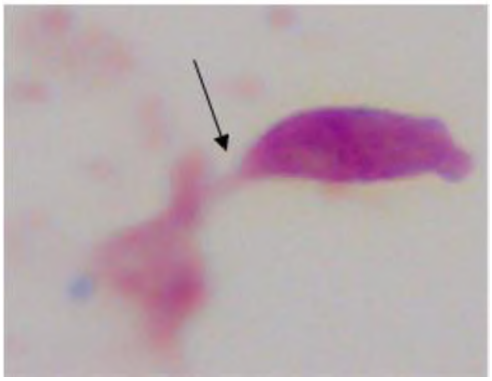

Figure 9. A single attachment (arrow) between a *Bodo caudatus and Colpodella* sp. trophozoite in myzocytosis stained with Sam-Yellowe's trichrome stain.

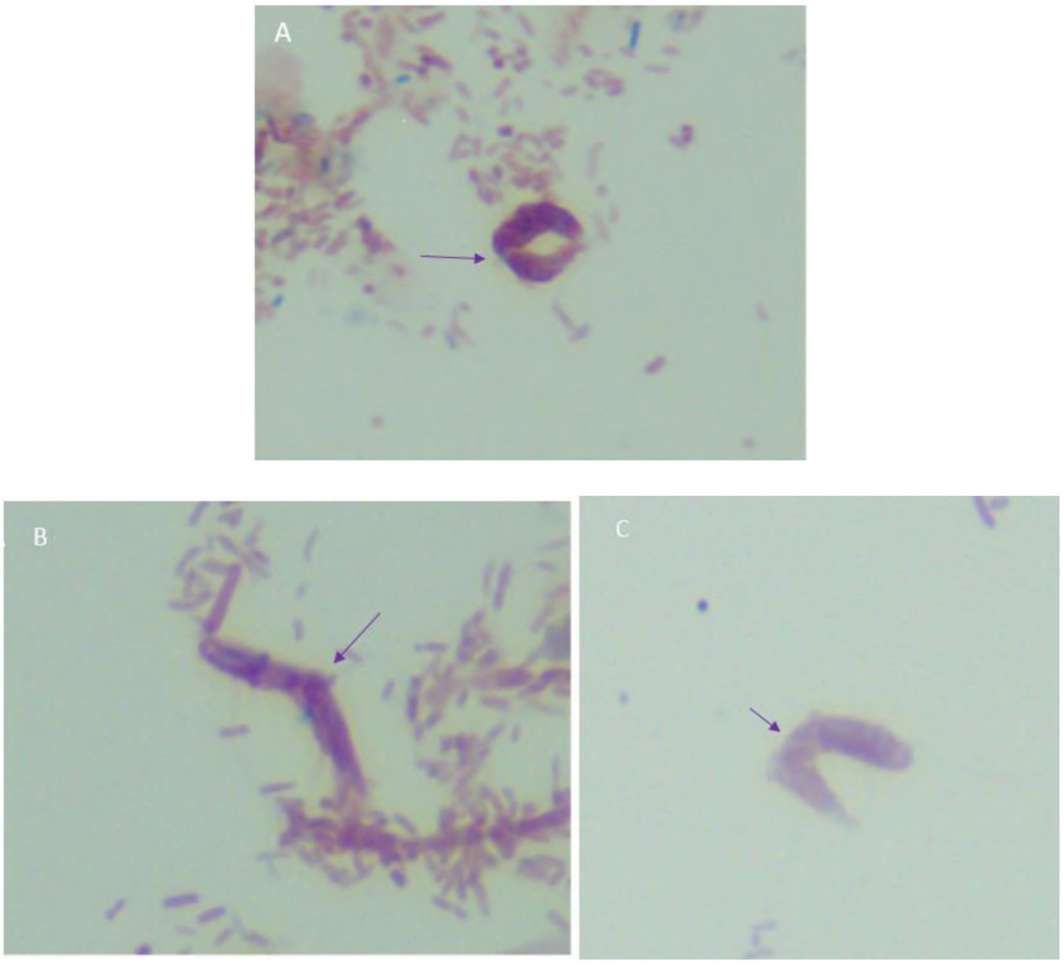

Figure 10 (A-C). Two immature *Colpodella* sp. trophozoites that have egressed from a cyst but have not completed cytokinesis (arrows). Cells were stained using Sam-Yellowe's trichrome stain.

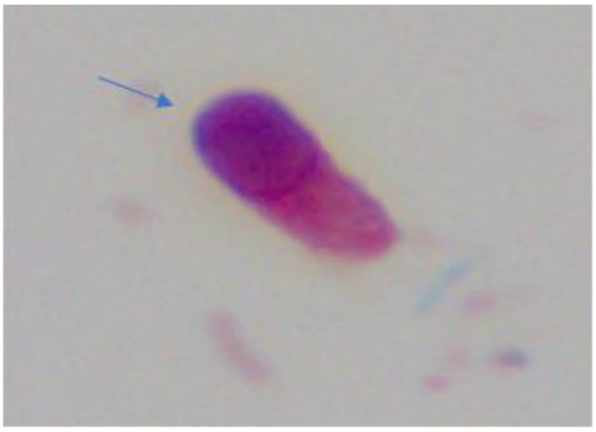

Figure 11. Sam-Yellowe's trichrome stain showing a *Colpodella* sp. precyst formed after myzocytosis and enlargement of the food vacuole (arrow). The anterior portion of the trophozoite disintegrates.

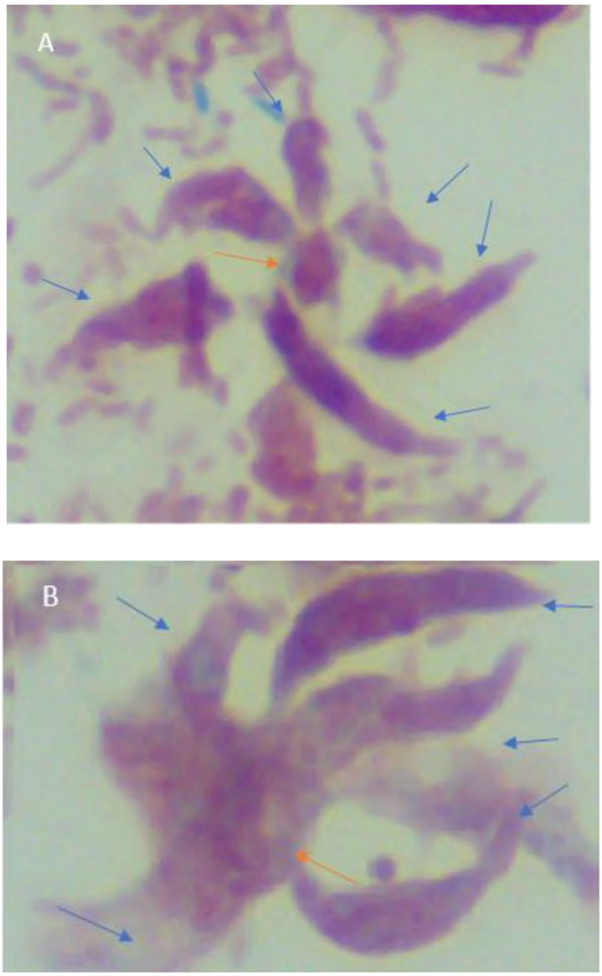

Figure 12 (panels A and B). Sam-Yellowe's trichrome stain showing multiple *Colpodella* sp. attacks on one *B. caudatus* prey. Orange arrows, *B. caudatus*. Blue arrows, *Colpodella* sp. trophozoites.

3.2 Time course Staining Using Sam-Yellowe's Trichrome

Time course experiments were performed to determine at what time point each life cycle stage occurred and to identify the predominant cyst stage during the resting stage of the life cycle. Six time course experiments were performed. The first four time courses were performed to observe the development of *Colpodella* sp. trophozoite and cyst stages (Figure 13 and Table 4). These time courses lasted thirty-six hours and cells were formalin-fixed for staining every 4 hours. At zero hours after subculture all that could be seen were a few *B. caudatus* and *Colpodella* sp. cysts (Figure 13 A i and ii). At four hours there were a few *Colpodella* sp. mature cysts, but there were many more *B. caudatus* cysts and trophozoites (Figure 13 B i and ii) which stain pink with Sam-Yelowe's trichrome stain. At 8 hours, more *B. caudatus* trophozoites were observed (Figure 13 C i and ii). At 12 hours *B. caudatus* trophozoites and mature *Colpodella* sp. cysts were observed with multiple nuclei (Figure 13 D i, *B. caudatus* and ii, *Colpodella* sp). At 16 hours (Figure 13 E, *Colpodella* sp. cysts (i) and *Colpodella* sp. trophozoites and *B. caudatus* in myzocytosis (ii) were observed. Precyct stages of *Colpodella* sp. were observed at 20 hours (Figure 13 F, i) along with mature *Colpodella* sp. cysts (Figure 13 F, ii). At 24 hours most *Colpodella* sp. trophozoites observed were in myzocytosis with *B. caudatus*, representing the most active time point of the life cycle (Figure 13 G i and ii). The arrows indicate the tubular tether formed between predator and prey. Cells in myzocytosis were still observed at 28 hours (Figure 13 H, i), along with encystation of *Colpodella* sp. (Figure 13 H, ii). At 32 hours, precyst stages of *Colpodella* sp. were observed (Figure 13 I, i and ii). Young trophozoites of *Colpodella* sp. (Figure 13 J, i) and *Colpodella* sp. cysts (Figure 13 J, ii) were observed at 36 hours

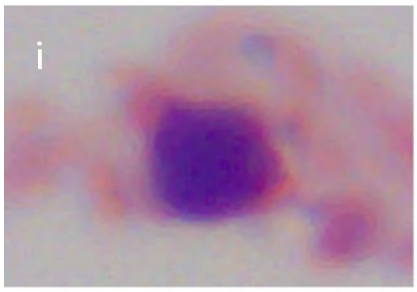

A

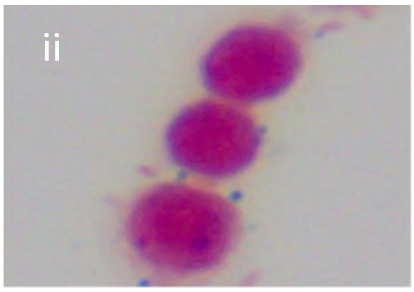

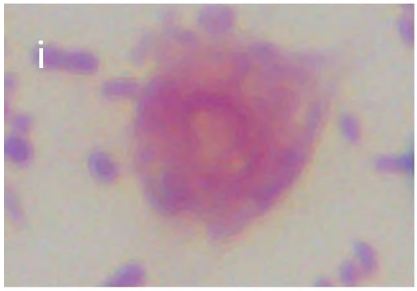

B

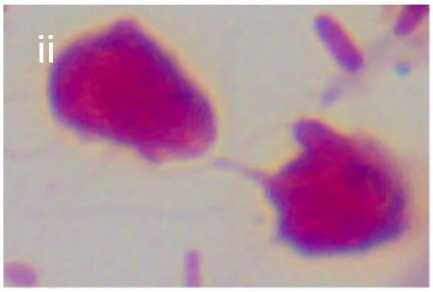

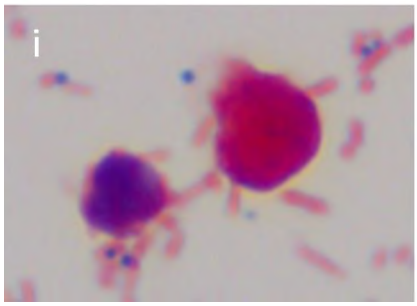

C

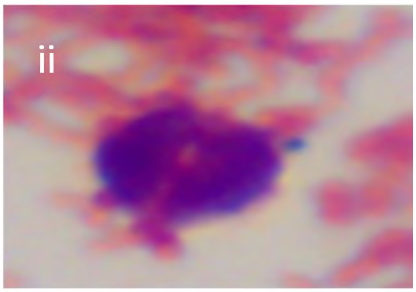

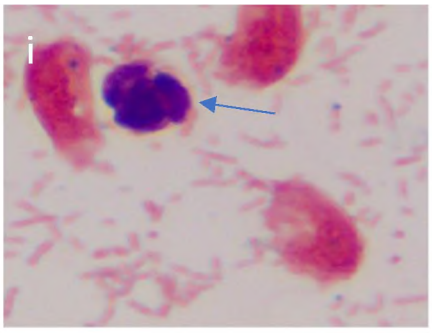

D

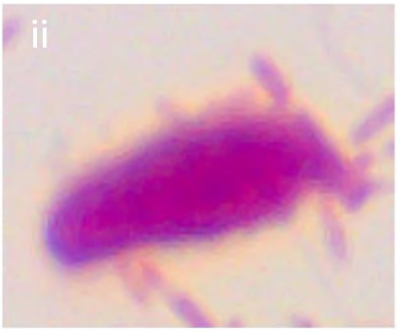

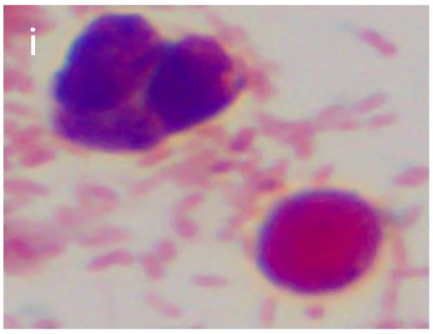

E

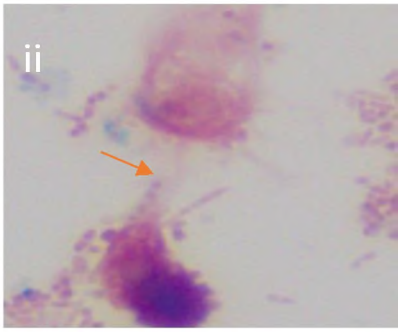

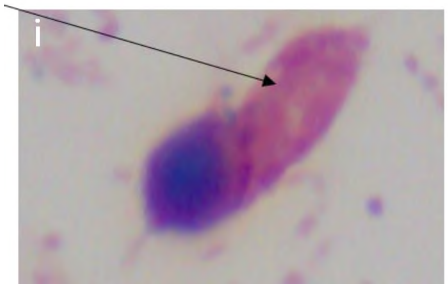

F

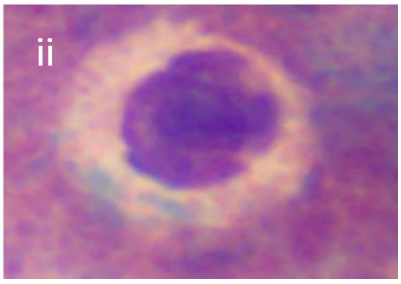

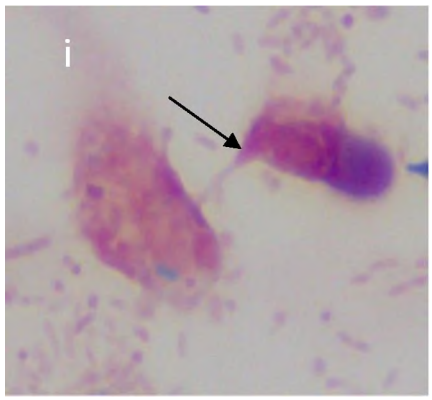

G

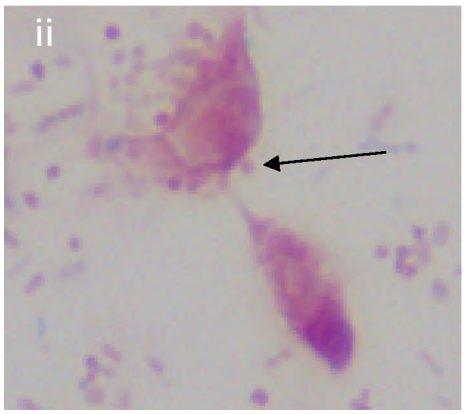

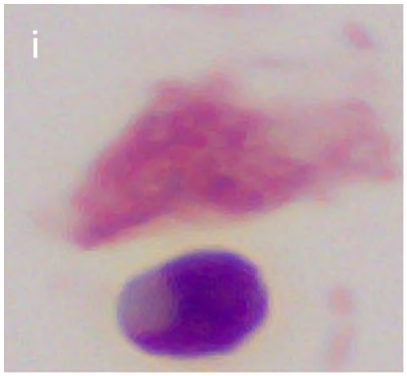

H

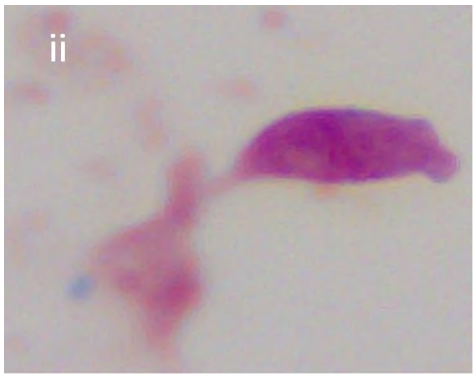

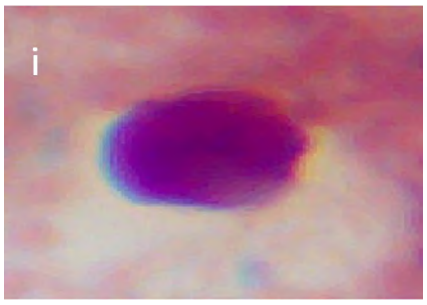

I

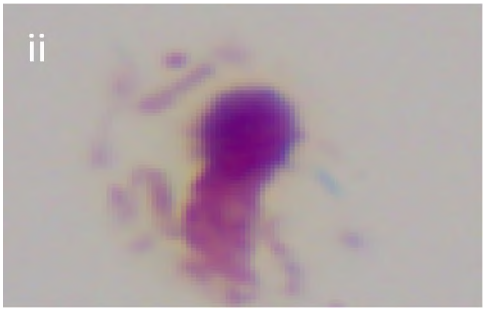

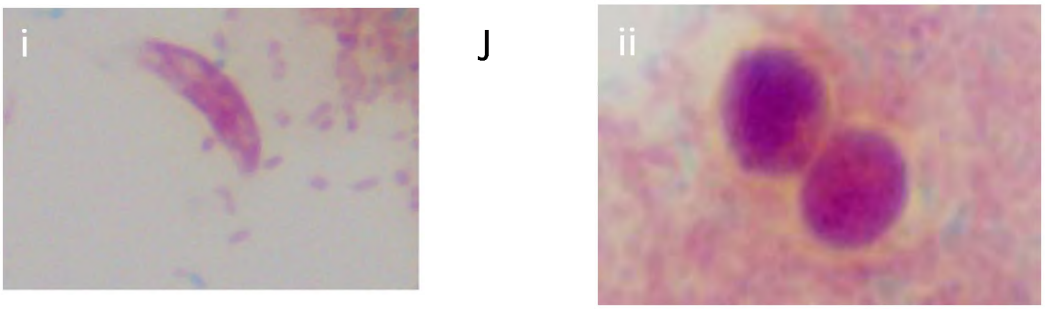

Figure 13. Representative life cycle stages of *Colpodella* sp. observed during a 36-hour time course experiment performed four times. Sam-Yellowe's Trichrome A stain was used for staining formalin-fixed cells. A. The culture at 0 hours with only cysts, both *Colpodella* sp. and *B. caudatus* cysts used for subculture. B, i and ii. At 4 hours when *B. caudatus* trophozoites have started to excyst. C, i and ii. At 8 hours, immature and mature *Colpodella* sp. cysts can be seen. D. *B. caudatus* (i) and *Colpodella* sp. cysts (ii). At 12 hours, *B. caudatus* trophozoites are active and *Colpodella* sp. cysts are maturing with a few early trophozoites egressing. E. At 16 hours, *Colpodella* sp. cysts (i) and *Colpodella* sp. attached to *B. caudatus* (ii) were observed (arrow). F. At 20 hours, *Colpodella* sp. precyst (i) and mature cyst (ii) were observed. The arrow points to the disintegrating anterior end of the trophozoite (arrow). G. i and ii. At 24 hours, the culture is most active with myzocytosis observed (arrows). *Colpodella* sp. trophozoites have egressed and myzocytosis is occurring. The tubular tethers attaching *Colpodella* sp. to the prey *B. caudatus* is indicated by the arrows. H. At 28 hours, *Colpodella* sp. cysts were observed (i) and cells in myzocytosis were also observed (arrow) (ii). I. i and ii. At 32 hours *Colpodella* sp. are starting to encyst by forming precysts where the anterior end disintegrates. J. At 36 hours, *Colpodella* sp. have mostly encysted into mature cysts. Transient *Colpodella* sp. cysts are still encysting (arrow) and young trophozoites (i) were observed along with cysts (ii).

Table 4. Time Course 1-4 observations and description of the life cycle stages and corresponding time points for each stage.

Time Point	Description
T0= 0 hours	Had a few *B. caudatus* cysts and young *Colpodella* sp. cysts
T1= 4 hours	A few *B. caudatus* trophozoites
T2= 8 hours	A little more *B. caudatus* trophozoites
T3= 12 hours	Many *B. caudatus* trophozoites
T4= 16 hours	Lots of *B. caudatus* trophozoites
T5= 20 hours	Many *B. caudatus* and a few *Colpodella* sp. trophozoites
T6= 24 hours	More *Colpodella* sp. trophozoites and first attachments
T7= 28 hours	*Colpodella* sp. display very long attachments and *B. caudatus* cysts starting to form, both species have many trophozoites
T8= 32 hours	Some attachments and more *B. caudatus* cysts forming, both species have many trophozoites
T9= 36 hours	Many *B. caudatus* cyst, *Colpodella* sp. are fewer in number
T10= 5 days	Saw *B. caudatus* cysts
T11= 10 days	Many *B. caudauts* cysts

3.3 Time Course 5 StainingUsing Sam-Yellowe's Trichrome

Time course five was performed to understand life cycle stage differentiation at the most active stages of the *Colpodella* sp. life cycle. The time course experiment lasted for

forty hours. Cells were formalin-fixed and stained every four hours till twenty-two hours. Between twenty-two and twenty-eight hours, cells were collected and formalin-fixed every hour. After twenty-eight hours, cells were collected every two hours till forty hours. Representative life cycle stages observed, and description of stages are shown in Figure 14 a nd Table 5. Cells were found to be most active during the twenty-two to thirty-hour time points. Multiple myzocytosis attachments were observed. Early and mature cysts were also seen as *Colpodella* sp. encysted. Precycts of *Colpodella* sp. were observed at 24 hours (Figure 14 A i and ii). Cells in myzocytosis Figure 14 B, i and a three-way cyst containing 3 juvenile trophozoites (Figure 14 B, ii) were observed at 25 hours. Demilune cysts of *Colpodella* sp. and cells attached in myzocytosis were observed at 26 hours as shown in Figure 14 C, i and ii, respectively. In these active stages of the life cycle, *Colpodella* sp. and *B. caudatus* trophozoites were observed attached in myzocytosis at 27 hours (Figure 14 D, i and ii). Demilune cysts of *Colpodella* sp. and cells in myzocytosis were observed at 28 hours (Figure 14 E, i and ii, respectively. At 29 hours encystment for both *Colpodella* sp. and *B caudatus* was observed. Figure 14 F shows a demilune cyst (i) and a mature cyst (ii) of *Colpodella* sp. At 30 hours precyst stages of *Colpodella* sp. were observed (Figure 14, i and ii). By 38 hours more mature cysts of *Colpodella* sp. were observed (Figure 14 H, i and ii). Among the mature cysts observed for *B. caudatus* and *Colpodella* sp. young *Colpodella* sp. trophozoites were also observed at the later stages of the life cycle (Figure 14 I, i).

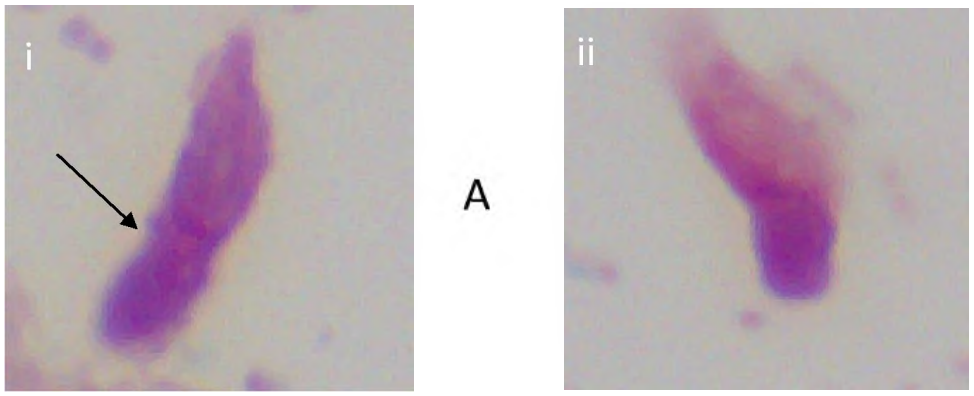
i
A
ii

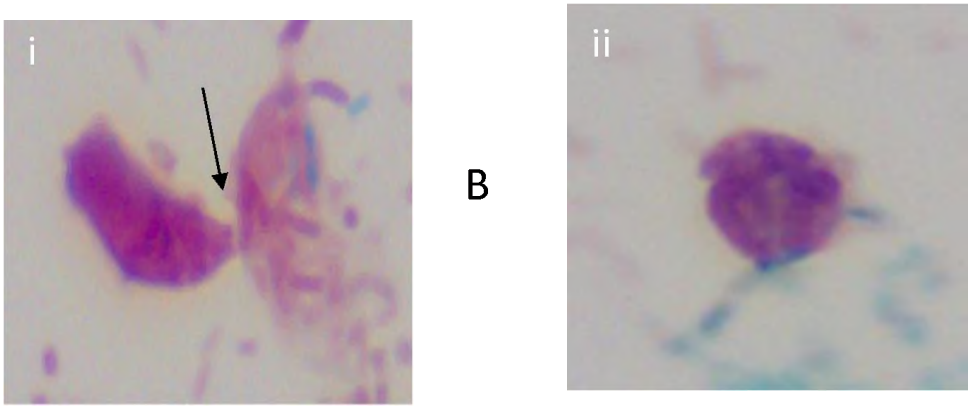
i
B
ii

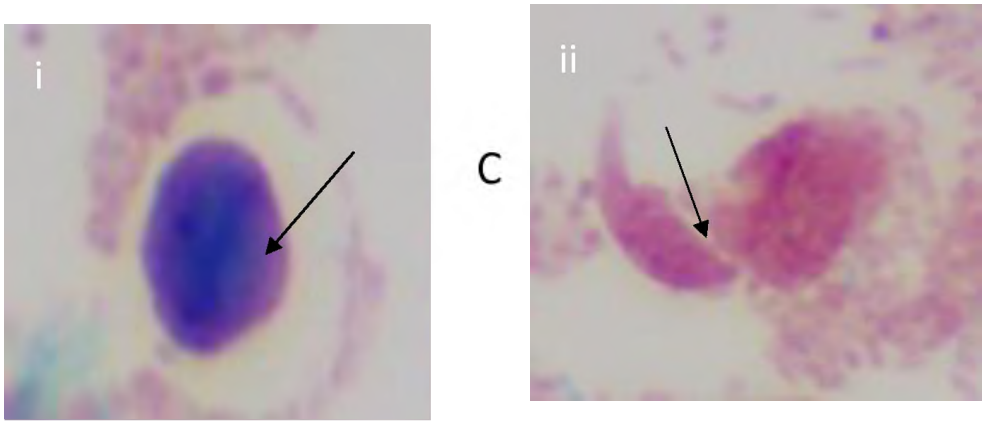
i
C
ii

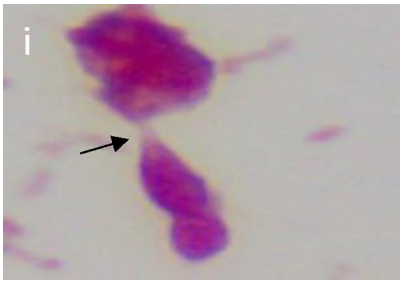

D

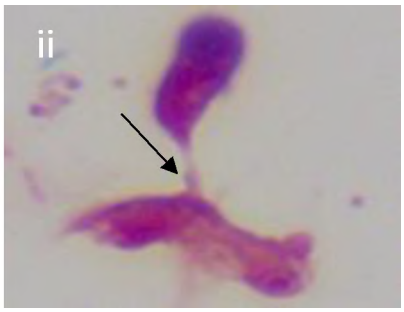

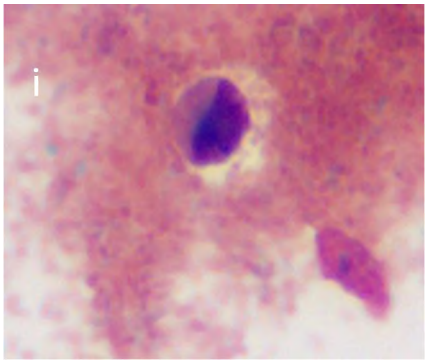

E

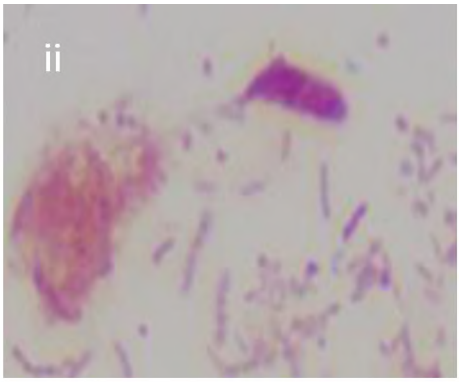

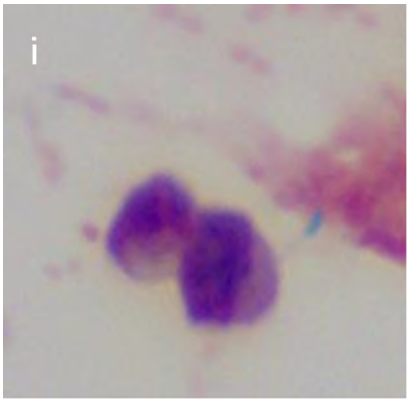

F

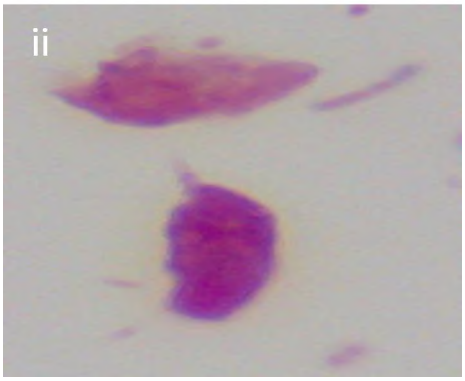

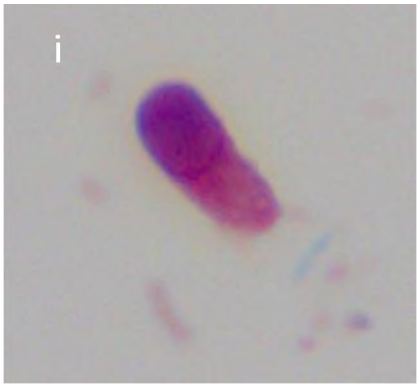

G

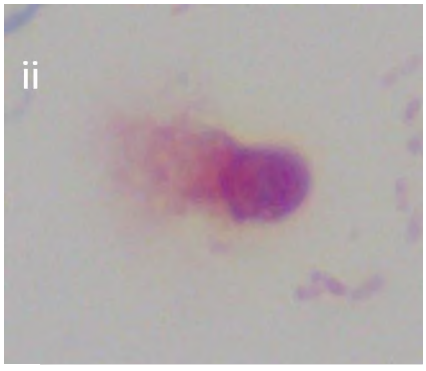

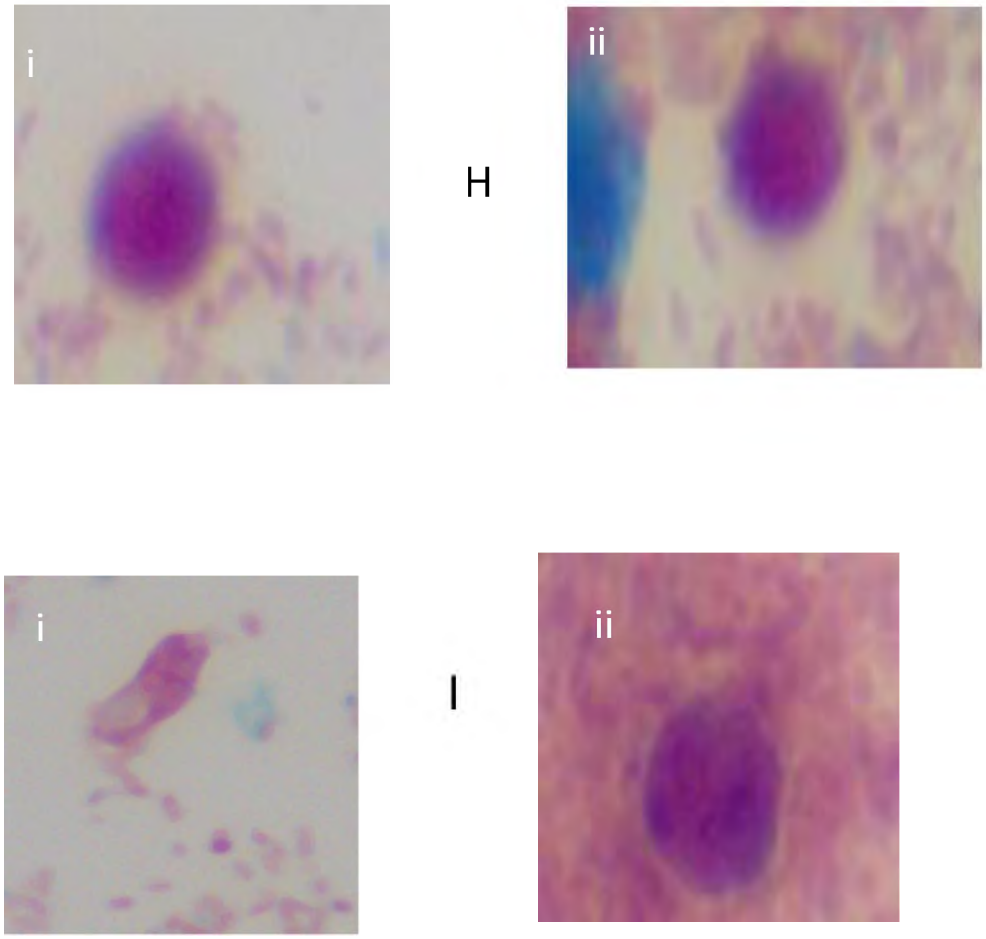

Figure 14. Representative life cycle stages of *Colpodella* sp. observed during a 40-hour time course experiment. Sam-Yellowe's Trichrome stain A was used for staining formalin-fixed cells. A, i and ii, at 24 hours, precyst stages of *Colpodella* sp. were observed (arrow). B, i (cells in myzocytosis) (arrow) and ii, three-way cyst of *Colpodella* sp. observed at 25 hours. C, i (demilune cyst of *Colpodella* sp.) (arrow) and ii (*Colpodella* sp. and *B. caudatus* trophozoites in myzocytosis) observed at 26 hours (arrow). D. i and ii show cells in myzocytosis (arrows). E. shows a demilune cyst of *Colpodella* sp. (i) and *Colpodella* sp. in myzocytosis with *B. caudatus* (arrow) (ii) at 28 hours. F. At 29 hours, a demilune (i) and mature cyst (ii) of *Colpodella* sp. were observed. G. i and ii, precyst stages of *Colpodella* sp. were observed at 30 hours. The precyst stages are shown with the anterior end disintegrating and fraying as the cyst is formed after feeding from the food vacuole. H. 38 hours, mature cysts of *Colpodella* sp. (i and ii) were observed. I. At 40 hours, mature cysts of *Colpodella* sp. (i) and trophozoites (ii) were observed.

Table 5. Time Course 1-4 observations and description of the life cycle stages and corresponding time points for each stage.

Time Point	Description
T0= 0 hours	Had a few *Bodo caudatus* cysts * (Need more sample)
T1= 4 hours	A few *Bodo caudatus* trophozoites and cysts
T2= 8 hours	A little more *B. caudatus* trophozoites
T3= 12 hours	More *B. caudatus* trophozoites and *Colpodella* sp. mature cyst
T4= 16 hours	Lots of *B. caudatus* trophozoites and first attachment, Saw *Colpodella* sp. early and late cyst
T5= 20 hours	Many *B. caudatus* trophozoites and *Colpodella* sp. late cysts
T6= 22 hours	Lots of *B. caudatus* trophozoites and some *Colpodella* sp. trophozoites, saw both early and mature cysts
T7= 24 hours	*B. caudatus* trophozoites *and Colpodella* sp. attachments, early *Colpodella* sp. cyst (2), mature *Colpodella* sp. cyst (4)
T8= 25 hours	*B. caudatus* trophozoites, many attachments, and saw a few *Colpodella* sp. early cysts
T9= 26 hours	*B. caudatus* trophozoites and *Colpodella* sp. attachments, many early *Colpodella* sp. cysts, *B. caudatus* start encysting
T10= 27 hours	*B. caudatus* trophozoites and cysts, some *Colpodella* sp. trophozoites with attachments, seeing *Colpodella* sp. encyst and early cysts
T11= 28 hours	*B. caudatus* trophozoites and cysts, *Colpodella* sp. trophozoites and attachments, Most mature *Colpodella* sp. cysts
T12= 29 hours	*B. caudatus* trophozoites and cysts, *Colpodella* sp. trophozoites and early cysts
T13= 30 hours	More *B. caudatus* cysts than trophozoites, many *Colpodella* sp. attachments and saw some early cysts
T14= 32 hours	*B. caudatus* cysts and trophozoites, *Colpodella* sp. trophozoites with a few attachments, a few early and late cysts
T15= 34 hours	*B. caudatus* cysts with a few trophozoites, one *Colpodella sp*. attachment, saw early *Colpodella* sp. cyst
T16= 36 hours	*B. caudatus* cysts and a few *Colpodella* sp. trophozoites
T17= 38 hours	*B. caudatus* cysts, saw a few *Colpodella* sp. trophozoites and mature cysts
T18= 40 hours	*B. caudatus* cysts
T19= 5 days	A few *B. caudatus* cysts, saw *Colpodella* sp. mature cyst
T20= 7 days	A few *B. caudatus* cysts

3.4 Time Course 6 Using Sam-Yellowe's Trichrome

Time course six was performed to identify the predominant *Colpodella* cyst stage in a resting culture. Cells were formalin-fixed for staining every twenty-four hours for eight days. In a second experiment day five and seven resting cultures were pooled and formalin-fixed for trichrome staining. The results show that the predominant *Colpodella* sp. life cycle stage in resting cultures for eight days were mature cysts with a single nucleus. Other mature cysts were observed with two or more nuclei and some demilune cysts were observed as well (Figure 15, panels A-H i and ii; Table 6). To determine the percentage of different cyst stages, cysts from the pooled day five and seven cultures were counted. One hundred cysts were counted on duplicate slides from cysts stained from day 5 and 7 cultures. Eighty five percent of the cysts were mature cysts on day 5 and 93% on day 7 (Table 7). A few *Colpodella* sp. *and B. caudatus* trophozoites excysted during these time points.

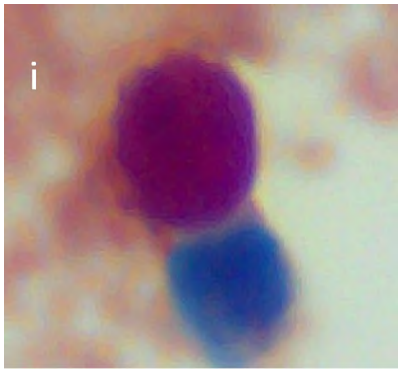

A

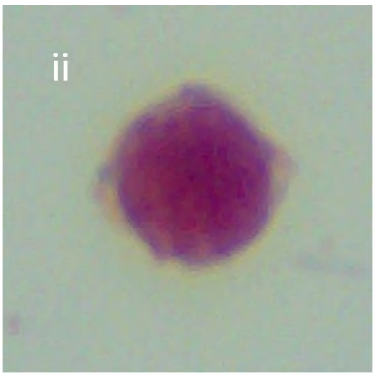

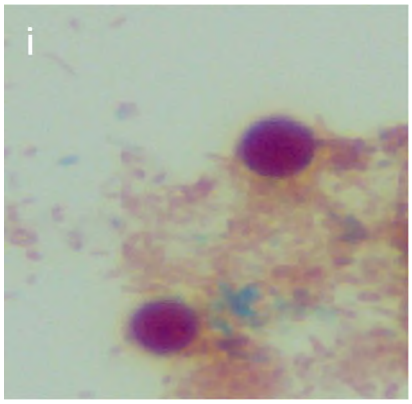

B

C

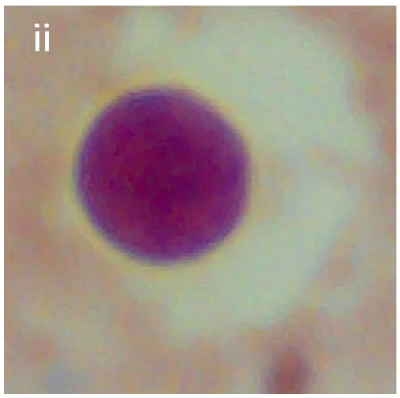

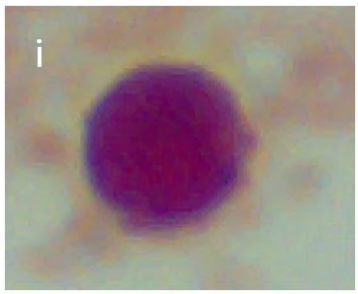

D

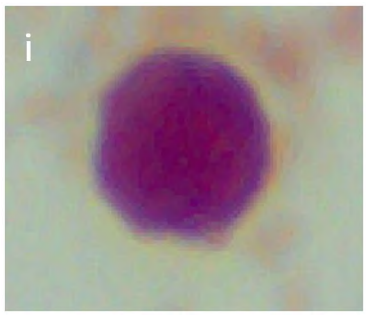

E

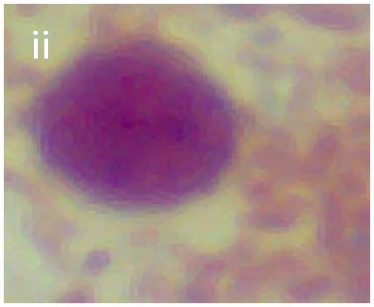

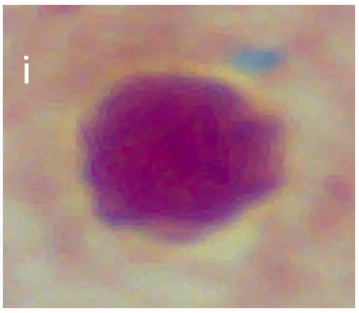

F

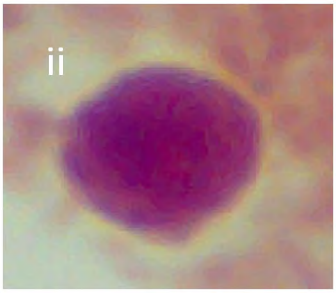

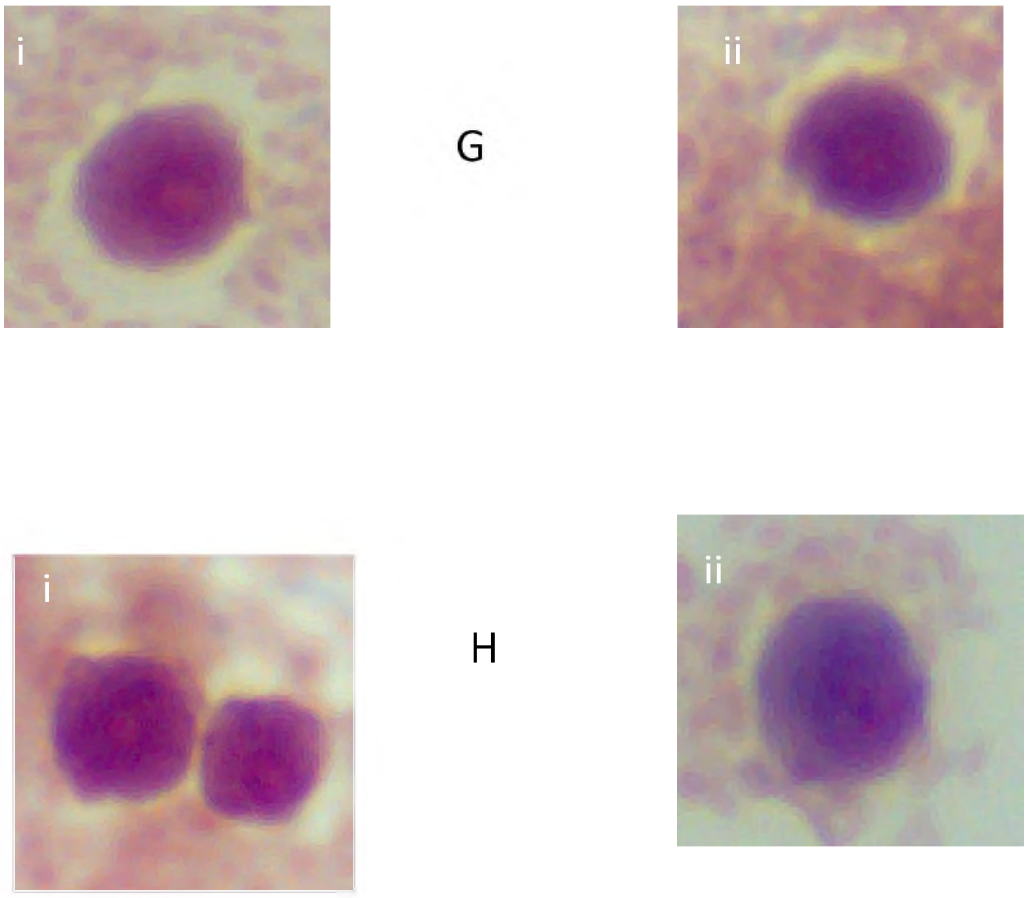

Figure 15. Figures representative of the predominant mature *Colpodella* sp. cyst stage in resting cultures from time course six. Diprotist cultures are asynchronous. A. Day 1, two mature *Colpodella* sp. cysts with one nucleus. B. Day 2, *Colpodella* sp. mature cysts. C. Day 3, *Colpodella* sp. mature cysts. D. Day 4, Predominant mature *Colpodella* sp. cysts. E. Day 5, *Colpodella* sp. mature cysts, F. Day 6, Shown are two *Colpodella* sp. mature cysts with one nucleus. G. Day 7, *Colpodella* sp. mature cyst and *Colpodella* sp. early cyst indicated by the demilune. H. Day 8, *Colpodella* sp. mature cysts.

Table 6. Time course 6 observations in resting culture after initial activity of the first 24 hours. *Colpodella* sp. mature cysts that had one nucleus were the most common.

Time point	Description
T0= Active Cells, 24 hours	Both *B. caudatus* and *Colpodella* sp. trophozoites were observed.
T1= 2 days	*Colpodella* sp. and *B. caudatus* cysts were identified. *Colpodella* sp. mature cysts with a single nucleus predominated the culture.
T2= 3 days	*Colpodella* sp. and *B. caudatus* cysts were identified. *Colpodella* sp. mature cysts with a single nucleus predominated the culture.
T3= 4 days	*Colpodella* sp. and *B. caudatus* cysts were identified. *Colpodella* sp. mature cysts with a single nucleus predominated the culture.
T4= 5 days	*Colpodella* sp. and *B. caudatus* cysts were identified. *Colpodella* sp. mature cysts with a single nucleus predominated the culture.
T5= 6 days	*Colpodella* sp. and *B. caudatus* cysts were identified. *Colpodella* sp. mature cysts with a single nucleus predominated the culture.
T6= 7 days	*Colpodella* sp. and *B. caudatus* cysts were identified. *Colpodella* sp. mature cysts with a single nucleus predominated the culture.
T7= 8 days	*Colpodella* sp. and *B. caudatus* cysts were identified. *Colpodella* sp. mature cysts with a single nucleus predominated the culture.

Table 7. Pooled *Colpodella* sp. cysts counted from day five and seven cultures. Cysts were counted to one hundred twice for each day for a total of four hundred. *Colpodella* sp. mature cysts are the predominant life cycle stage in resting cultures. The average of both cyst stages were accounted for in each day.

Day & Slide #	Early Cyst	Mature Cyst	*Colpodella* trophozoite	*Bodo* trophozoite	*Colpodella* Precyst
Day 5 #1	19	81	0	1	2
Day 5 #2	12	88	0	0	1
Day 5 Avg.	15	85	0	1	2
Day 7 #1	6	94	1	0	0
Day 7 #2	9	91	0	2	1
Day 7 Avg.	7	93	1	1	1

3.5 Immunofluorescence of *Colpodella* sp. in Diprotist Culture using Antiserum 686

Indirect Immunofluorescence was performed with cells in diprotist culture. The antibody against *P. falciparum* rhoptry protein, RhopH3 was used to identify life cycle stages in the diprotist culture that were cross reactive with the antibodies. Background reactivity was obtained with *B. caudatus* cysts (Figure 16A). *Colpodella* sp. in myzocytosis with *B. caudatus* showed intense antibody reactivity with antiserum 686. Reactivity was also seen in the tubular tether and weakly in the *B. caudatus* prey (Figure 16 B and C). The negative control NRS was not reactive with *Colpodella* sp. and *B. caudatus* stages (Figure 16 D).

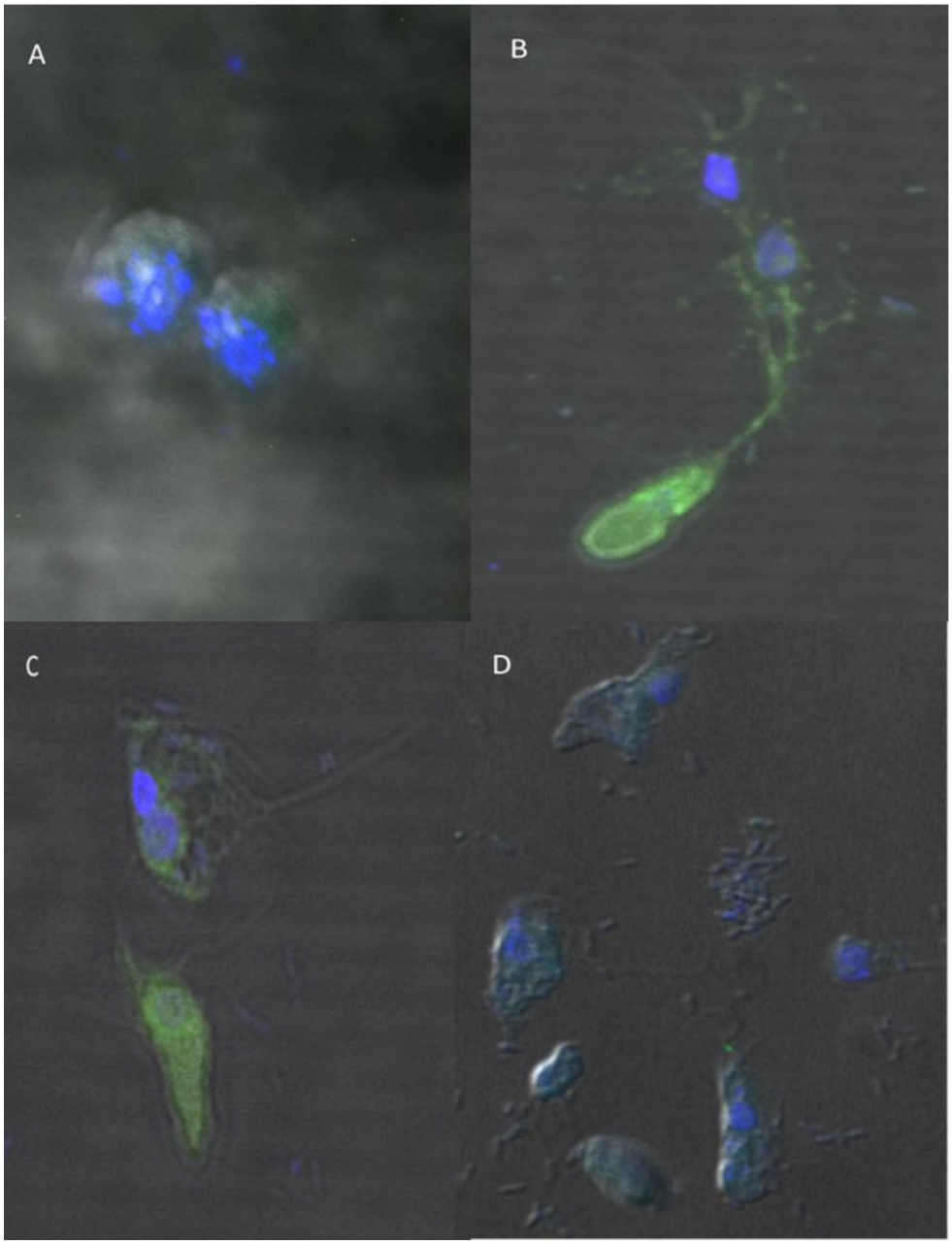

Figure 16. Immunofluorescence microscopy of diprotist culture using antiserum 686 specific for *P. falciparum* rhoptry protein, RhopH3. A. *B. caudatus* cysts showing no cross reactivity with the antiserum. B. Antiserum 686 cross reacted with *Colpodella* sp. proteins in the cytoplasm and in the tubular tether used for attachment with the prey. C. *Colpodella* sp. trophozoite is shown in myzocytosis with *B. caudatus*. Antiserum 686 cross reacted with proteins in the cytoplasm of *Colpodella* sp. Both *Colpodella* sp. and *B. caudatus* are in myzocytosis with cross reactivity displayed in the tether in the section closest to the predator. D. Normal rabbit serum (NRS) negative control with no reactivity with *B. caudatus* and *Colpodella sp.* trophozoites and *Colpodella* sp. precysts. DAPI staining shows the nucleus and kinetoplast in *B. caudatus* and the nucleus in *Colpodella sp.*

3.6 Immunofluorescence of *Colpodella* sp. in Time Course Experiments

Immunofluorescence was performed on life cycle stages in the time course experiments to identify stages that would cross react with the RhopH3 specific antibody. Normal rabbit serum was used as a negative control serum. The results show that *Colpodella* sp. and some *B. caudatus* trophozoites and cysts cross reacted with antiserum 686. DAPI shows the nucleus of each protist and the kinetoplast made up of mitochondrial DNA can only be seen in *B. caudatus.* Through DAPI staining nuclear contents from *B. caudatus* being aspirated into the food vacuole of *Colpodella* sp. during myzocytosis were also visualized. The number of nuclei in mature cysts of *Colpodella* sp. stained with DAPI could be counted. Differential interference contrast microscopy allowed the morphology of life cycle stages to be identified, as well as revealing their flagella. *Bodo caudatus* cysts in diprotist culture at 18 hours were not reactive with antiserum 686 (Figure 17). *Colpodella* sp. precysts and *B. caudatus* trophozoites were also not reactive with antibody at 20 hours (Figure 18 and 19). Only background staining was observed. At 22 hours, similarly no reactivity was obtained with *Colpodella* sp. precyst and *B. caudatus* trophozoites (Figure 20 and 21).

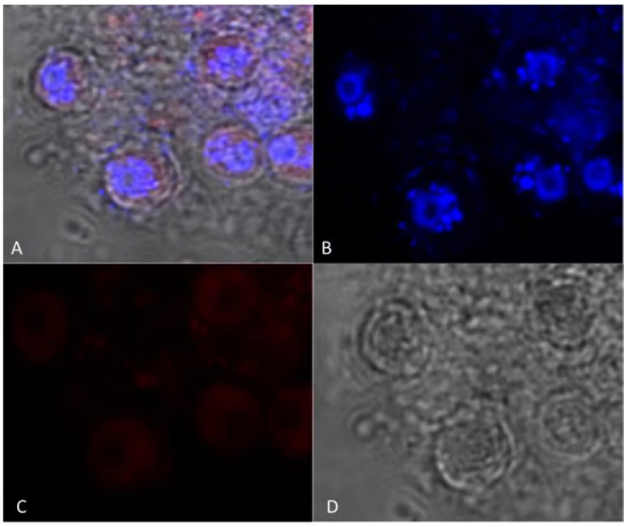

Figure 17. IFA of formalin-fixed cells in diprotist culture at time point four (18 hours). Antiserum 686 1:100 was used in IFA. A. Merged image of five *B. caudatus* cysts showing DAPI, DIC, and antibody reactivity. The ring nuclei are characteristic of DAPI stained *B. caudatus*. B. DAPI stained nuclei. C. Background reactivity was observed with the cysts. D. Differential interference contrast (DIC) image reveals the cyst morphology.

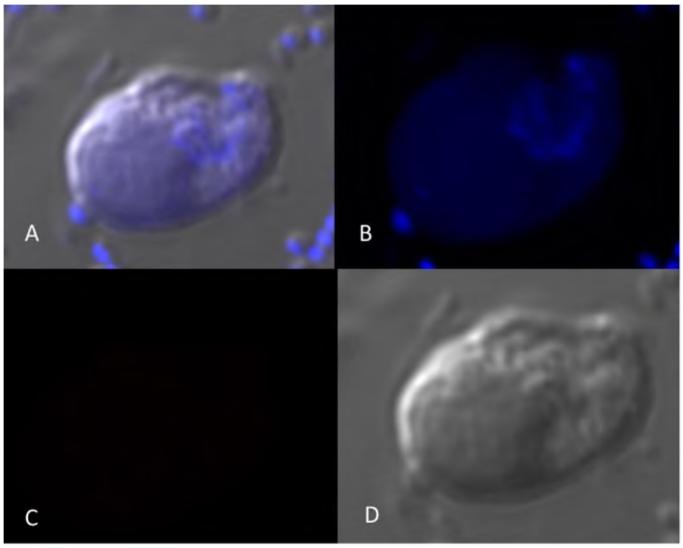

Figure 18. IFA of formalin-fixed cells in diprotist culture at time point five (20 hours). Antiserum 686 1:100 was used in IFA. Antiserum 686 did not cross react with *Colpodella* sp. proteins in the precyst. A. A *Colpodella* precyst captured with merged imaging of DIC, DAPI, and antibody 686. A single nucleus can be seen. B. DAPI image showing nucleus inside the *Colpodella* precyst. C. No reactivity with antibody. D. DIC image of the *Colpodella* sp. precyst showing the morphology.

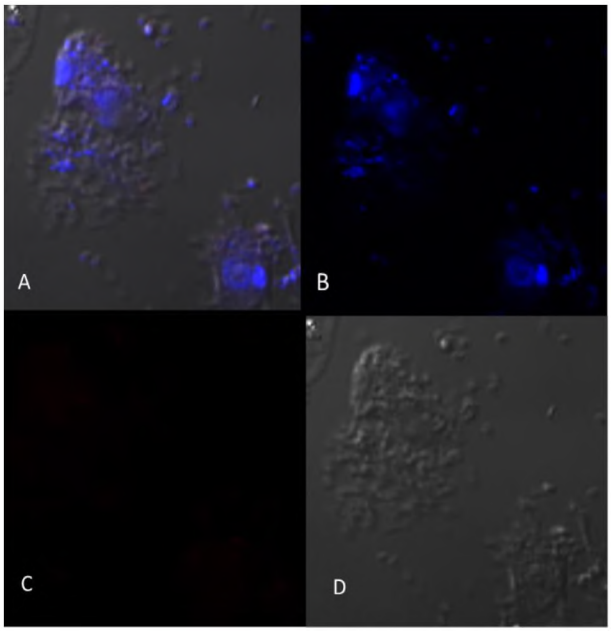

Figure 19. IFA of formalin-fixed cells in diprotist culture at time point five (20 hours). Antiserum 686 1:100 was used in IFA. A. Merged image (DIC, Antibody, and DAPI) showing two *B. caudatus* trophozoites among some bacteria. The kinetoplasts stains very bright with DAPI compared to the central nucleus in *B. caudatus* trophozoites. B. DAPI stain of the two *B. caudatus trophozoites* showing the kinetoplast. C. There is no antibody cross reactivity with *B. caudatus* trophozoites. D. DIC image of *B. caudatus* trophozoites and their morphology.

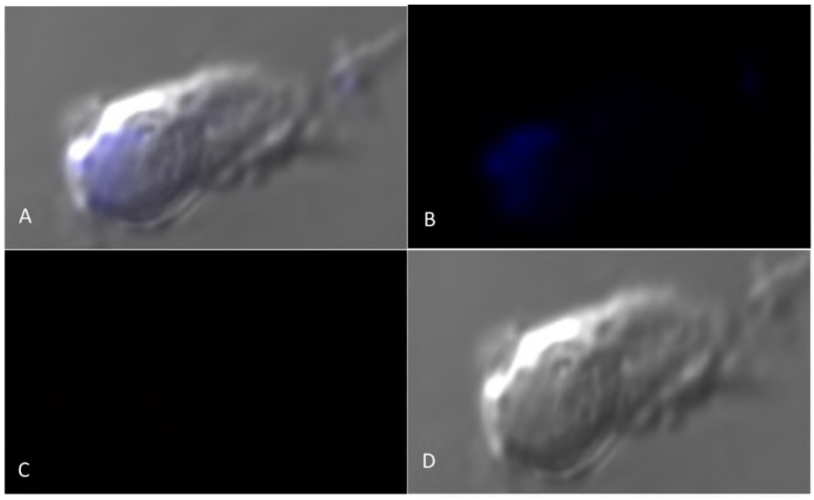

Figure 20. IFA of formalin-fixed cells in diprotist culture at time point six (22 hours). Antiserum 686 1:100 was used in IFA. A. Merged image of a *Colpodella* sp. precyst which has just finished feeding. It is losing the anterior portion and a cyst is forming in the posterior food vacuole. The nucleic contents are stained in the food vacuole of the *Colpodella* sp. indicating the successful aspiration of its prey, *B. caudatus*. B. DAPI stain shows a faint nucleus and the contents that were sucked out of the prey and into the food vacuole. C. There is no antibody reactivity seen in the *Colpodella* sp. precyst and Anti-686. D. DIC shows the posterior food vacuole turning into a circular *Colpodella* sp. cyst.

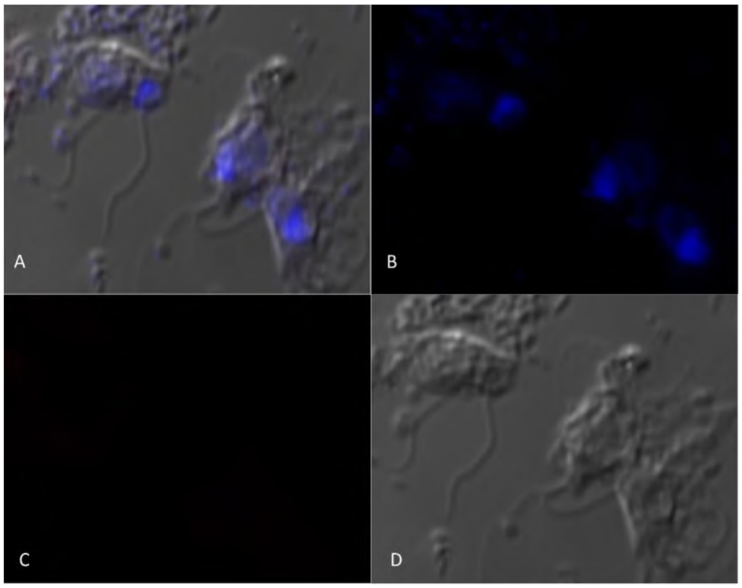

Figure 21. IFA of formalin-fixed cells in diprotist culture at time point six (22 hours). Antiserum 686 1:100 was used in IFA. A. Merged image observes three *B. caudatus* trophozoites with their flagella displayed. B. DAPI shows the *B. caudatus* trophozoites bright stained kinetoplast and nucleus. C. There is no cross reactivity between the *B. caudatus* trophozoites and antiserum 686. D. DIC shows the morphology of each *B. caudatus* trophozoite and their flagella used for locomotion.

Figure 22 shows *B. caudatus* trophozoites at 24 hours. There was no antibody reactivity with the cells. *Colpodella* sp. trophozoites were observed with strong RhopH3 antibody reactivity within the cytoplasm at 25 hours (Figure 23). *B. caudatus* present in culture at 26 hours were not reactive with antibody (Figure 24). At 27 hours, formalin-fixed *Colpodella* sp. trophozoites were reactive with antiserum 686, mostly at the anterior portion of the cell. Reactivity was observed on *B. caudatus* trophozoites (Figure 25 and 26). At 28 and 29 hours, antibody reactivity was not observed (Figure 28 and 29). *Colpodella* sp. trophozoites attached in myzocytosis showed weak reactivity when reacted with antibody as seen in Figure 29.

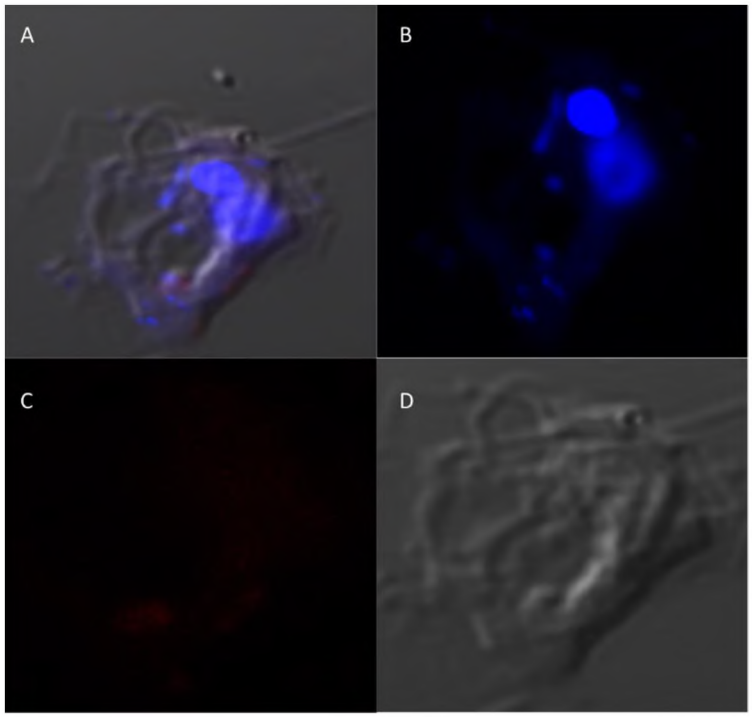

Figure 22. IFA of formalin-fixed cells in diprotist culture at time point seven (24 hours). Antiserum 686 1:100 was used in IFA. A. Merged view of a single mature *B. caudatus* trophozoite. B. DAPI stained the prominent kinetoplast and nucleus of the trophozoite. C. There is no reactivity seen between antiserum 686 and *B. caudatus*. D. DIC shows a mature *B. caudatus* trophozoite morphology and flagella.

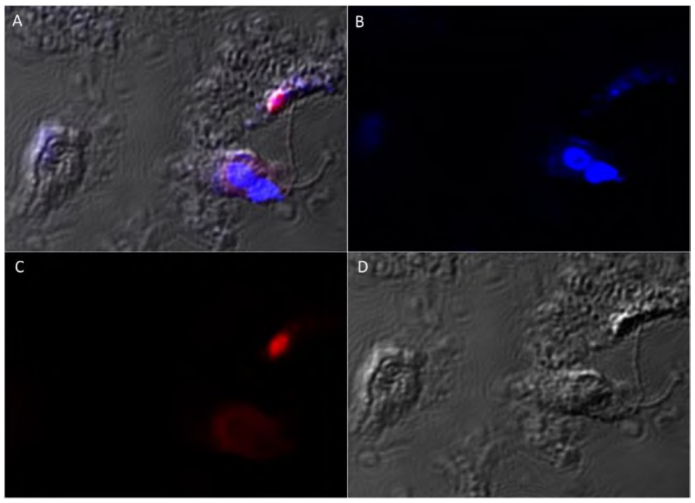

Figure 23. IFA of formalin-fixed cells in diprotist culture at time point eight (25 hours). Antiserum 686 1:100 was used in IFA. A. Merged image shows a *Colpodella* sp. and *B. caudatus* trophozoites. B. The DAPI stain shows the kinetoplast of *B. caudatus* and nuclei of both trophozoites. C. Antibody reactivity (red) was observed in *Colpodella* sp. trophozoites within the cytoplasm. Background reactivity was also obtained on *B. caudatus* trophozoite. D. DIC shows the shape of *Colpodella* sp. and *B. caudatus* along with their flagella.

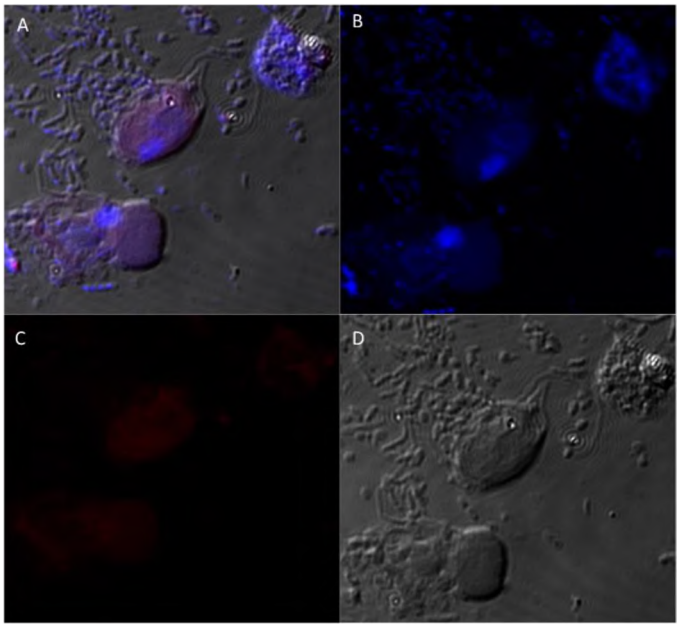

Figure 24. IFA of formalin-fixed cells in diprotist culture at time point nine (26 hours). Antiserum 686 1:100 was used in IFA. A. Merged image shows two *B. caudatus* trophozoites. B. The kinetoplast and nuclei are seen in both *B. caudatus*. C. There is no cross reactivity of antiserum 686 with *B. caudatus* proteins. D. The flagella and shape of the cells are shown with DIC imaging.

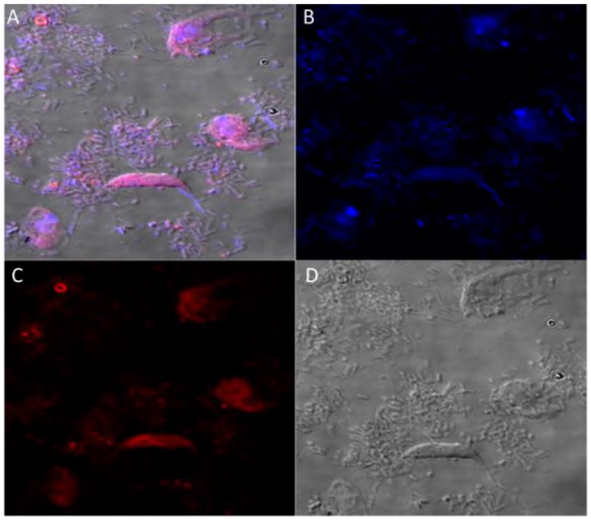

Figure 25. IFA of formalin-fixed cells in diprotist culture at time point ten (27 hours). Antiserum 686 1:100 was used in IFA. A. Merged image shows a single *Colpodella* sp. trophozoite among three *B. caudatus* trophozoites. B. Using DAPI, the *Colpodella* sp. nucleus is seen in the center of the cell. C. Antibody reactivity was observed at the anterior portion of the *Colpodella* sp. trophozoite and in some *B. caudatus* trophozoites. D. The DIC images show the shape of the predator and prey trophozoites.

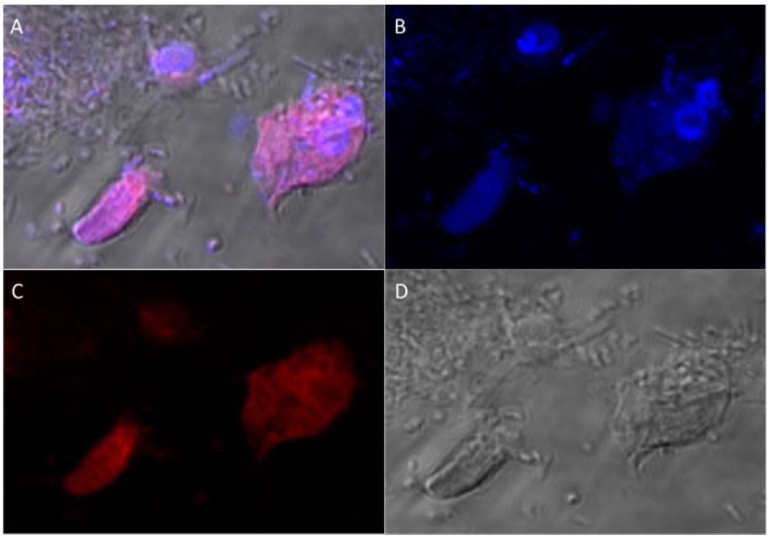

Figure 26. IFA of formalin-fixed cells in diprotist culture at time point ten (27 hours). Antiserum 686 1:100 was used in IFA. A. Merged image of a young *Colpodella* sp. trophozoite beside two *B. caudatus* trophozoites. B. DAPI stained nuclei, *Colpodella* sp. has a nucleus in the center of the cell, the *B. caudatus* nuclei and kinetoplasts are also visualized. C. Antibody reactivity observed at the apical end of *Colpodella* sp. and in *B. caudatus*. D. DIC shows the morphology of the cells.

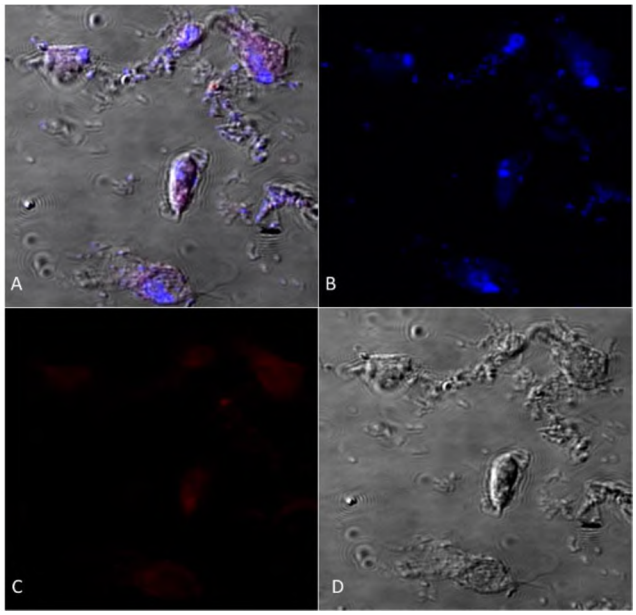

Figure 27. IFA of formalin-fixed cells in diprotist culture at time point eleven (28 hours). Antiserum 686 1:100 was used in IFA. A. Merged image with a mature *Colpodella* sp. precyst in the middle. The posterior food vacuole is large and showing a precyst starting to form. Four *B. caudatus* trophozoites were also observed. B. DAPI shows the nucleus and aspirated DAPI stained contents in the food vacuole of the *Colpodella* sp. trophozoite. The *B. caudatus* kinetoplasts and nuclei are visualized. C. Background antibody reactivity was observed in the predator and prey trophozoites. D. DIC image shows the shape and size of each trophozoite.

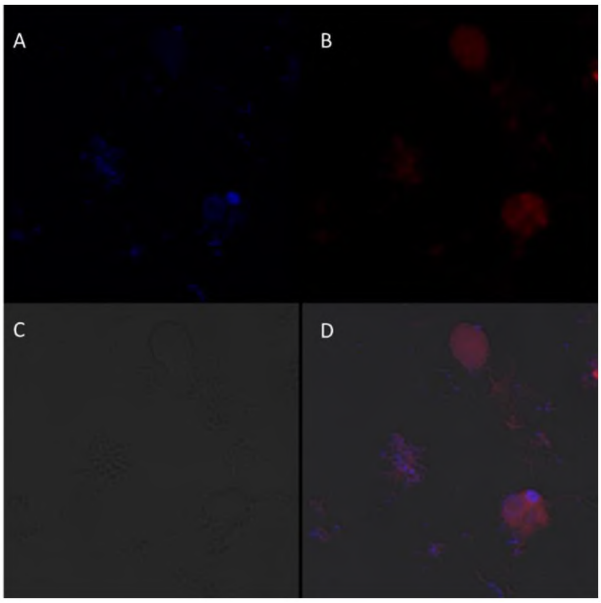

Figure 28. IFA of formalin-fixed cells in diprotist culture at time point twelve (29 hours). Antiserum 686 1:100 was used in IFA. A. DAPI-stained image showing *B. caudatus cysts* with nuclei and kinetoplast. B. Weak reactivity of antiserum 686 is seen in the cysts. C. The DIC image for this panel did not appear. D. merged images with DIC, antibody reactivity, and DAPI.

At 30 hours, both protist species are encysting. *Colpodella* sp. precysts are shown with weak antibody reactivity. In *Colpodella* sp. attached to *B. caudatus* in myzocytosis, weak reactivity was observed in the anterior portion of the cells (Figure 29).

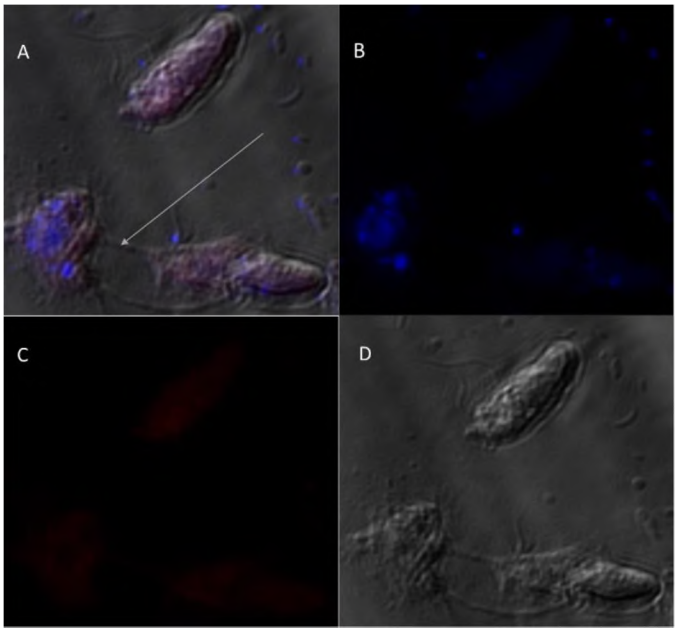

Figure 29. IFA of formalin-fixed cells in diprotist culture at time point thirteen (30 hours). Antiserum 686 1:100 was used in IFA. A. Merged image shows two *Colpodella* sp. trophozoites, one attached to a *B. caudatus* trophozoite (arrow). A long tubular tether can be seen attached to both cells. The nucleus of each protist can be seen by DAPI staining. B. Kinetoplast and nucleus of *B. caudatus* can be seen using DAPI. Contents can be seen aspirated from the prey into the *Colpodella* sp. food vacuole. C. Weak antibody reactivity was observed in *Colpodella* sp. and *B. caudatus* trophozoites. D. DIC, the tubular tether can be seen tethering the *Colpodella* sp. to the prey. The heterodynamic flagella are also observed.

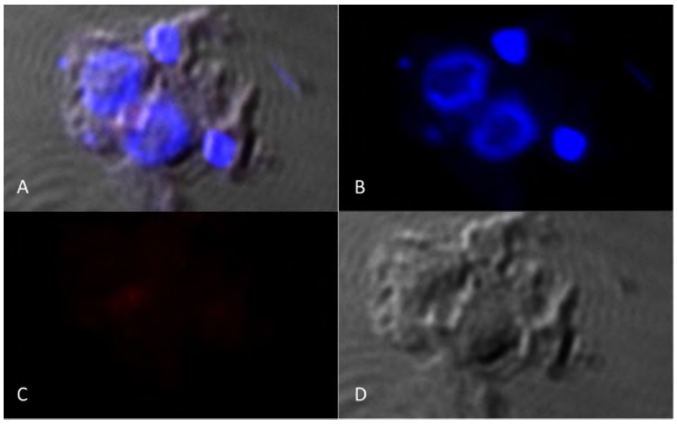

Figure 30. IFA of formalin-fixed cells in diprotist culture at time point fourteen (32 hours). Antiserum 686 1:100 was used in IFA. A. Merged image of two *B. caudatus* trophozoites side by side. B. Kinetoplast and nuclei of each *B. caudatus* trophozoite shown by DAPI staining. C. No antibody reactivity was observed. D. DIC imaging of *B. caudatus* morphology.

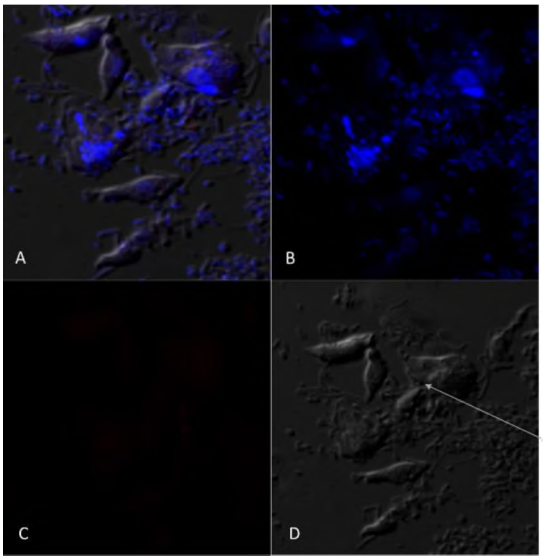

Figure 31. IFA of formalin-fixed cells in diprotist culture at time point fourteen (32 hours). Antiserum 686 1:100 was used in IFA. A. Merged image of many *Colpodella* sp. trophozoites (6) surrounding one *B. caudatus* trophozoite. The nuclei of the *Colpodella* sp. can be identified and a close attachment was observed. B. DAPI stain shows nuclei and kinetoplasts of *B. caudatus* and nuclei of *Colpodella* sp. C. No antibody reactivity was observed. D. Attachment was seen between a *B. caudatus* trophozoite and *Colpodella* sp. trophozoite (arrow). Morphology of the many *Colpodella* sp. can be observed.

At 32 hours (Figure 30 and 31) and 34 hours (Figure 32 and 33) is when most of *B. caudatus* and *Colpodella* sp. have encysted. *Colpodella* sp. mature cysts can be observed. Cross reactivity with antiserum 686 is shown very faintly in the cysts (Figure 34 and 35).

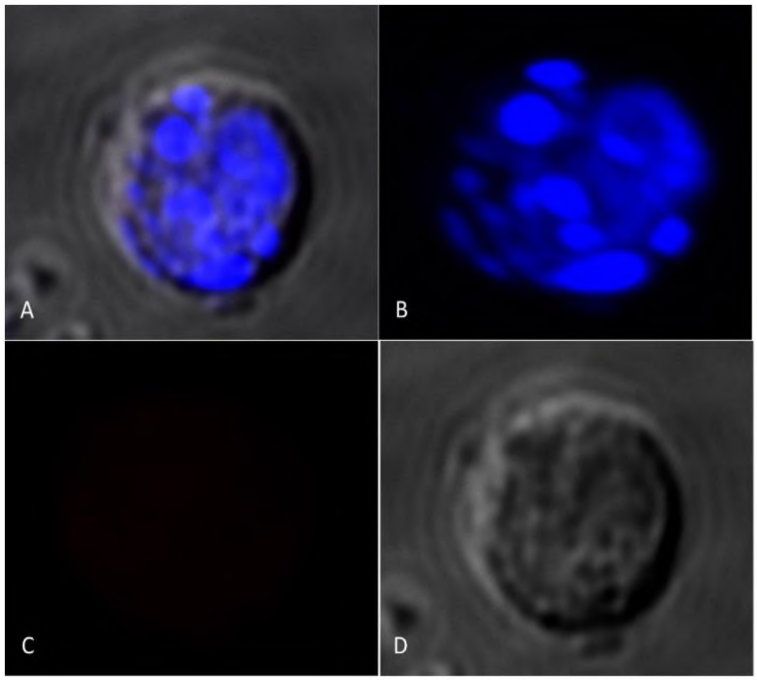

Figure 32. IFA of formalin-fixed cells in diprotist culture at time point fifteen (34 hours). Antiserum 686 1:100 was used in IFA. A. Merged image of a *B. caudatus* cyst. B. DAPI image showing the ring nucleus, and kinetoplast of the *B. caudatus* trophozoite bacteria inside the cyst. C. No antibody reactivity was observed with the cyst. D. Morphology of *B. caudatus* cyst is seen with DIC.

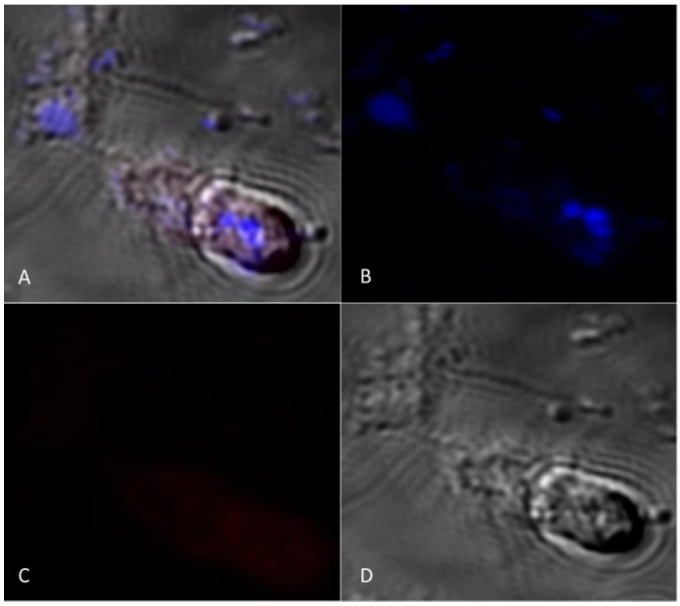

Figure 33. IFA of formalin-fixed cells in diprotist culture at time point fifteen (34 hours). Antiserum 686 1:500 was used in IFA. A. Merged image was taken and shows a *Colpodella* sp. trophozoite feeding on *B. caudatus* prey in myzocytosis. DAPI stained aspirated contents of the prey can be seen in the large food vacuole. The tether attaching the two cells together can also be seen. Background antibody staining was observed. B. DAPI staining shows the nucleus of both cells and the cytoplasmic contents from the prey in the posterior food vacuole of *Colpodella* sp. C. Background antibody reactivity (red) was observed. D. The DIC image shows the morphology of both *Colpodella* sp. and *B. caudatus* trophozoites including the point of attachment.

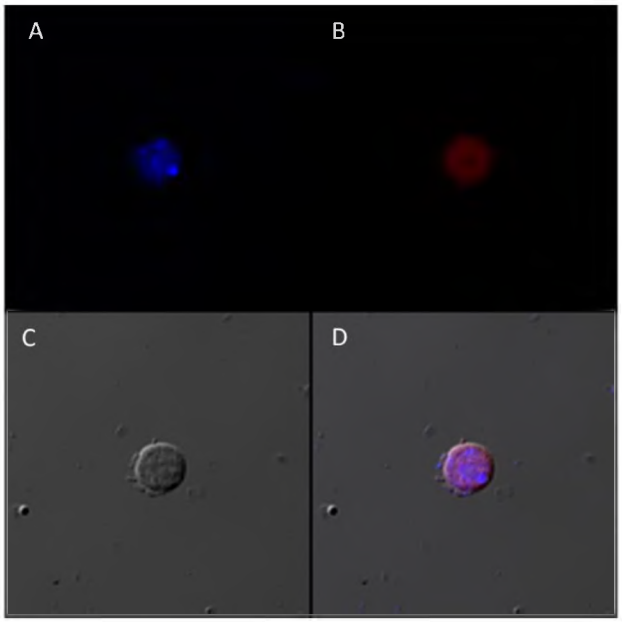

Figure 34. IFA of formalin-fixed cells in diprotist culture at time point sixteen (36 hours). Antiserum 686 1:100 was used in IFA. A. DAPI image showing a single *B. caudatus* cyst with a nucleus and kinetoplast. B. Antibody cross reactivity was observed with the cyst. C. DIC shows the shape of the cyst. D. merged images with DIC, antibody and DAPI.

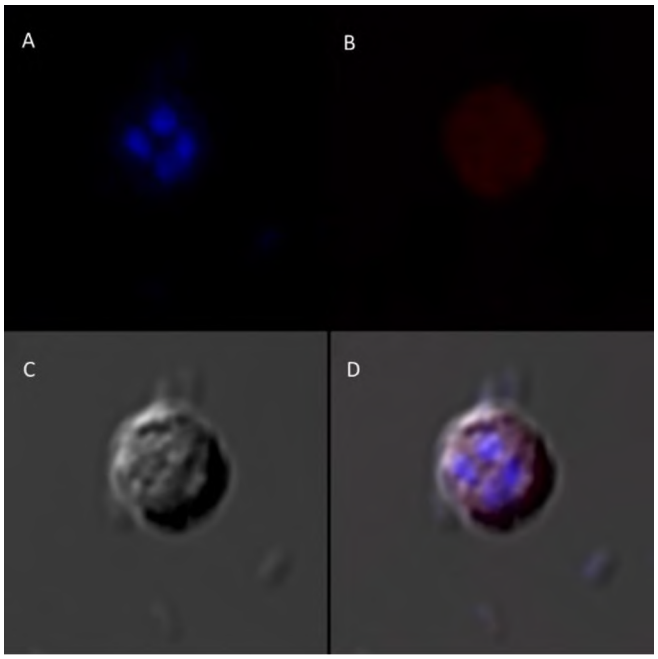

Figure 35. IFA of formalin-fixed cells in diprotist culture at time point sixteen (36 hours). Antiserum 686 1:100 was used in IFA. A. DAPI image showing a single mature *Colpodella* sp. cyst with four nuclei. B. Weak antibody cross reactivity was observed with the cyst. C. DIC shows the shape of the cyst. D. merged images with DIC, antibody, and DAPI.

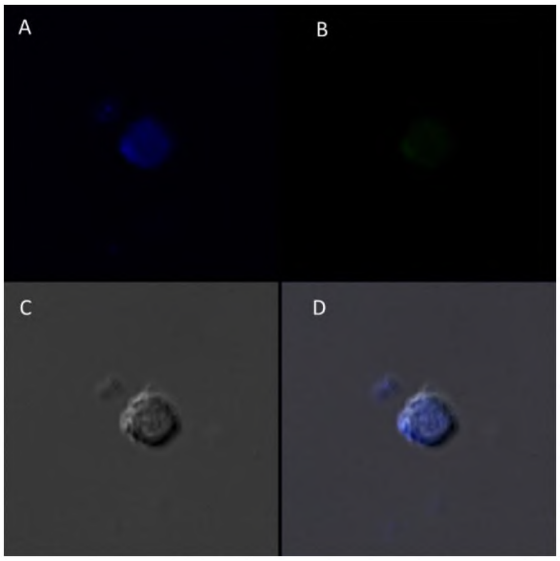

Figure 36. IFA of formalin-fixed cells in diprotist culture at time point seventeen (38 hours). Antiserum 686 1:100 was used in IFA. A. DAPI image showing a single *Colpodella* sp. mature cyst with a nucleus. B. No antibody reactivity was observed in the cysts. C. DIC shows the shape of the cyst. D. merged images with DIC, antibody, and DAPI.

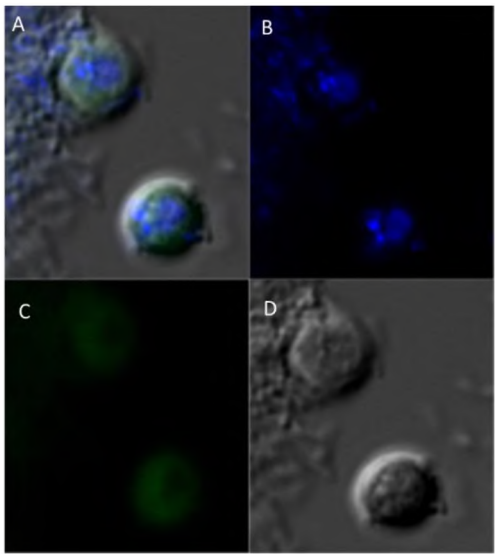

Figure 37. IFA of formalin-fixed cells in diprotist culture at time point seventeen (38 hours). Antiserum 686 1:100 was used in IFA. A. Merge of DAPI, DIC and antibody. DAPI stain identifies two *B. caudatus* cysts. B. DAPI staining shows the nuclei of both cysts. C. Background antibody reactivity (green) was observed. D. DIC shows the shape of the cysts.

3.7 Immunofluorescence with Normal Rabbit and Mouse Serum

Polyclonal rabbit antibodies and monoclonal antibodies specific for *P. falciparum* proteins were used for IFAs with *Colpodella* sp. and *B. caduatus* proteins to determine if the antibodies would cross react with *Colpodella* sp. proteins and to identify structures reactive with the antibodies. Normal rabbit and mouse serum were used as negative controls. No reactivity was observed on *Colpodella* sp. or *B. caudatus* trophozoites and cysts with normal rabbit (Figures 38-41) and mouse (Figures 42-44) normal sera. Both DIC microscopy and DAPI allowed us to identify the morphology of different life cycle stages and identify the nucleus and kinetoplast by confocal microscopy. DIC images of *Colpodella* sp. and *B. caudatus* in myzocytosis is shown in Figure 39 A and C, and in Figure 41. A free swimming *Colpodella* sp. trophozoite showing the heterodynamic flagella is shown in Figure 40. In Figure 42, DIC images show the morphology of *Colpodella* sp. attached to prey in myzocytosis with aspirated DAPI stained contents of the prey in the posterior food vacuole of *Colpodella* sp. The DAPI stained central nucleus of a free swimming *Colpodella* sp. trophozoite is shown in Figure 44.

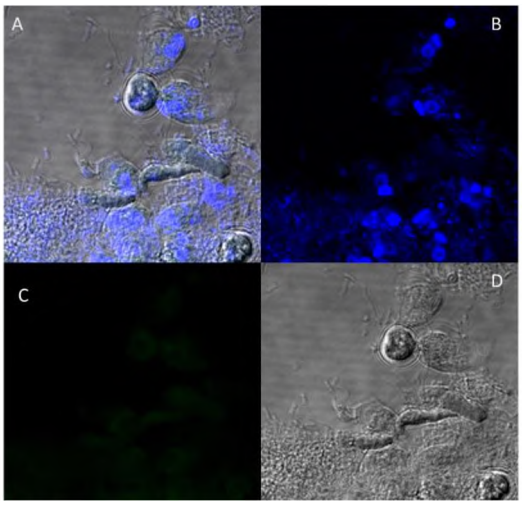

Figure 38. Normal rabbit serum, 1:100 was used as a negative control. There was no reactivity with proteins of C*olpodella* sp. and *Bodo caudatus*. A. Merge of DAPI, NRS and DIC images show a *Colpodella* sp. trophozoite feeding upon a *B. caudatus* trophozoite. The nucleus and kinetoplasts of *B. caudatus* are stained intensely by DAPI while the nucleus of *Colpodella* sp. is less intense but can be seen. B. DAPI staining shows the nuclei of both flagellates and the *B. caudatus* kinetoplast. C. There was no reactivity with NRS. D. DIC image shows morphology of *Colpodella* sp. and prey.

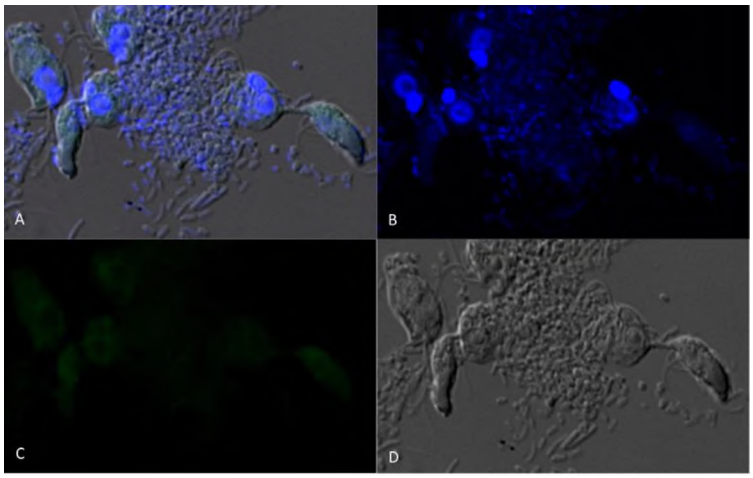

Figure 39. Normal rabbit serum, 1:100 was used as a negative control. Weak background reactivity was observed. The merged image shows two separate attachments of *Colpodella* sp. and *B. caudatus* trophozoites. B. DAPI staining shows the nucleus of *Colpodella* sp. and *B. caudatus*. C. Weak background reactivity was observed on cells with NRS. D. DIC images show the attachment of *Colpodella* sp. and the tubular tethers.

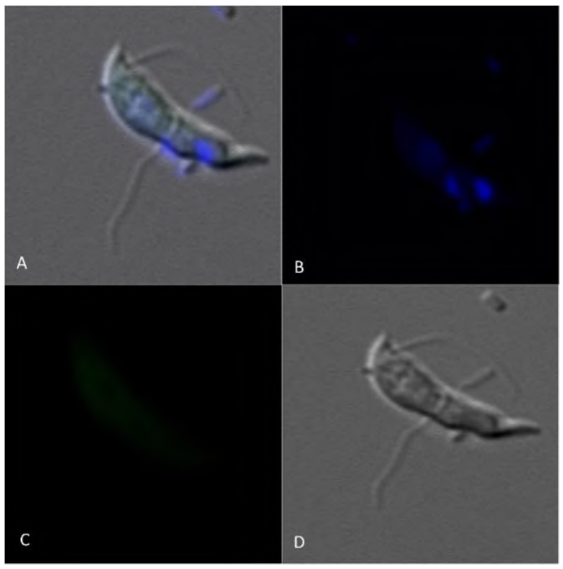

Figure 40. Normal rabbit serum, 1:100 was used as a negative control. There was no reactivity with proteins of *Colpodella* sp. Cells were formalin-fixed and incubated with normal rabbit serum. A. The merged image shows a single immature *Colpodella* sp. trophozoite. B. The DAPI stain shows the nucleus. C. There was reactivity observed with NRS. D. DIC shows the shape of the *Colpodella* sp. trophozoite and the flagella were also observed.

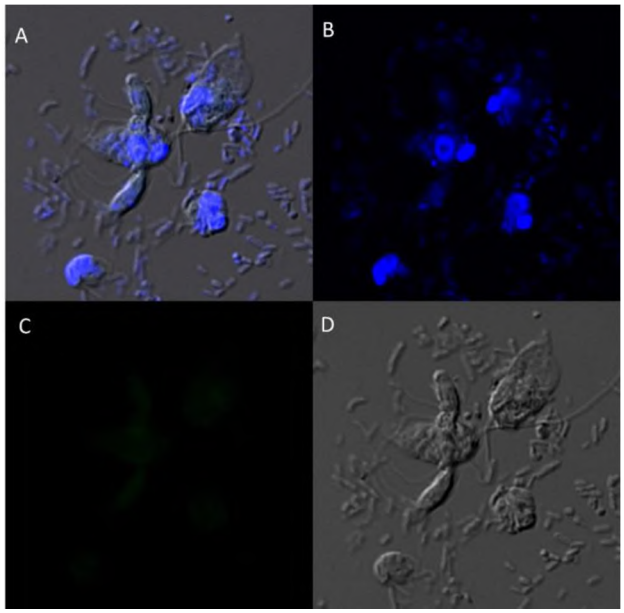

Figure 41. Normal rabbit serum, 1:1000 was used as a negative control. There was no reactivity with proteins of C*olpodella* sp. and *Bodo caudatus*. A. DIC, NRS and DAPI image shows a double attachment, two *Colpodella* sp. trophozoites in myzocytosis with one *B. caudatus* trophozoite. B. DAPI image shows the nucleus and DAPI stained aspirated contents of the prey can be seen in the posterior of the *Colpodella* sp. trophozoite. The cytoplasmic contents from the prey are being aspirated into the posterior food vacuole of *Colpodella* sp. C. There was no reactivity with normal rabbit serum. D. DIC image showing morphology of cells and flagella.

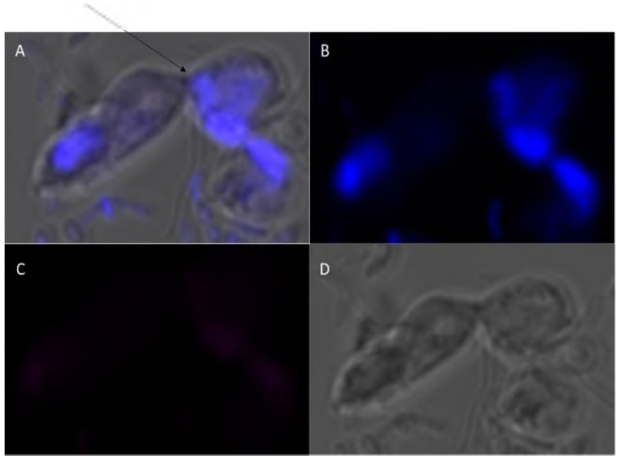

Figure 42. Normal mouse serum, 1:100 was used as a negative control. There was no reactivity with proteins of C*olpodella* sp. and *B. caudatus*. The merged image shows a *Colpodella* sp. trophozoite attached to a *B. caudatus* trophozoite. B. DAPI staining shows the nuclei in both cells. The DAPI stained contents aspirated from the prey can be visualized as blue in the posterior food vacuole of *Colpodella* sp. C. There was no reactivity with NMS. D. DIC showing the morphology of the cells in myzocytosis.

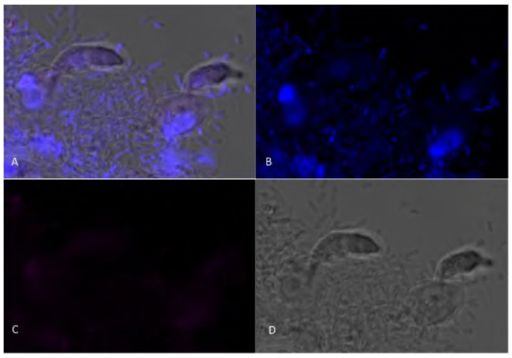

Figure 43. Normal mouse serum, 1:100 was used as a negative control. There was no reactivity with proteins of C*olpodella* sp. and *B. caudatus*. A. The merged image shows two *Colpodella* sp. trophozoites feeding on two separate *B. caudatus* trophozoites. B. DAPI stained nuclei in both the predator and prey trophozoites can be seen. C. No reactivity was observed with NMS. D. DIC image shows the morphology of predator and prey in myzocytosis.

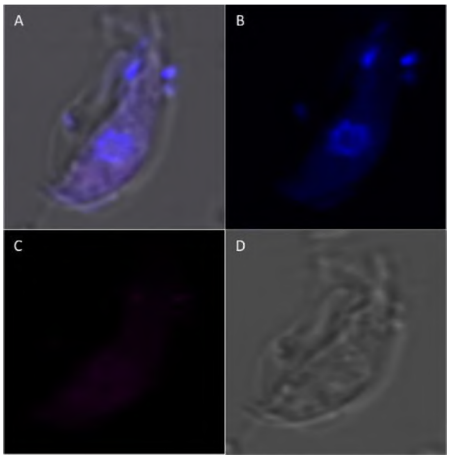

Figure 44. Normal mouse serum, 1:100 was used as a negative control. There was no reactivity with proteins of C*olpodella* sp. and *B. caudatus*. A. The merged image shows a *Colpodella* sp. trophozoite with a central nucleus and flagella. B. DAPI staining shows the nucleus in the center of the cell. C. No reactivity was observed with NMS. D. DIC image shows the shape of the cells and flagella.

3.8 Immunofluorescence of *Colpodella* sp. with Antisera IMC3, IMC7, Py235, EBA175, AMA1 and PL2

Different antibodies against known apical and non-apical proteins of *P. falciparum* and *Toxoplasma gondii* were used in IFA. We wanted to know if antigens recognized by these antibodies could be localized in *Colpodella* sp. Antisera were diluted

at 1:50, 1:100, 1:200, 1:500, and 1:1000. There was no cross reactivity observed with Py235 antisera and proteins of *Colpodella* sp. (Figures 44 and 46). The antibody is specific for the 235 kDa rhoptry protein of *P. yoelii*, which is a rodent parasite. Only faint background reactivity was observed. IMC3 is an inner membrane complex protein found in apicomplexans and was identified in *Colpodella* sp. and weakly in *B. caudatus* (Figures 47-49). Anti-IMC3 FLR which recognizes the full-length antigen was observed reactive with the anterior portion of *Colpodella* sp. trophozoites (Figures 50-52) and weakly in *B. caudatus*. AMA1 is a microneme protein used in cell invasion among parasitic apicomplexans. Intense cross reactivity was obtained with the antibodies on *Colpodella* sp. trophozoites and weakly on *B. caudatus* trophozoites (Figures 53-55). The cross reactivity with anti-AMA1 antibody in *Colpodella* sp. trophozoites was observed towards the apical end. IMC7 is another inner membrane complex protein identified in apicomplexan parasites. There was no reactivity with anti-IMC7 antibody as the reactivity was observed as background reactivity. (Figures 56 and 57). Plasmepsin II is an aspartic protease located in the food vacuole of *P. falciparum* where it degrades hemoglobin. Cross reactivity was observed between the antisera and antigen in *Colpodella* sp. trophozoites feeding on *B. caudatus* in myzocytosis (Figures 58 and 59). Reactivity was observed in *B. caudatus* trophozoites attached to *Colpodella* sp. In Figure 59, the posterior portion of *Colpodella* sp. is intensely reactive with anti-Plasmepsin II. Weak antibody reactivity was observed in unattached *B. caudatus* trophozoites (Figures 58-59). EBA175 is a microneme protein that functions in *P. falciparum* merozoite invasion. It is used to initiate invasion of red blood cells. Antibody cross reactivity was

identified in *Colpodella* sp. at the anterior portion of the cell and weakly in *B. caudatus* (Figures 60-63).

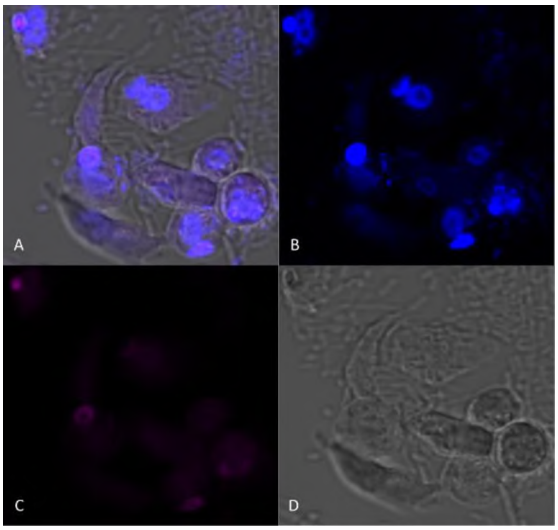

Figure 45. IFA of formalin-fixed cells in diprotist culture. Antibody Py 235 1:100 was used in IFA. A. The merged image shows a single and a double attachment between *Colpodella* sp. and *B. caudatus* trophozoites and few free *B. caudatus* trophozoites and one cyst. B. DAPI staining shows the nuclei of both predator and prey. C. There was no reactivity with Anti-Py235 antibodies and the proteins of *Colpodella* sp. and *B. caudatus*. D. DIC image shows the morphology of cells in close attachments.

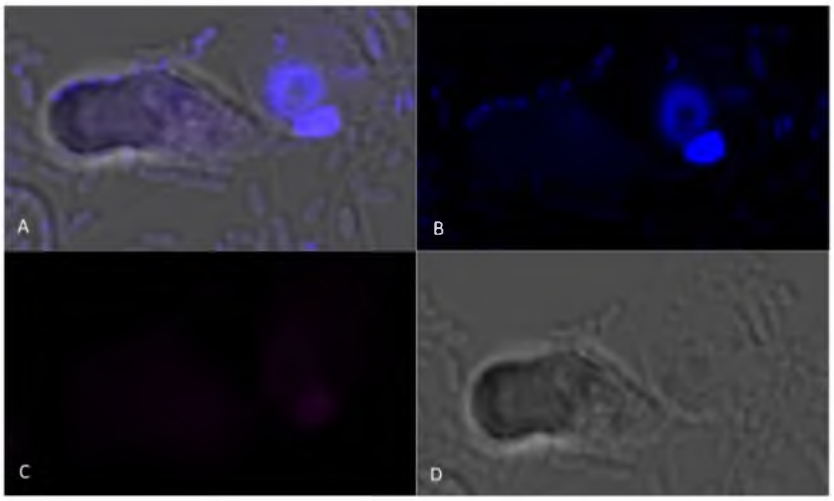

Figure 46. IFA of formalin-fixed cells in diprotist culture. Antibody Py 235 1:100 was used in IFA. A. The merged image shows a mature *Colpodella* sp. trophozoite feeding on a *B. caudatus* trophozoite. The posterior food vacuole is enlarged followed feeding in preparation for encystation. B. DAPI staining shows the nuclei of both trophozoites and the kinetoplast of *B. caudatus*. C. There was no reactivity with antibody Py235. D. DIC image shows the close attachment and the enlarged posterior food vacuole.

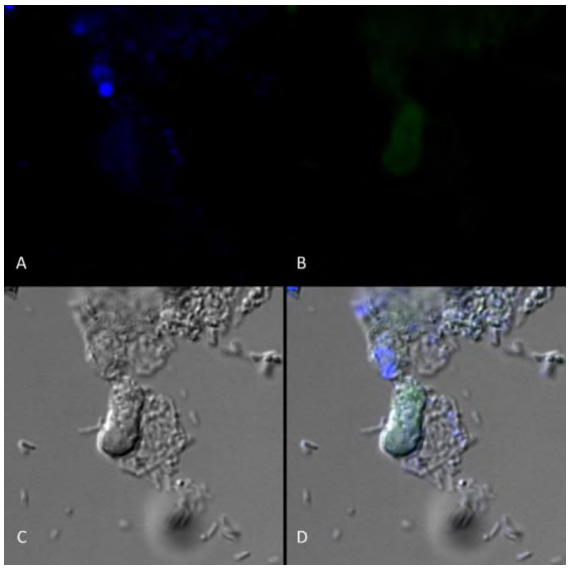

Figure 47. IFA of formalin-fixed cells in diprotist culture. Anti-IMC31:1000 was used in IFA. A. DAPI image shows a *B. caudatus* trophozoite with a nucleus and kinetoplast. B. Weak antibody reactivity was observed in *Colpodella* sp. C. The morphology of a *Colpodella* sp. trophozoite attached to its prey with a large food vacuole was seen in DIC image. D. Merged image of DAPI, antibody and DIC showing weak antibody reactivity and morphology of the cells.

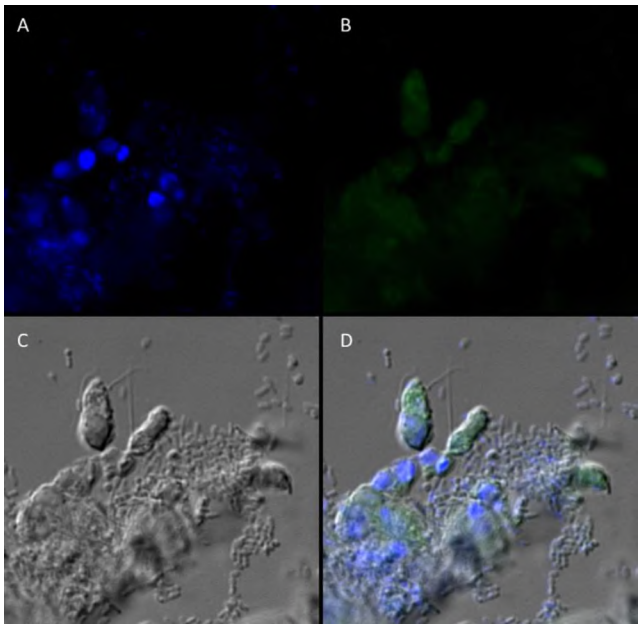

Figure 48. IFA of formalin-fixed cells in diprotist culture. Anti-IMC3 antibody 1:1000 was used in IFA. A. DAPI image shows the nuclei of *Colpodella* sp. and *B. caudatus* trophozoites. The kinetoplasts of *B. caudatus* were also observed. B. Weak antibody reactivity (green) was observed on *Colpodella* sp. trophozoites. Some trophozoites of *B. caudatus* were weakly reactive with the antibody. C. DIC image shows the morphology of both predator and prey with a double attachment from two *Colpodella* sp. trophozoites on one *B. caudatus* trophozoite observed. D. Merged image with DIC, antibody, and DAPI stain. Antibody reactivity can be seen in trophozoites of *Colpodella* sp.

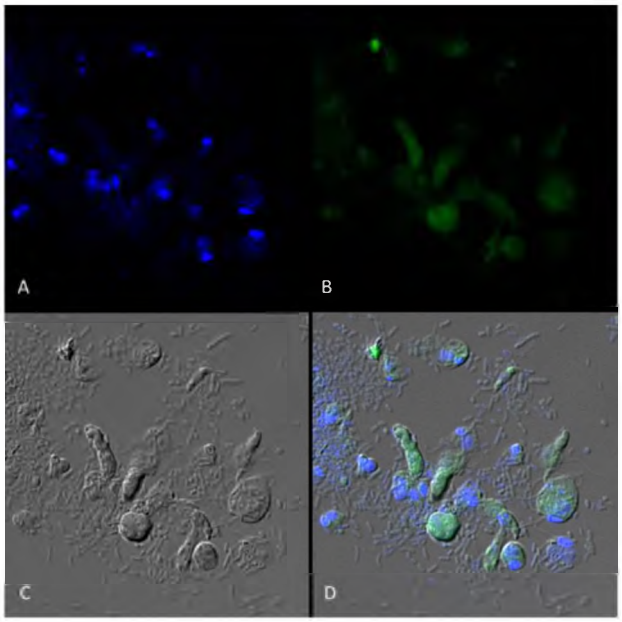

Figure 49. IFA of formalin-fixed cells in diprotist culture. Anti-IMC3 antibody 1:1000 was used in IFA. A. DAPI image shows the nuclei in both *Colpodella* sp. trophozoites and *B. caudatus*, while the kinetoplasts are only in *B. caudatus*. B. Antibody reactivity (green) was observed in *Colpodella* sp. trophozoites and cysts. C. DIC image shows multiple *Colpodella* sp. trophozoites with a few feeding pairs. D. Merged image with DIC, antibody and DAPI stain. Antibody reactivity was observed in *Colpodella* sp. trophozoites.

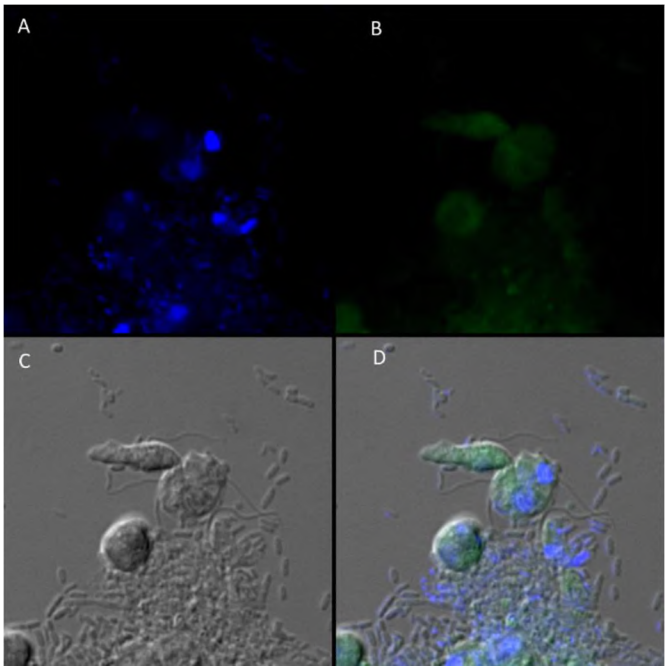

Figure 50. IFA of formalin-fixed cells in diprotist culture. Anti-IMC3 FLR antibody 1:50 was used in IFA. A. DAPI image shows a *Colpodella* sp. trophozoite attached to a *B. caudatus* trophozoite in myzocytosis and a *Colpodella* sp. cyst with three nuclei. There are also other *B. caudatus* trophozoites shown in the image. B. Cross reactivity shows up in all cells imaged. C. DIC shows the closeness of the attachment and the *Colpodella* sp. flagella. D. Merged image with DIC, antibody and DAPI stain.

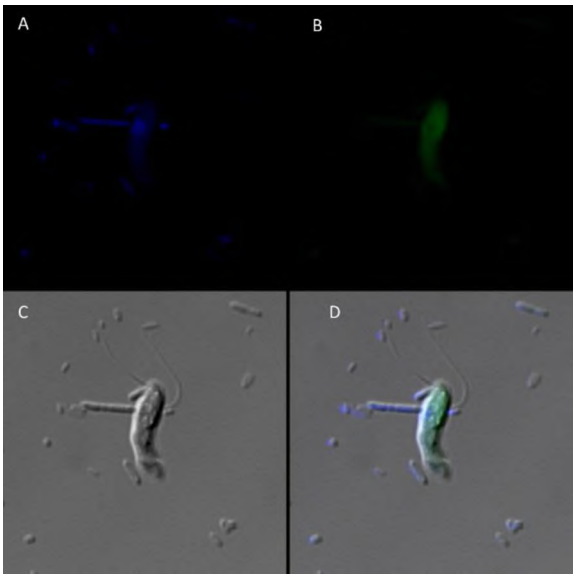

Figure 51. IFA of formalin-fixed cells in diprotist culture. Anti-IMC3 FLR antibody 1:50 was used in IFA. A. DAPI image shows a single immature *Colpodella* sp. trophozoite with a nucleus. B. Antibody reactivity was observed with *Colpodella* sp. proteins. C. DIC shows the slender shape of the trophozoite along with the heterodynamic flagella. D. Merged image with DIC, antibody and DAPI stain.

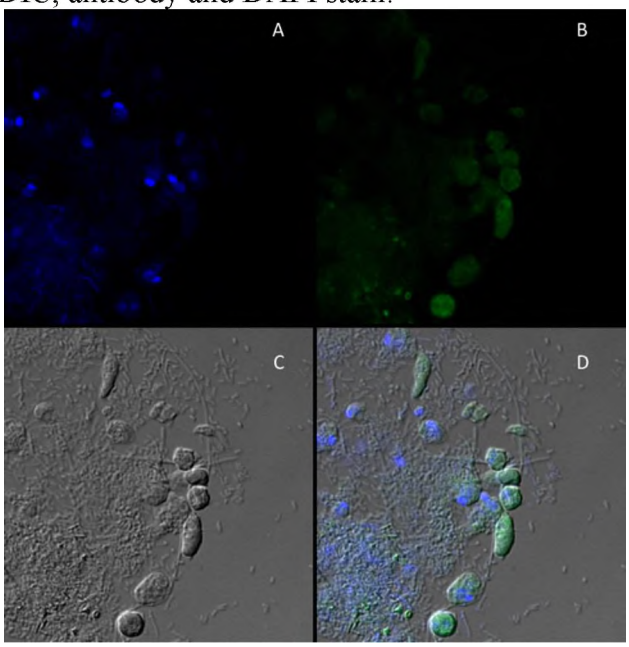

Figure 52. IFA of formalin-fixed cells in diprotist culture. Anti-IMC3 FLR antibody 1:100 was used in IFA. A. DAPI image shows a *Colpodella* sp. trophozoites free and also attachaed to *B. caudatus*. A *Colpodella* sp. cyst with two nuclei and *B. caudatus* trophozoites were also observed. *Bodo caudatus* trophozoites are identified by the presence of a nucleus and a kinetoplast. B. Antibody reactivity was observed in *Colpodella* sp. with most of the reactivity observed in the feeding *Colpodella* sp. trophozoite. C. DIC shows the tubular tether that forms during myzocytosis between the *Colpodella* sp. trophozoite and *B. caudatus* as well as the shape of each cell. D. Merged image with DIC, antibody and DAPI stain.

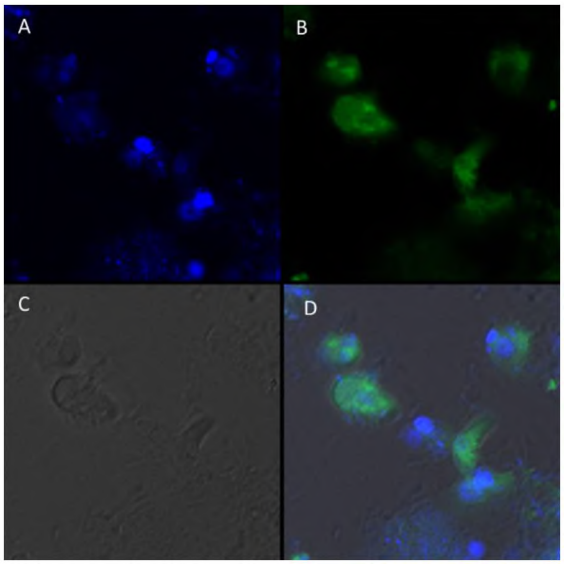

Figure 53. IFA of formalin-fixed cells in diprotist culture. Anti-AMA1 1:50 was used in IFA. A. DAPI image shows the nuclei of both *Colpodella* sp. and *B. caudatus* trophozoites. The kinetoplast of *B. caudatus* is stained brightly. B. Antibody reactivity was observed in *Colpodella* sp. trophozoites mostly at the apical end, and weakly on *B. caudatus* trophozoites. Antibody reactivity is shown in green and reveals a single attachment between predator and prey on the lower right of the panel with most of the reactivity observed in the *Colpodella* sp. trophozoite and in the *Colpodella* sp. precyst. C. DIC image shows the attachment and a *Colpodella* sp. precyst that is losing its anterior portion. D. Merged image with DIC, antibody and DAPI stain.

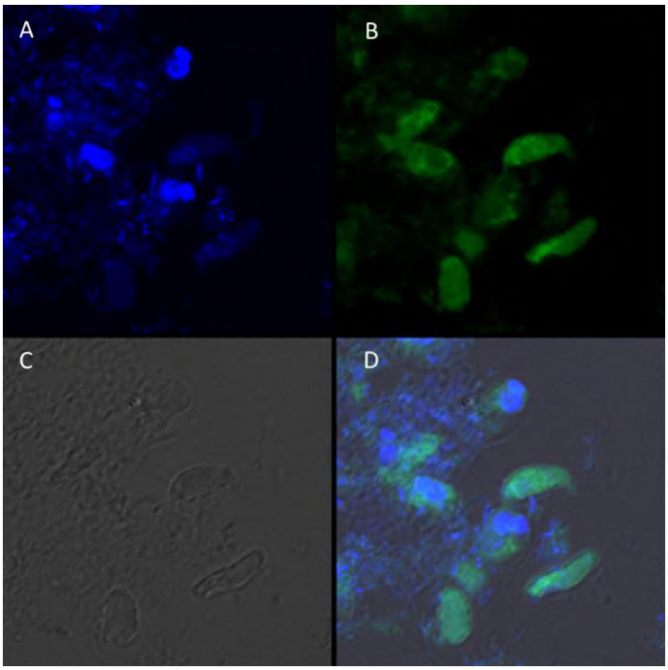

Figure 54. IFA of formalin-fixed cells in diprotist culture. Anti-AMA1 antibody 1:200 was used in IFA. A. DAPI stained cells show the nuclei of two *Colpodella* sp. trophozoites and precyst along with *B. caudatus* trophozoites with a nucleus and kinetoplast. B. Reactivity was observed with the AMA1 specific antibody most intensely at the apical end of *Colpodella* sp. trophozoites. The *B. caudatus* trophozoite attached to *Colpodella* sp. trophozoite and free trophozoite in top right of the panel show background reactivity. C. DIC image shows the morphology of *Colpodella* sp. and *B.caudatus* trophozoites and cells attached in myzocytosis. D. Merged image with DIC, antibody and DAPI stain.

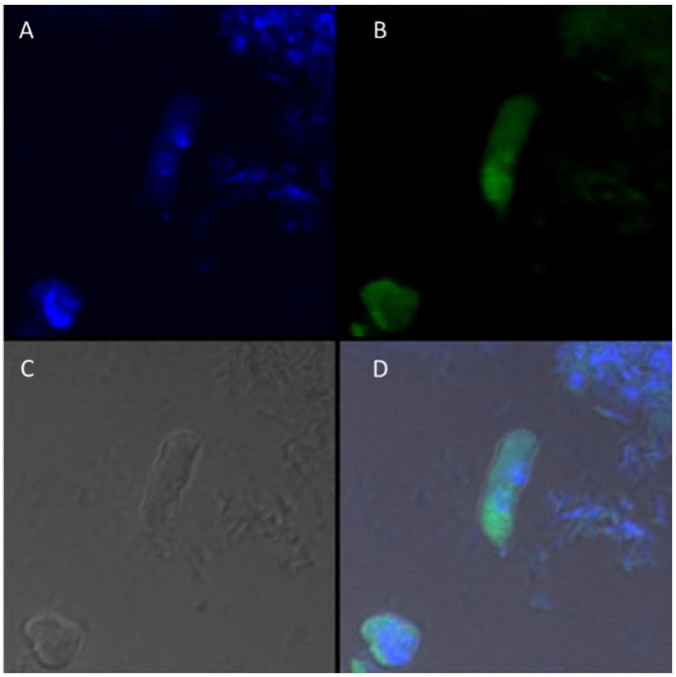

Figure 55. IFA of formalin-fixed cells in diprotist culture. Anti-AMA1 1:200 was used in IFA. A. DAPI image shows a *Colpodella* sp. trophozoite, cyst and *B. caudatus* trophozoites with their nuclei. The *Colpodella* sp. trophozoite has already fed as DAPI stained aspirated contents from the prey can be seen behind the central nucleus in its posterior food vacuole. B. Intense antibody reactivity was observed in the apical end of the *Colpodella* sp. trophozoite and in the cyst. C. DIC image shows the morphology of the *Colpodella* sp. and *B. caudatus* trophozoites. D. Merged image with DIC, antibody and DAPI stain.

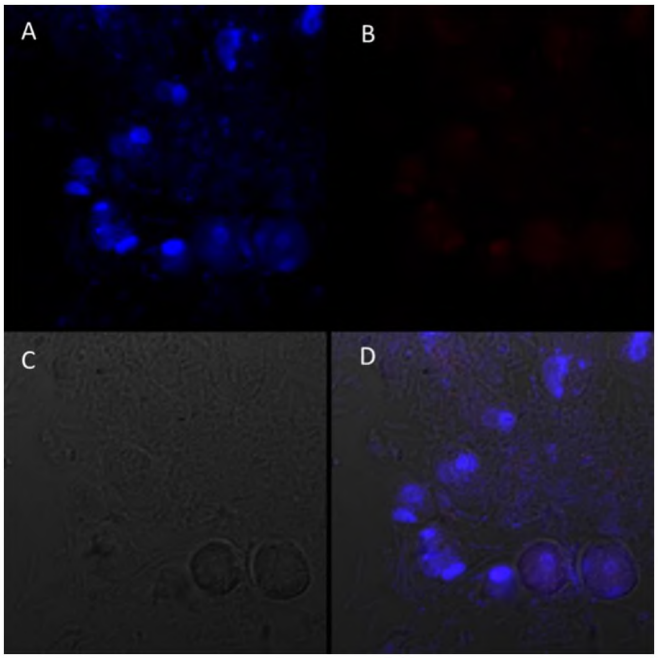

Figure 56. IFA of formalin-fixed cells in diprotist culture. Anti-IMC7 1:50 was used in IFA. A. DAPI image shows many *B. caudatus* cysts and trophozoites along with two mature cysts of *Colpodella* sp. One *Colpodella* sp. cyst has two nuclei and the second *Colpodella* sp. cyst has three nuclei indicating synchronous and asynchronous division. B. There was no antibody reactivity with the cells and cysts. C. DIC image shows the morphology of the trophozoites and cysts. D. Merged image with DIC, antibody and DAPI stain.

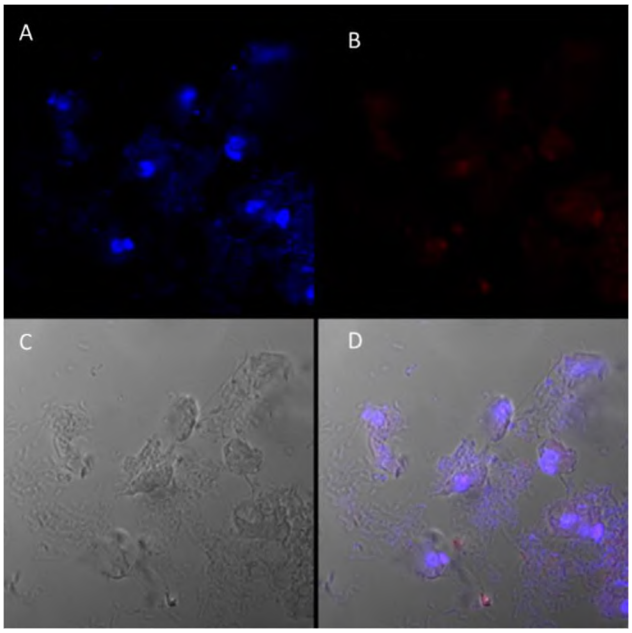

Figure 57. IFA of formalin-fixed cells in diprotist culture. Anti-IMC7 1:50 was used in IFA. A. DAPI stained image shows the nuclei and kinetoplasts of *B. caudatus* trophozoites and trophozoites of *Colpodella* sp. feeding in the top left. B. There was no antibody reactivity with the trophozoites. C. DIC image captures the close attachment during myzocytosis and the morphology of predator and prey trophozoites. D. Merged image with DIC, antibody and DAPI stain.

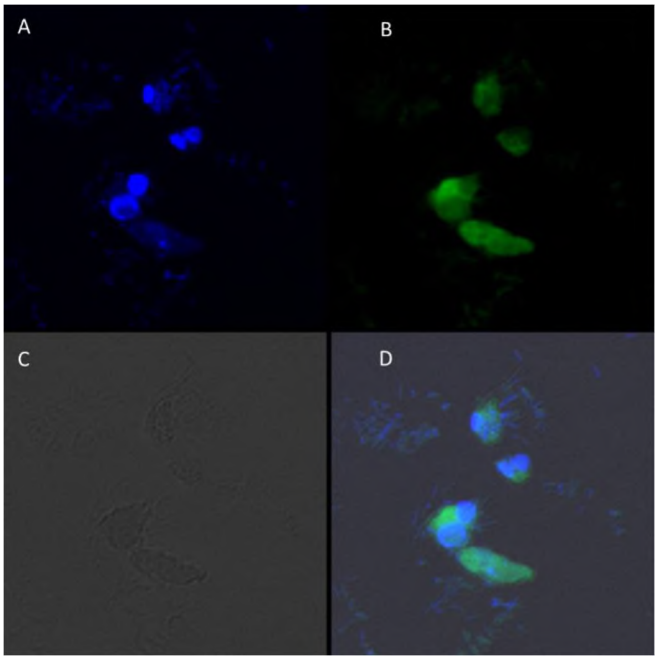

Figure 58. IFA of formalin fixed cells in diprotist culture. Anti-plasmepsin II 1:100 was used in the IFA. A. DAPI image shows a *Colpodella* sp. attached to a *B. caudatus* trophozoite, there are two other *B. caudatus* imaged. A nucleus is stained in every cell, but only *B. caudatus* trophozoites display the bright kinetoplast. B. Cross reactivity with plasmepsin 2 is observed in all protist cells as green. C. DIC imaging captures the shape of the protist's along with the close attachment during myzocytosis. D. Merged image with DIC, antibody reactivity, and DAPI stain.

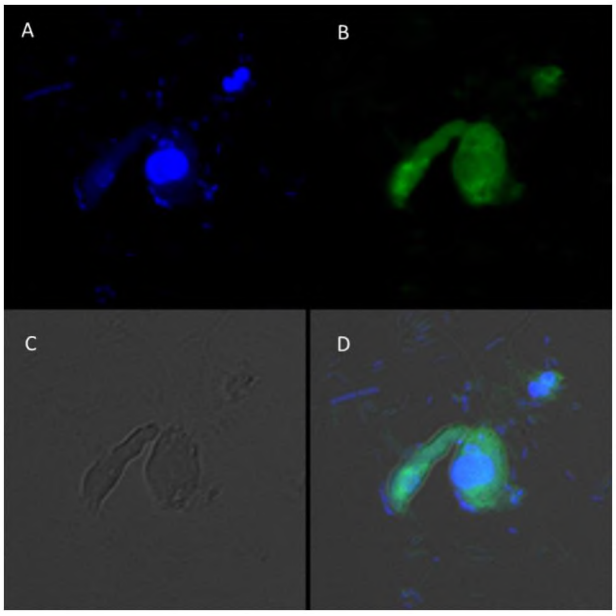

Figure 59. IFA of formalin-fixed cells in diprotist culture. Anti-plasmepsin II 1:100 was used in IFA. A. DAPI image shows the nucleus and kinetoplast *B. caudatus* and the nucleus of *Colpodella* sp. trophozoite in a close attachment. The nucleus is visualized in each protist. B. Intense antibody reactivity was observed in the posterior food vacuole of *Colpodella* sp. and weakly within the prey. C. DIC image shows the angle of the attachment and the morphology of the predator and prey cells. D. Merged image with DIC, antibody and DAPI stain.

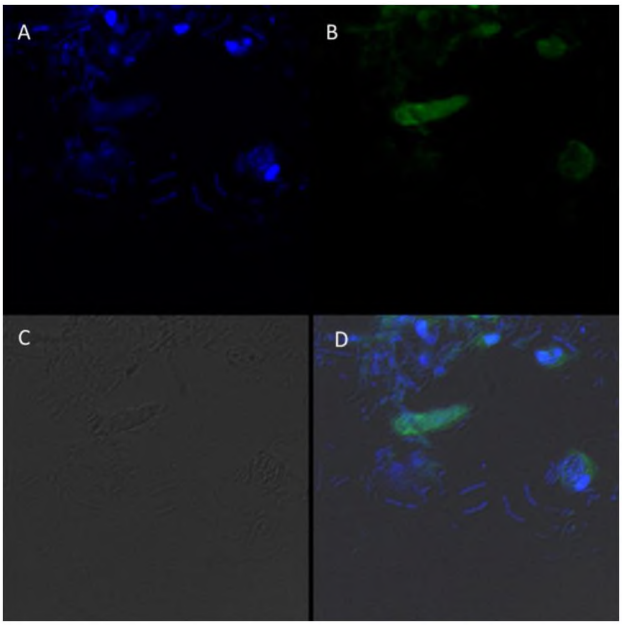

Figure 60. IFA of formalin-fixed cells in diprotist culture. Anti-EBA175 1:50 was used in IFA. A. DAPI image shows a mature *Colpodella* sp. trophozoite with a central nucleus. Trophozoites of *B. caudatus* were imaged with a nucleus and kinetoplast. B. Antibody reactivity was observed in the cytoplasm of *Colpodella* sp. trophozoites. Background antibody reactivity was observed in trophozoites of *B. caudatus*. C. DIC imaging captures the morphology of *Colpodella* sp. and *B. caudatus* trophozoites. D. Merged image with DIC, antibody and DAPI stain.

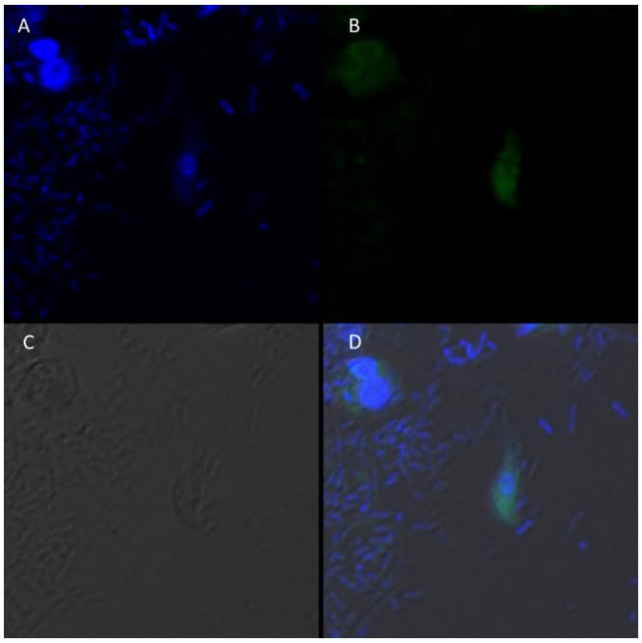

Figure 61. IFA of formalin-fixed cells in diprotist culture. Anti-EBA175 1:50 was used in IFA. A. DAPI image shows a single *Colpodella* sp. and *B. caudatus* trophozoite whose nuclei can be observed. B. Antibody reactivity was observed at the anterior portion of *Colpodella* sp. with weak background antibody reactivity observed in the trophozoite of *B. caudatus*. C. Morphology of the predator and prey trophozoites is captured with DIC. D. Merged image with DIC, antibody and DAPI stain.

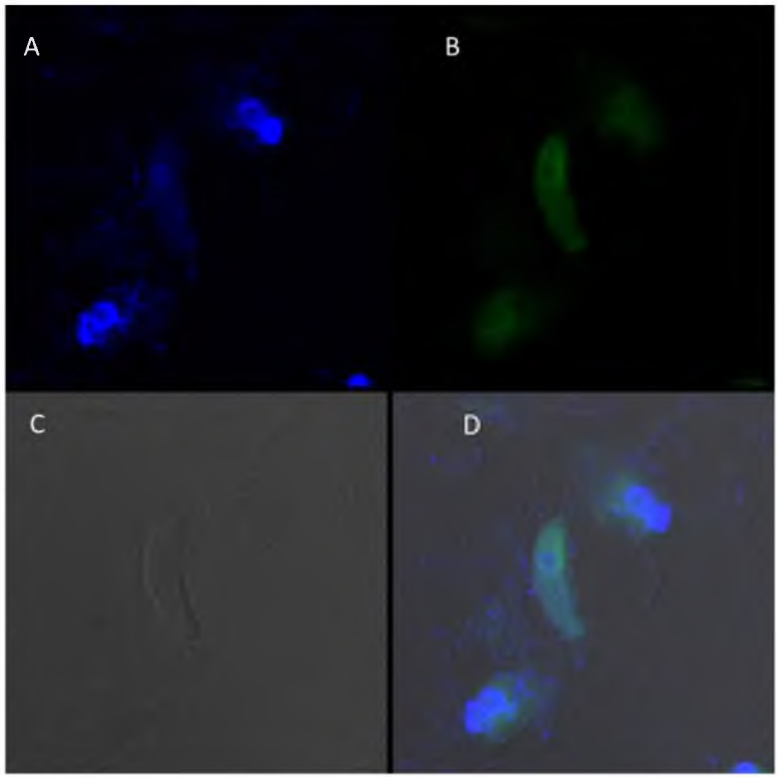

Figure 62. IFA of formalin-fixed cells in diprotist culture. Anti-EBA175 1:100 was used in IFA. A. DAPI image shows a mature *Colpodella* sp. trophozoite beside two trophozoites of *B. caudatus*. A nucleus is shown in each cell with *B. caudatus* showing a brightly stained kinetoplast and nucleus and the central nucleus of *Colpodella* sp. is less intense. B. Antibody reactivity was observed in the apical end of *Colpodella* sp. trophozoites and around the nucleus. Background antibody reactivity was observed in trophozoites of *B. caudatus* seen on either side of the *Colpodella* sp. trophozoite C. DIC image captures the morphology of *Colpodella* sp. and *B. caudatus* trophozoites. D. Merged image with DIC, antibody and DAPI stain.

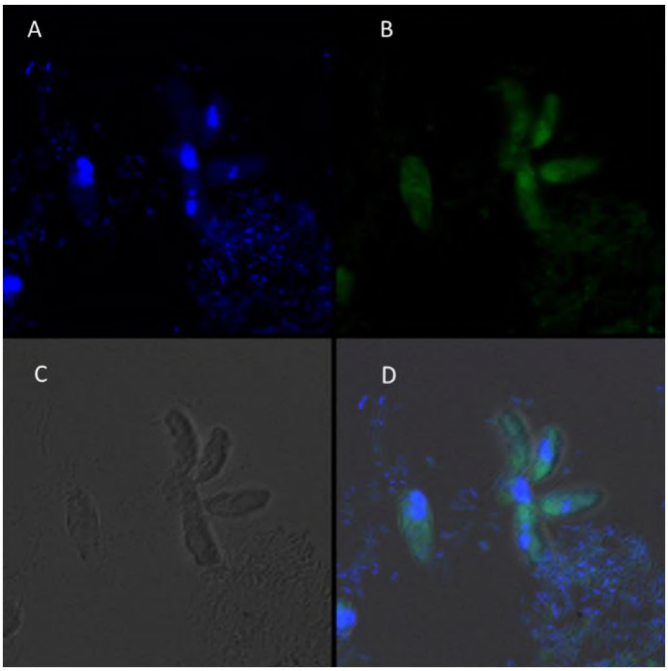

Figure 63. IFA of formalin-fixed cells in diprotist culture. Anti-EBA175 1:200 was used in IFA. A. DAPI image shows four *Colpodella* sp. nuclei beside a *B. caudatus* trophozoite. B. Intense antibody reactivity was observed at the apical ends of the four feeding *Colpodella* sp. trophozoites. Weak antibody reactivity was observed in a *B. caudatus* trophozoite. C. DIC image shows the proximity of each attachment and the morphology of the cells. D. Merged image with DIC, antibody and DAPI stain.

3.9 Transmission Electron Microscopy

Diprotist cultures were prepared for TEM to investigate the ultrastructure of *Colpodella* sp. life cycle stages. The results show that *Colpodella* sp. cysts can have both asymmetric and symmetric division as both odd and even-numbered juvenile trophozoites were observed within mature cysts. *Colpodella* sp. also develop asynchronously within the cyst as some juvenile trophozoites develop faster than others. Developing trophozoites, still undifferentiated, were observed still attached to the remnants of the food vacuole (residual body) (Figure 64, panels A and B). The flagella could be seen within the cyst (panel B). Two undifferentiated trophozoites can be seen in panels C and D. One trophozoite is more advanced in development than the other in panel

D demonstrating asynchrony in development. In panel E, seven juveniles were observed within a cyst. Asynchronous development was observed where one trophozoite already showing a developed pseudoconoid can be seen. The *Colpodella* sp. cyst wall is very thin compared to the thick cyst wall of *B. caudatus* shown in panel F. *Bodo cadautus* also has a large central nucleus within the cyst.

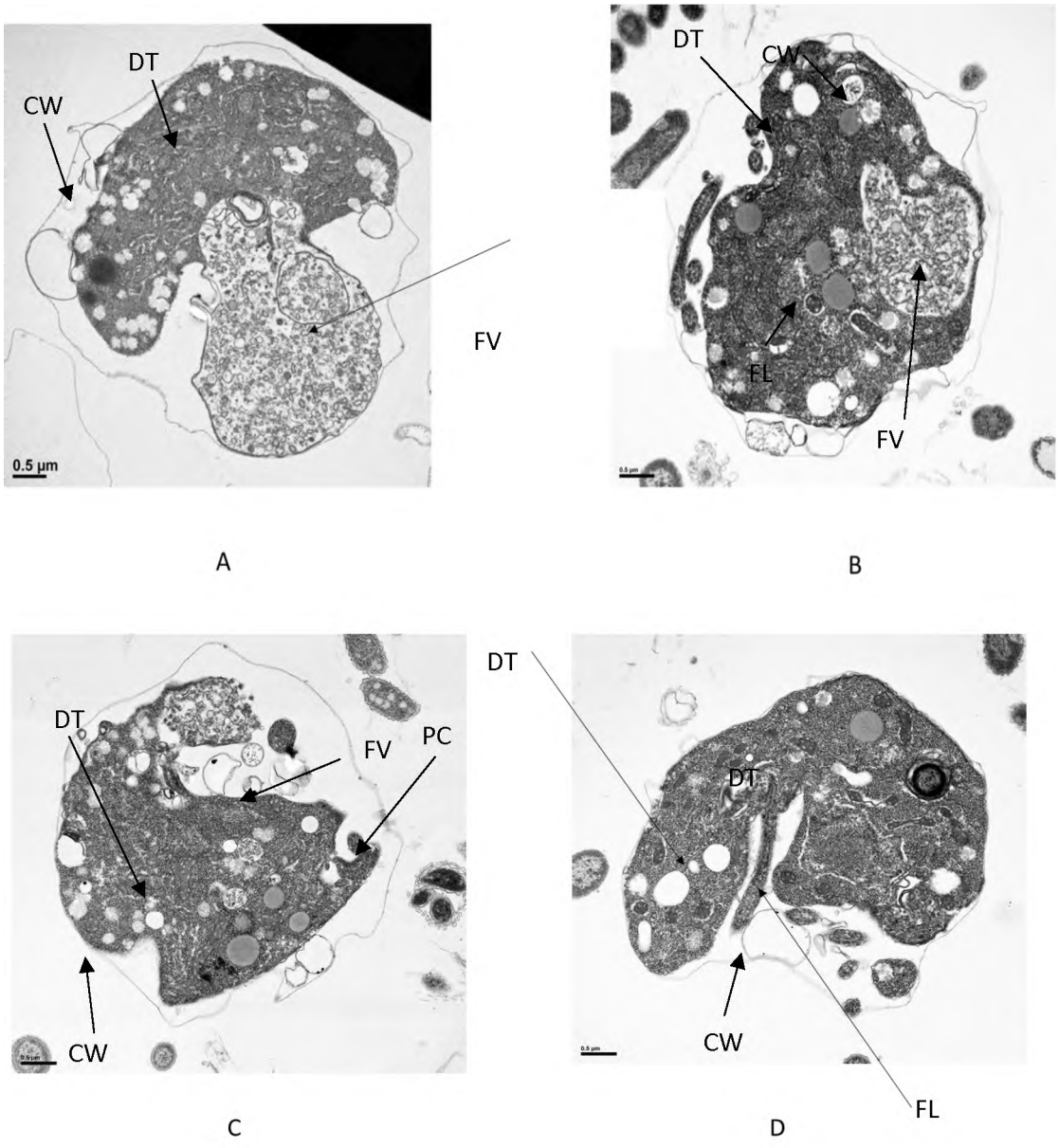

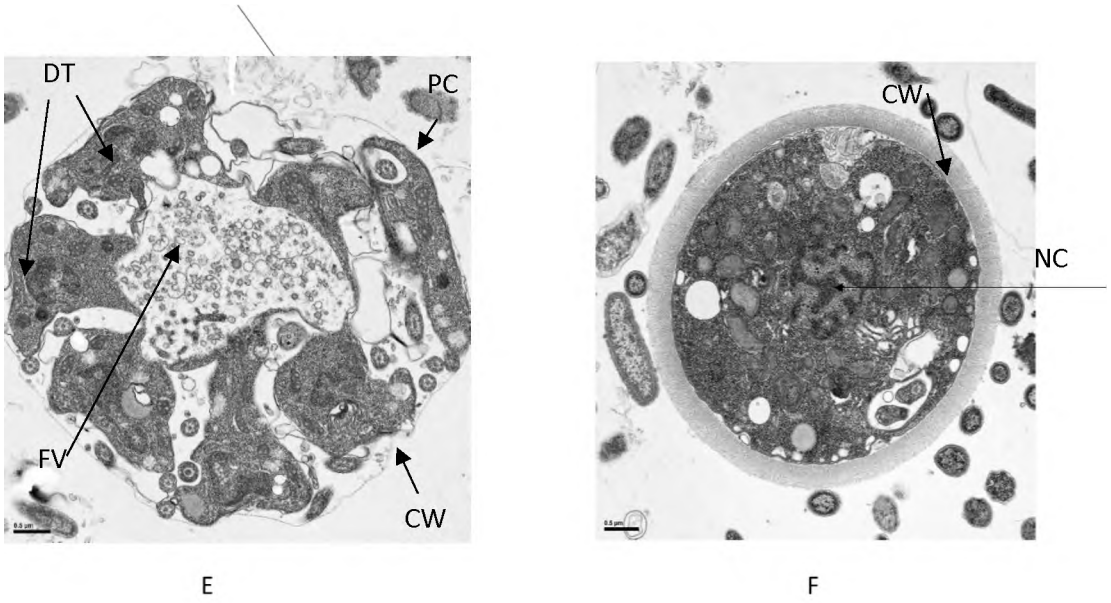

Figure 64. Transmission electron microscopy images showing asynchronous and asymmetric division of *Colpodella* sp. cysts. *Colpodella* cysts have a thin cyst wall. A. This is an early *Colpodella* sp. cyst with a large food vacuole (arrow) and undifferentiated trophozoites. B. This is an early *Colpodella* sp. cyst showing undifferentiated contents of the cyst. Flagella are present within the cyst. Thin cyst wall is identified (arrow) C. A cyst with *Colpodella* sp. trophozoites becoming recognizable. The pseudoconoid of the trophozoite on the right was observed, but it is still early in division and a remnant food vacuole was also seen. D. A mature *Colpodella* sp. cyst, farther along in division with a recognizable trophozoite showing the posterior portion (top arrow) of the trophozoite along with a visible flagellum (bottom arrow). E. A mature asymmetric and asynchronous *Colpodella* sp. cyst was observed with seven trophozoites. The trophozoite on the far right is farthest along in development as the pseudoconoid (arrow) can be seen. F. A *B. caudatus* cyst is shown with a thick cyst wall (top arrow) and can be differentiated from the very thin wall of *Colpodella* sp. cysts. The nucleus is seen in the middle (arrow). (CW, cyst wall; DT, developing trohpzoite; FL, flagella; FV, food vacuole; NC, nucleus).

3.10 Summary of the Life Cycle of Colpodella sp.

The life cycle of *Colpodella* sp. is shown in Figure 65. Based on the life cycle stages identified by Sam-Yellowe's trichrome staining, DIC microscopy, DAPI staining and ultrastructure investigated by TEM, the transitions through the life cycle of *Colpodella* sp. are summarized as shown from steps A-J. *Colpodella* sp. trophozoites attach to *B. caudatus* prey (A) and feed by myzocytosis, after which trophozoites begin to

undergo encystation by first forming the precyst (B, C) which differentiates into the early demilune cyst (D). The most active stage of the life cycle in culture is between 20-30 hours after subculture with peak activity at 24-28 hours. *Colpodella* sp. encyst in culture to form transient and long-term cysts. Transient cysts excyst and release trophozoites in the active phase of the culture. Long term (mature resting) cyst can survive in culture for up to 14 days (E). The demilune cysts (D) mature and divide to form two trophozoites (F) then divide to form more than two trophozoites (G, H). Multinucleate cysts can contain up to ten nuclei. Cysts with four and seven nuclei are depicted (G, H). Trophozoites egress as individual trophozoites (I, J) or egress as a pair still attached at the anterior end with incomplete cytokinesis (J'). The duration of the life cycle in culture is 36 hours. The precyst stage, multinucleate cysts, asymmetric and asynchronous division, and egress of paired juveniles with incomplete division are previously undocumented events for *Colpodella* species.

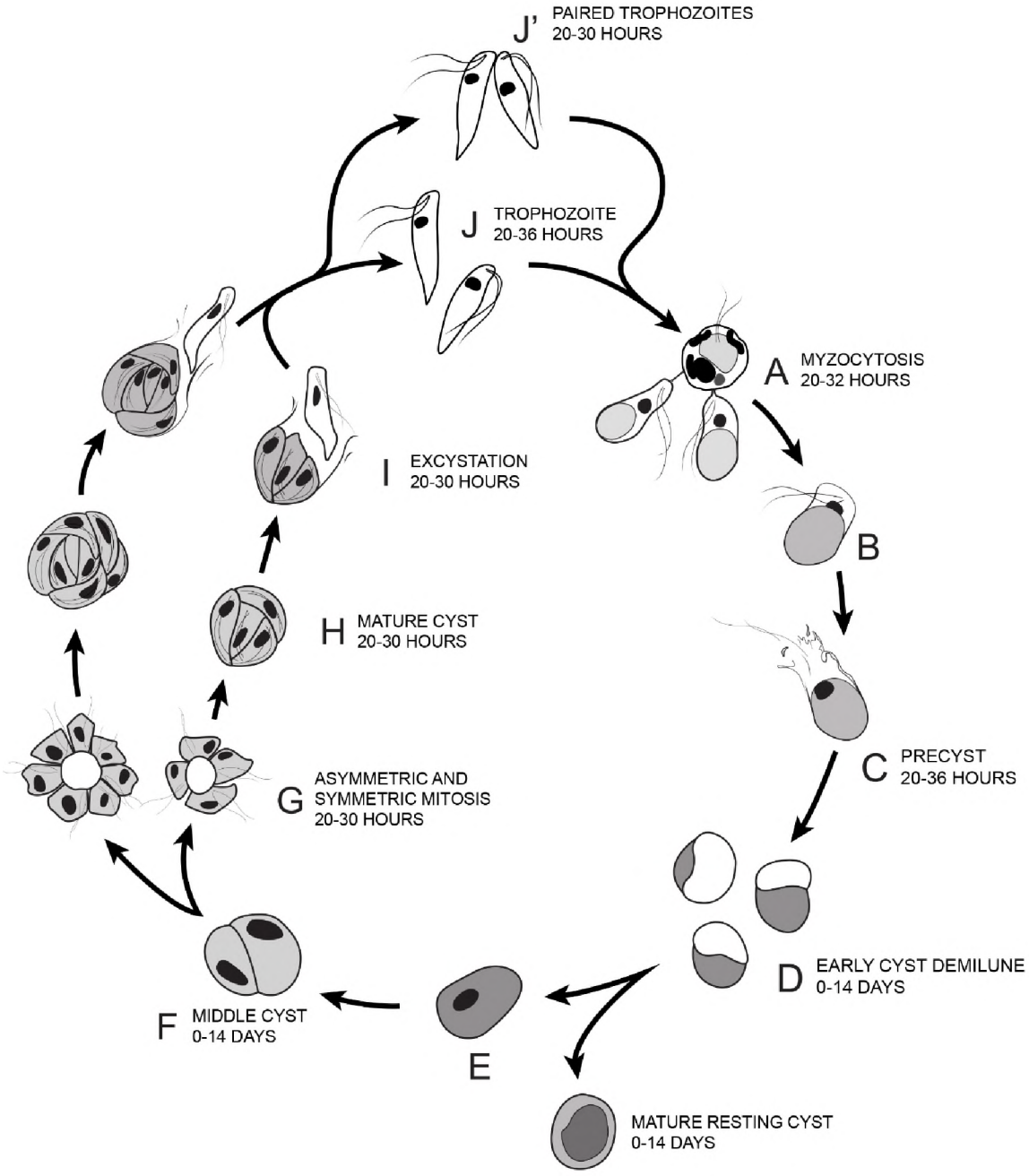

Figure 65. Illustration of the life cycle of *Colpodella* sp. (ATCC 50594) cultured in Hay medium. A. Once trophozoites egress from cysts they begin feeding on *B. caudatus* prey. Two trophozoites are depicted feeding in the process of myzocytosis. Active cultures with predator-prey attachments are seen 20-32 hours after subculture. The posterior food vacuole in *Colpodella* sp. enlarges during feeding. B. Encystment begins after feeding. C. Precyst showing anterior portion of trophozoite with a "frayed" appearance. Precysts are seen 20-36 hours after subculture. D. Early demilune cysts can be seen in culture during the active phase of the culture or in resting cultures (0-14 days after subculture). E. Mature cyst stages found in active and resting cultures can be seen in culture 0-14 days after subculture. Mature *Colpodella* sp. cysts with two or more nuclei are observed in

active cultures, as transient cysts are formed at this stage. The one nucleus cyst is predominant in the resting culture. F. Two-way cysts of *Colpodella* sp. can be seen in culture, 0-14 days after subculture. G. Following mitosis, development of the four-way cyst is most common. Asymmetric cysts containing three, five and seven nuclei were observed in culture, in addition to symmetric cysts containing four, six or eight nuclei. Four and seven nuclei cysts are depicted and can be seen in culture 20-30 hours after subculture. H. Mature cysts with young trophozoites can be seen 20-30 hours after subculture. I. Excystation (egress) and release of young trophozoites. J. Juvenile trophozoites can egress individually at 20-36 hours after subculture or rarely, juvenile trophozoites in pairs still attached can egress from cysts and complete cytokinesis outside the cyst (J' seen 20-30 hours after subculture). Paired trophozoites can egress from symmetric or asymmetric cysts. Free swimming young trophozoites egressed from cysts attach to prey to repeat the life cycle. The life cycle of C*olpodella* sp. lasts 36 hours.

CHAPTER IV

DISCUSSION

Colpodella sp. (ATCC 50594) is a predator protist that feeds on another protist, *B. caudatus,* as prey by performing myzocytosis. Contents of the prey are aspirated into a posterior food vacuole in *Colpodella* sp. Through protein, DNA, and RNA analysis it was discovered that *Colpodella* sp. is phylogenetically closely related to Apicomplexan parasites such as *Plasmodium* species and the plastid containing *Chromera velia* (Kuvardina et al. 2002; Janouskovec et al. 2015). In this study, *Colpodella* sp. was grown in tissue culture flasks in Hay medium (Yadavalli and Sam-Yellowe 2017; Sam-Yellowe and Yadavalli 2018) and used in a number of different experiments with the aim of investigating the life cycle and identification of the specific time points for each life cycle stage. Six time course experiments were conducted using formalin-fixed cells stained with Sam-Yellowe's trichrome (Sam-Yellowe et al. 2019) stain to view the cells. The objective of the first four time course experiments was to identify all the life cycle stages present in *Colpodella* sp. and to construct a general life cycle that will aid future investigations of *Colpodella* sp. and help in the identification of infective stages in opportunistic human infections caused by *Colpodella* species. Cells were collected for fixation and staining every four hours from hour zero until thirty-six

hours. Through the first four time course experiments, the most active part of the life cycle was identified between 20 and 30 hours. A fifth time course was performed where cells were collected for fixation and staining every four hours until twenty-two hours and then cells were collected every hour until hour thirty was reached. After thirty hours, cells were formalin-fixed every two hours up to forty hours. A last time course; time course six, was performed to identify the predominant stage of *Colpodella* sp. in a resting culture. Cysts were counted from pooled day five and seven cultures fixed and stained with Sam-Yellowe's trichrome to confirm the predominant cyst stage. The diprotist culture is asynchronous and the predator has two major life cycle stages that are characterized by a trophozoite and cyst stage. Using the time course experiments, we wanted to identify when each of the life cycle stages predominates in culture and what corresponding time points could be used for their identification.

Previously undocumented stages were identified in the diprotist culture using Sam-Yellowe's trichrome stains, confocal and DIC microscopy and TEM. Precyst stages, asymmetric and asynchronous cyst stages and multinucleate stages were identified. The egress of paired juvenile trophozoites of *Colpodella* sp. that complete cytokinesis outside the cyst were also identified. Immunofluorescence and confocal microscopy was performed to identify cross reactivity of antibodies specific for apical complex antigens of *P. falciparum* in the diprotist culture. Antibodies specific for apical complex proteins of *P. falciparum* and nonapical complex proteins was also used in IFA with DAPI used to stain the nuclei of the predator and prey. The morphology of each protist was identified by DIC microscopy. Antiserum 686 specific for the RhopH3 rhoptry protein reacted with *Colpodella* sp. trophozoites in free swimming trophozoites

and in trophozoites attached to *B. caudatus* in myzocytosis similar to previous reports (Sam-Yellowe et al. 2019). In some cell preparations, reactivity of the antibody was weak, and some background reactivity was observed in *B. caudatus*. The microneme specific antibodies against AMA-1 (Crewther et al. 1990) and EBA175 (Sim et al. 1990) also reacted with the apical end of *Colpodella* sp. trophozoites. There are no antibodies against apical complex proteins or food vacuole proteins of *Colpodella* species. The use of microneme and plasmepsin II specific antibodies in immunofluorescent assay studies to characterize *Colpodella* species proteins has not been performed previously. The specific structures containing the cross-reactive proteins are unknown. Antibodies against IMC3 cross reacted with proteins on *Colpodella* sp. with a more diffuse staining pattern. There was no reactivity with antibodies against IMC7 and Py235. Interestingly, the antibodies against plasmepsin II, an aspartate protease found in the food vacuole of *P. falciparum* reacted with proteins in the posterior section of feeding *Colpodella* sp. suggestive of a similar localization to the posterior food vacuole of *Colpodella* sp. (Silva et al. 1996). This is the first time that antibodies specific to *P. falciparum* EBA175, AMA1, plasmepsin II and *P.yoelii* 235 kDa rhoptry protein have been used in IFA on *Colpodella* sp. In a proteomic study of the dinoflagellate *Perkinsus marinus*, liver stage antigen 3, merozoite surface protein 3 of *P. falciparum* and Py235 rhoptry protein of *P. yoelii* were identified (Leibowitz et al. 2017). These experiments will need to be repeated to confirm the data obtained in this study. Transmission electron microscopy was performed to investigate the ultrastructure of *Colpodella* sp. in the diprotist culture. Asymmetric multinucleate cyst stages were identified.

Colpodella sp. is a protist with very little known about the life cycle stages and the timing of stage transitions. Other *Colpodella* species have been investigated to identify life cycle stages but much remains unknown. *Colpodella pseudoedax* life cycle stages have been reported as having cyst and trophozoite stages but the trophozoites of this *Colpodella* species were reported to perform binary fission (Mylnikov 2009). In this study binary fission was not observed in *Colpodella* sp. (ATCC 50594) after multiple passages in Hay medium culture, in time course experiments, staining and viewing live cultures using an inverted microscope with live imaging of the cultures. Even though binary fission was not observed, we cannot rule out the occurrence of binary fission in the ATCC maintained species as the cultures have not been in culture long-term. Investigations of *C. vorax* demonstrates the presence of some similarities and differences with the ATCC maintained species of *Colpodella* (Brugerolle 2002; Vazac et al. 2018). Both species of *Colpodella* have trophozoites that excyst and feed through myzocytosis. The cysts of *C. vorax* are shown to be symmetric, having four nuclei per cyst. Differences observed in the *C. vorax* life cycle include trophozoites fusing together after excystation (Brugerolle 2002; Vazac et al. 2018), which was not observed in the ATCC maintained species. In *Colpodella* sp. we have shown that there can be mature cysts with asymmetric and asynchronous division during the mitosis process. This has not been reported in other species. Among other relatives of *Colpodella* species such as described in *C. velia*, three life cycle stages were discovered in the life cycle of *C. velia* (Obornik et al 2011), which are coccoid, cysts and flagellates. The prevalence of each of these life cycle stages depended upon the culture conditions. The oval coccoid stage was the most abundant in every culture condition. They were able to find that these cells

undergo binary fission, and another round of division can lead to a cyst or flagellate stage. The transformation from coccoid stage to motile stage takes a few minutes and is usually in response to light stimulus. Most of the flagellate cells were observed between day 7 and day 11 in the culture and after a few hours the motile cells usually transformed back into coccoid cells. Investigators proposed that these organisms evolved into flagellate stages to either get away from intense light or to find nutrients. The *C. velia* cysts can hold a symmetric or asymmetric number of coccoid or trophozoite cells similar to the life cycle found in the *Colpodella* sp. investigated in this study. *Viterella brassicaformis* is another chromerid that was discovered recently in a coral. The life cycle was investigated and demonstrated to follow two different pathways in which autosporangia can excyst to release non-motile autospores and zoosporangia which give rise to motile zoospores (Obornik et al. 2012). The cysts can contain a symmetric number of cells from two to four but further investigation using electron microscopy showed *C. velia* can have more than four cells and be asymmetric in a cyst during mitosis (Portman et al. 2014). *Colpodella* sp. has a very similar life cycle to *C. velia* in that it can have asymmetric number of trophozoites during excystation but does not excyst non-motile cells like those described for chromerids. Another difference in the chromerid life cycle is that most of the flagellated cells are observed a week after subculturing, unlike *Colpodella* sp. where the most active stages are at day one in a 36-hour life cycle. The cultures are primarily resting and encysted after 36 hours. When counting the number of cysts form pooled day five and seven cultures, the predominant cyst stage identified was a mature *Colpodella* sp. cyst with one nucleus. Comparing this to the studies on *C. velia* we see these life cycles are similar, having resting cysts or coccoid cells in culture most

of the time. Using other *Colpodella* species and similar life cycle studies with chromerids we are able compare the life cycles of these important relatives of the parasitic apicomplexans.

Time courses, electron, and confocal microscopy were used to investigate the life cycle of *Colpodella* sp. The first four time course experiments analyzed with Sam-Yellowe's trichrome stain revealed that the prey, *B. caudatus,* excysts much earlier than the predator approximately four hours after subculturing. The prey dominates in the culture until about twenty hours when *Colpodella* sp. begins to egress from their cysts. Young trophozoites of *Colpodella* sp. emerge and begin myzocytosis lasting between twenty and thirty hours in culture. Once twenty-eight hours has been reached, *B. caudatus* trophozoites will start to encyst earlier than the *Colpodella* sp. trophozoites. At thirty hours is when *Colpodella* sp. started to encyst and around thirty-six hours the culture is mostly quiet with only a few predator and prey trophozoites remaining. After the diprotist cultures have encysted they remain encysted until they are subcultured and are viable up to 14 days. The cells must be subcultured by 14 days or the cysts start to deteriorate, and the cell yield is low. Data from time course experiments 1-4 demonstrated that the most active part of the life cycle is between twenty and thirty hours. Many active *Colpodella* sp. trophozoites were seen attached to their prey between twenty-four to twenty-eight hours after subculturing. At thirty hours the *Colpodella* sp. started to encyst and by 36 hours, the culture was mostly encysted. The cultures looked the same from 36 to 40 hours. Time course six was performed to identify the predominant cyst stage in the diprotist resting cultures. Sam-Yellowe's trichrome stain

was used to stain and observe cysts for each timepoint every twenty-four hours for eight days.

Diprotist cultures are asynchronous so there is no uniformity in the life cycle stages found for each protist. Cysts were counted from pooled day five and seven cultures to confirm the predominant cyst stages. An active culture was observed at one day after subculturing in support of the data obtained from time course experiments 1-5. This confirmed that there was *B. caudatus* and *Colpodella* sp. trophozoites performing myzocytosis. Looking through each of the eight days of stained slides the primary cyst stage identified for *Colpodella* sp. in resting cultures was a mature cyst with a single nucleus. Slides stained from pooled day five and seven slides were counted to determine the percentage of each cyst stage. One hundred cysts were counted on duplicate slides. Eighty to ninety percent of the *Colpodella* sp. cyst were of this type. Not all *Colpodella* sp. cysts were mature with a single nucleus, some had multiple asymmetric nuclei or symmetric nuclei with two or more juvenile trophozoites. Early *Colpodella* sp. demilune cysts were also counted but there only seemed to be a relatively small number of them. Even though these cultures are primarily resting, free swimming predator and prey trophozoites, encysting and excysting during these time points were also detected. Although challenging to achieve synchronous cultures when working with the free-living alveolates, the use of synchronous cultures would help to confirm these results. Investigations of life cycles of *C. velia* and *V. brassicaformis* also used nonsynchronized cells due to culture conditions used (Obornik et al. 2011; Obornik et al. 2012, Portman et al. 2014).

Single predator prey attachments were the most common pairings observed, similar to reports of other *Colpodella* species (Simpson and Patterson 1996; Brugerolle 2002; Mylnikov 2009). Two to three predators on one prey can also occur. In the most active stage of the life cycle observed in the present study, five to six predators feeding on one prey were observed. The *Colpodella* sp. "crowd" of trophozoites feeding on a single prey with multiple attachments and different lengths of the tubular tethers has not been reported previously. One of the reasons for so many *Colpodella* sp. attaching to one prey may have to do with smaller number of prey available when the majority of *Colpodella* sp. trophozoites egress from cysts. *Colpodella* sp. trophozoites exceed the number of *B. caudatus* trophozoites because of early prey encystation. This has only been observed in culture and may be different in their natural environment. If we know the life cycle, we can isolate and culture *Colpodella* sp. from their habitat and know the life cycle timing and stages we should expect.

Electron microscopy images identified the ultrastructure of *Colpodella* sp. and *B. caudatus* cysts. The cysts of *Colpodella* sp. have a very thin cyst wall and a remanent food vacuole associated with undifferentiated trophozoites. The electron microscopy images confirmed that cysts of *Colpodella* sp. can have asymmetric division which has not been previously observed. Results also showed that the mitosis in mature *Colpodella* sp. cysts is asynchronous, meaning that not all the trophozoites develop and differentiate at the same rate within the cyst. Inside the cysts *Colpodella* sp. trophozoites that are more developed can be visualized showing a pseudoconoid, mitochondria, and defined nucleus. *B. caudatus* cysts can be easily differentiated by the thickness of their wall. They are also seen to have a nucleus and kinetoplast. Both protists show parts of

their flagella inside the cysts. Not much information is known about the process of cell division inside the cysts of *Colpodella* species. Mitotic kinases have not been identified in *Colpodella* species.

Transmission electron microscopy images show that division in *Colpodella* sp. cysts is similar to schizogony found in some parasitic apicomplexans. Schizogony is the asexual reproduction of merozoites through rounds of multiple fission found in parasites such as *P. falciparum* and *Eimeria* (Gubbels et al. 2020). This happens during closed mitosis where the nuclear envelope remains intact and intranuclear mitotic spindle interacts with the centromeres. Another form of apicomplexan reproduction is called endodyogeny, in which there is a single round of mitosis that produces two identical daughter cells (Gubbels et al. 2020). *Toxoplasma gondii* is an example of an apicomplexan parasite that uses endodyogeny in cell division. *Colpodella* sp. seems to fit into schizogony because they develop into multiple trophozoites within a single cyst. The cyst can hold a symmetric number or asymmetric number of trophozoites between one and eight that were observed.

It is crucial to understand the life cycle of *Colpodella* sp. to help with studies that are involved in isolating different stages of the life cycle such as the cysts and trophozoites. Life cycle stages causing infection can also be identified. There have been two case studies reported from China showing that two separate women were infected with *Colpodella* species as the DNA sequence was isolated using PCR (Yuan et al. 2012; Jiang et al. 2018). The life cycle stages that caused the infection and pathogenesis are unidentified so it would help knowing the life cycle. Knowing the life cycle can also help in any protein or DNA studies. As of now we are unsure of what genes are activated and

what proteins are translated during each stage of the life cycle. Investigators interested in isolating a specific protein or performing proteome analysis can study different stages of the life cycle. Furthermore, identifying genes conserved in *Colpodella* sp. that have been identified among the parasitic apicomplexans can help with phylogenetic studies. Reactivity of antibodies against the microneme proteins, EBA175 and AMA1 used for merozoite invasion in *P. falciparum* will need to be confirmed by identifying the genes encoding these proteins. The gene encoding AMA1 is highly conserved among the parasitic apicomplexans (Tyler et al. 2011; Chesne-Seck et al. 2005; Tonkin et al. 2013). Understanding the role played by the apical complex proteins may provide additional insights to help understand the origins of intracellular parasitism.

LITERATURE CITED

1. Anderson-White BR, Ivey FD, Cheng K, Szatanek T, Lorestani A, Beckers CJ, Ferguson DJ, Sahoo N, Gubbels MJ (2007) A family of intermediate filament-like proteins is sequentially assembled into the cytoskeleton of *Toxoplasma gondii*. Cell Microbiol. 13:18-31.
2. Bargieri D, Lagal V, Andenmatten N, Tardieux I, Meissner M, Ménard R (2014) Host cell invasion by apicomplexan parasites: the junction conundrum. PLoS Pathog. 10:e1004273. doi: 10.1371/journal.ppat.1004273. PMID: 25232721; PMCID: PMC4169498.
3. Beck JR, Chen AL, Kim EW, Bradley PJ (2014) RON5 Is Critical for Organization and Function of the *Toxoplasma* Moving Junction Complex. PLoS Pathogens, 10. doi:10.1371/journal.ppat.1004025
4. Bonniec SL, Deregnaucourt C, Redeker V, Banerjee R, Grellier P, Goldberg DE, Schrével J (1999) Plasmepsin II, an acidic hemoglobinase from the *Plasmodium falciparum* food vacuole, is active at neutral pH on the host erythrocyte membrane skeleton. J Biol Chem. 274: 14218-14223.
5. Brossier F, Sibley LD (2005) *Toxoplasma gondii*: Microneme protein MIC2. The International Journal of Biochemistry; Cell Biology, 37: 2266-2272.
6. Brugerolle G (2002) *Colpodella vorax*: ultrastructure, predation, life-cycle, mitosis, and phylogenetic relationships. European Journal of Protistology, 38: 113-125.

7. Cavalier-Smith T, Chao E (2004) Protalveolate phylogeny and systematics and the origins of Sporozoa and dinoflagellates (phylum Myzozoa nom. nov.). European Journal of Protistology, 40: 185-212.
8. Chesne-Seck ML, Pizarro JC, Vulliez-Le Normand B, Collins CR, Blackman MJ, Faber BW, Remarque EJ, Kocken CH, Thomas AW, Bentley GA (2005) Structural comparison of apical membrane antigen 1 orthologues and paralogues in apicomplexan parasites. Mol Biochem Parasitol. 144: 55-67.
9. Combe A, Moreira C, Ackerman S, Thiberge S, Templeton TJ, Ménard R (2009) TREP, a novel protein necessary for gliding motility of the malaria sporozoite. International Journal for Parasitology, 39: 489-496.
10. Crewther PE, Culvenor JG, Silva A, Cooper JA, Anders RF (1990) *Plasmodium falciparum*: Two antigens of similar size are located in different compartments of the rhoptry. Exp Parasitol. 70: 193-206.
11. Dubey R, Harrison B, Dangoudoubiyam S, Bandini G, Cheng K, Kosber A, Agop-Nersesian C, Howe DK, Samuelson J, Ferguson DJP, Gubbels MJ (2017) Differential Roles for Inner Membrane Complex Proteins across *Toxoplasma gondii* and *Sarcocystis neurona* Development. mSphere. 2: e00409-17.
12. Egarter S, Andenmatten N, Jackson AJ, Whitelaw JA, Pall G, et al. (2014) The *Toxoplasma* Acto-MyoA Motor Complex Is Important but Not Essential for Gliding Motility and Host Cell Invasion. PLoS ONE 9: e91819.
13. Frenal K, Polonais V, Marq JB, Stratmann R, Limenitakis J, et al. (2010) Functional dissection of the apicomplexan glideosome molecular architecture. Cell Host Microbe 8: 343–357.

14. Giovannini D, Spath S, Lacroix C, Perazzi A, Bargieri D, et al. (2011) Independent roles of apical membrane antigen 1 and rhoptry neck proteins during host cell invasion by apicomplexa. Cell Host Microbe 10: 591–602
15. Goodenough U, Roth R, Kariyawasam T, He A, Lee JH (2018) Epiplasts: Membrane Skeletons and Epiplastin Proteins in Euglenids, Glaucophytes, Cryptophytes, Ciliates, Dinoflagellates, and Apicomplexans. mBio. 9: e02020-18.
16. Gubbels M, Keroack CD, Dangoudoubiyam S, Worliczek HL, Paul AS, Bauwens C, . . . Duraisingh MT (2020) Fussing About Fission: Defining Variety Among Mainstream and Exotic Apicomplexan Cell Division Modes. Frontiers in Cellular and Infection Microbiology. 10: 269
17. Gubbels MJ, Duraisingh MT (2012) Evolution of apicomplexan secretory organelles. International Journal for Parasitology. 42: 1071-1081.
18. Gubbels MJ, Lehmann M, Muthalagi M, Jerome ME, Brooks CF, Szatanek T, Flynn J, Parrot B, Radke J, Striepen B, White MW (2020) Forward Genetic Analysis of the Apicomplexan Cell Division Cycle in *Toxoplasma gondii*. PLoS Pathog 4: e36.
19. Hale VL, Watermeyer JM, Hackett F, Vizcay-Barrena G, Ooij CV, Thomas JA, . . . Saibil HR (2017) Parasitophorous vacuole poration precedes its rupture and rapid host erythrocyte cytoskeleton collapse in *Plasmodium falciparum* egress. Proceedings of the National Academy of Sciences. 114: 3439-3444.
20. Holder AA, Freeman RR (1981) Immunization against blood-stage rodent malaria using purified parasite antigens. Nature. 294: 361-364.

21. Janouskovec J, Tikhonenkov D, Burki F, Howe A, Kolisko M, Mylnikov P, Keeling P (2015) Factors mediating plastid dependency and the origins of parasitism in apicomplexans and their close relatives. PNAS. 112: 10200-10207.

22. Jiang J, Jiang R, Chang Q, Zheng Y, Jiang B, Sun Y, et al. (2018) Potential novel tick-borne *Colpodella* species parasite infection in patient with neurological symptoms. PLOS Neglected Tropical Diseases, 12: e0006546.

23. Joseph SJ, Fernández-Robledo JA, Gardner MJ, El-Sayed NM, Kuo C, Schott EJ, . . . Vasta GR (2010) The Alveolate *Perkinsus marinus*: Biological Insights from EST Gene Discovery. BMC Genomics. 11: 228.

24. Kennedy M, Wang J, Zhang Y, Miles A, Chitsaz F, Saul A, Long C, Miller L, Stowers A (2002) In Vitro Studies with Recombinant *Plasmodium falciparum* Apical Membrane Antigen 1 (AMA1): Production and Activity of an AMA1 Vaccine and Generation of a Multiallelic Response. Infection and Immunity. 70: 6948-6960

25. Kono M, Heincke D, Wilcke L, Wai Ying Wong T, Bruns C, Herrmann S, Spielmann T, Gilberger TW (2016) Pellicle formation in the malaria parasite. J Cell Sci. 129: 673–680.

26. Kuarvdina O, Leander B, Aleshin V, Myl'nikov A, Keeling P, Simdyanov T (2002) The Phylogeny of Colpodellids (Alveolata) Using Small Subunit rRNA Gene Sequences Suggests They are the Free-living Sister Group to Apicomplexans. The Journal of Eukaryotic Microbiology. 49: 498-504.

27. Leander B, Kuvardina O, Aleshin V, Mylnikov A, Keeling P (2003) Molecular Phylogeny and Surface Morphology of *Colpodella edax* (Alveolata): Insights into

the Phagotrophic Ancestry of Apicomplexans. The Journal of Eukaryotic Microbiology. 50: 334-340.

28. Leibowitz MP, Tavares GC, Pereira FL, Perdigão C Azevedo V, Figueiredo, HC (2017). Shotgun Label-Free Proteomic Analyses of the Oyster Parasite *Perkinsus marinus*. Journal of Proteomics And Genomics Research, 2: 13-21.
29. McFadden G, Yeh E (2017) The apicoplast: now you see it, now you don't (Apicomplexa). International Journal for Parasitology. 47: 137-144.
30. Meissner M, Schluter D, Soldati D (2002) Role of *Toxoplasma gondii* myosin A in powering parasite gliding and host cell invasion. Science. 298: 837–840.
31. Mital J, Meissner M, Soldati D, Ward GE (2005) Conditional expression of *Toxoplasma* gondii apical membrane antigen-1 (TgAMA1) demonstrates that TgAMA1 plays a critical role in host cell invasion. Mol Biol Cell. 16: 4341–4349.
32. Mohd A, Ridzuan M, Moon RW, Knuepfer E, Black S, Holder AA, Green JL (2012) Subcellular Location, Phosphorylation and Assembly into the Motor Complex of GAP45 during *Plasmodium falciparum* Schizont Development. PLoS ONE. 7: e33845.
33. Moore R, Oborník M, Janouškovec J, Chrudimský T, Vancová M, Green D, et al. (2008) A photosynthetic alveolate closely related to apicomplexan parasites. Nature. 451: 959-963.
34. Murata E, Tokunaga N, Tachibana M, Tsuboi T, Torii M, et al. (2012) The investigation of the mechanism how malaria sporozoites invade salivary glands. Molecular Approaches to Malaria Meeting 2012. Abstract Book. Lorne, Australia. 12: 394-400.

35. Mylnikov A (2009) Ultrastructure and phylogeny of colpodellids (*Colpodellida*, Alveolata). Biology Bulletin. 36: 582-590.

36. Myl'nikova Z, Myl'nikov A (2008) The morphology of predatory flagellate *Colpodella pseudoedax* Mylnikov et Mylnikov, 2007 (*Colpodellida*, Alveolata). Inland Water Biology. 2: 199-204.

37. Okamoto N, Keeling P (2014) A Comparative Overview of the Flagellar Apparatus of Dinoflagellate, Perkinsids and Colpodellids. Microorganisms. 2: 73-91.

38. Olmo J, Esteban G, Finlay B (2011) New records of the ectoparasitic flagellate *Colpodella gonderi* on non-Colpoda ciliates (*Colpodella*). International Microbiology. 207-211.

39. Orbornik M, Vanocova M, Lai D, Janouskovec J, Keeling P, Lukes J (2011) Morphology and Ultrastructure of the Photosynthetic Relative of Apicomplexa, *Chromera velia* (Chromerids). Institute of Parasitology. Protist. 162: 115-130.

40. Orbornik M, Modry D, Lukes M, Cernotikova-Stribrna E, Cihlar J, Tersarova M, Kotabova E, Vancova M, Prasil O, Lukes J (2012) Morphology, Ultrastructure and Life Cycle of *Vitrella brassicaformis* n. sp., n. gen., a Novel Chromerid from the Great Barrier Reef (Chromerid). Biology Centre, Institute of Parasitology. Protist. 163: 306-323

41. Peixoto L (2009) Using Evolutionary Genomics to Elucidate Parasite Biology and Host-Pathogen Interactions. Publicly Accessible Penn Dissertations. 38.

42. https://repository.upenn.edu/edissertations/38

43. Portman N, Foster C, Walker G, Šlapeta J (2014) Evidence of intraflagellar transport and apical complex formation in a free-living relative of the apicomplexa. Eukaryot Cell. 13: 10-20.

44. Roberts L, Janovy Jr J, Nadler S, Schmidt GD, Larry S. Roberts' Foundations of Parasitology, Ninth Edition. (2013).

45. Sam-Yellowe T, Addepalli K, Yadavalli R, Peterson JW (2019) New trichrome stains identify cysts of *Colpodella* sp. (Apicomplexa) and *Bodo caudatus*. International Microbiology. 23: 303-311.

46. Sam-Yellowe T, Yadavalli R, Fujioka H, Peterson JW, Drazba J (2019) RhopH3, rhoptry gene conserved in the free-living alveolate flagellate *Colpodella* sp. (Apicomplexa). European Journal of Protistology. 71: 125637.

47. Sam-Yellowe T, Yadavalli R (2018) Giemsa Staining and Antibody Characterization of *Colpodella* sp. (Apicomplexa). Microbiol Modern Tech. 3: 103

48. Schnepf E, Deichgräber G (1984) "Myzocytosis", a kind of endocytosis with implications to compartmentation in endosymbiosis. Naturwissenschaften. 71: 218–219.

49. Shen B, Sibley LD (2014) *Toxoplasma* aldolase is required for metabolism but dispensable for host-cell invasion. Proc Natl Acad Sci U S A. 111: 3567–3572.

50. Siddall M, Reece K, Nerad T, Burreson E. (2001) Molecular Determination of the Phylogenetic Position of a Species in the Genus *Colpodella* (Alveolata). American Museum Novitates. 3314: 1-12.

51. Sim BK, Orlandi PA, Haynes JD, Klotz FW, Carter JM, Camus D, Zegans ME, Chulay JD (1990) Primary structure of the 175K *Plasmodium falciparum* erythrocyte binding antigen and identification of a peptide which elicits antibodies that inhibit malaria merozoite invasion. J Cell Biol. 111:1877-1884.

52. Simpson A, Patterson D, (1996) Ultrastructure and identification of the predatory flagellate *Colpodella pugnax* Cienkowski (Apicomplexa) with a description of *Colpodella turpis* n. sp. and a review of the genus. Systematic Parasitology. 33: 187–198.

53. Silva A, Lee A, Gulnik S, Maier P, Collins J, Bhat T, Collins P, Cachau R, Luker K, Gluzman I, Francis S., Oksman A., Goldberg D, Erickson J (1996) Structure and inhibition of plasmepsin II, a hemoglobin-degrading enzyme from *Plasmodium falciparum*. Proceedings of the National Academy of Sciences. 93: 0034-10039.

54. Sultan AA, Thathy V, Frevert U, Robson KJ, Crisanti A, et al. (1997) TRAP is necessary for gliding motility and infectivity of *Plasmodium* sporozoites. Cell. 90: 511–522

55. Templeton T, Pain A (2015) Diversity of extracellular proteins during the transition from the 'proto-apicomplexan' alveolates to the apicomplexan obligate parasites. Parasitology. 143: 1-17.

56. Tonkin ML, Crawford J, Lebrun ML, Boulanger MJ (2013) *Babesia divergens* and *Neospora caninum* apical membrane antigen 1 structures reveal selectivity and plasticity in apicomplexan parasite host cell invasion. Protein Sci. 22: 114-127.

57. Tyler JS, Treeck M, Boothroyd JC (2011) Focus on the ringleader: the role of AMA1 in apicomplexan invasion and replication. Trends Parasitol. 27: 410-420.

58. Vazač J, Füssy Z, Hladová I, Killi S, Oborník M (2018) Ploidy and Number of Chromosomes in the Alveolate Alga *Chromera velia*. Protist. 169: 53-63.

59. Yadavalli R, Sam-Yellowe T (2017) Developmental stages identified in the trophozoite of the free-living Alveolate flagellate *Colpodella* sp. (Apicomplexa). Int Microbiol. 20: 178-183.

60. Yang JC, Blanton RE, King CL, Fujioka H, Aikawa M, Sam-Yellowe TY (1996) Seroprevalence and specificity of human responses to the *Plasmodium falciparum* rhoptry protein Rhop-3 determined by using a C-terminal recombinant protein. Infect Immun. 64: 3584-3591.

61. Yuan CL, Keeling PJ, Krause PJ, Horak A, Bent S, Rollend L, Hua XG (2012) *Colpodella* spp.-like parasite infection in woman, China. Emerg Infect Dis. 18:125-127.